Oxidative dehydrogenation of *n*-octane over molybdate based catalysts

by

Mohamed I. Fadlalla

November 2014

Oxidative dehydrogenation of *n*-octane over molybdate based catalysts

by

Mohamed I. Fadlalla

(MSc)

Submitted in the fulfillment of the academic requirements for the degree of Doctor of Philosophy in the School of Chemistry and physics, University of KwaZulu-Natal, Durban, South Africa.

November 2014

NOTE: This thesis has been prepared according to Format 3 as outlined in the guidelines from the Collage of Agriculture, Engineering and Science which state:

This is a thesis in which the chapters are written as a set of discrete research papers, with an Overall Introduction and Final Discussion. These research papers would not be published yet, but at least one paper would have been submitted for publication. The references are reformatted to a uniform standard.

As the candidate's supervisor, I have approved this thesis for submission

Prof. Holger B. Friedrich _____ Date_____

Abstract

The oxidative dehydrogenation of *n*-octane over different molybdates was investigated using a continuous flow fixed bed reactor in the temperature range of 350-550 °C at 50 °C intervals. Molybdates investigated in this study were synthesized by the co-precipitation method and characterized by powder and *in situ* (oxidation and reduction) X-Ray diffraction (XRD), BET-surface area measurements, inductively coupled plasma-optical emission spectroscopy (ICP-OES), Raman spectroscopy, scanning electron microscopy (SEM), temperature programmed reduction (TPR) and temperature programmed oxidation (TPO). Molybdates focus of this study was magnesium molybdate (MM) and cobalt molybdate (CM). In the case of magnesium molybdate, catalysts with different magnesium : molybdenum ratios were synthesized (*i.e.* 0.87, 0.98, 1.06 and 1.25 magnesium : molybdenum). While for cobalt molybdate the ratio of cation to molybdenum was kept near the stoichiometric ratio.

The influence of the synergistic effect between molybdenum trioxide and molybdate was investigated using MM. An increase of the molybdenum content in the catalysts resulted in an increase in the surface area of the catalysts and in the TPR results the intensity of the reduction peak corresponding to molybdenum trioxide increased as the molybdenum content increased, which marked an increase in the *n*-octane conversion. The preliminary catalytic testing was at a gas hourly space velocity (GHSV) of 4000 h^{-1} and carbon to oxygen ratio of 8:3 C:O. The highest conversion of *n*-octane and selectivity to value added products (*i.e.* octenes and aromatics) was obtained over the two catalysts with near stoichiometric ratio of molybdenum / magnesium (*i.e.* MM 0.98 and 1.06). The surface acidity of the catalysts was altered by varying the molybdenum content, which in return influenced the selectivity of the catalyst. Used catalyst characterization by Raman spectroscopy showed all catalysts were still dominated by the magnesium molybdate phase after the reaction.

Both molybdates (*i.e*. MM and CM) with a near stoichiometric ratio of cation : molybdenum were tested under different oxidation environments ranging from oxygen lean to oxygen rich environments (*i.e*. carbon : oxygen ratio of 8:0, 8:1, 8:2, 8:3 and 8:4). The conversion of *n*-octane over all molybdates increased as the oxygen concentration in the reaction feed increased. The carbon to oxygen ratio also greatly influences the selectivity of the catalyst. In general terms as the oxygen concentration increased the selectivity to octenes decreased and selectivity to aromatics increased, while the selectivity to COx increased and peaked at the reaction temperature close to the onset reduction temperature of the catalyst. The chemical stability of the catalyst was also altered by the oxygen concentration as determined by characterization of the used catalyst by powder XRD and Raman spectroscopy. In the case of MM and CM the initial phases of the catalyst was maintained and stable under moderate to oxygen rich environments (*i.e*. 8:2, 8:3 and 8:4 carbon : oxygen), while under oxygen lean environments (*i.e*. 8:0 and 8:1 carbon : oxygen) phase segregation takes place and molybdenum oxide dominates the catalysts.

The effect of the cation in the molybdate structure was highlighted by comparing the activity and selectivity of the magnesium molybdate catalyst and the cobalt molybdate catalyst under *iso*-conversion and *iso*-thermal conditions. Magnesium molybdate seems to favor olefin formation, while cobalt molybdate favors aromatics, based on the *iso*-conversion results. Considering the iso-thermal comparison between the two molybdates, the data indicate that cobalt molybdate is more active than magnesium molybdate.

Preface

The experimental work described in this thesis was carried out in the School of Chemistry and Physics in the University of KwaZulu Natal, Westville campus, Durban. Starting from July 2011 under the guidance and supervision of Professor Holger B. Friedrich.

These studies represent original work by the author and have not otherwise been submitted in any form for any degree or diploma to any tertiary institution. Where use has been made of work of other it is duly acknowledged in the text.

_____

Mohamed I. Fadlalla

B.Sc (Honours), MSc (University of Kwa zulu Natal, Westville campus)

Declaration 1

Plagiarism

I, Mohamed I. Fadlalla

1. The research reported in this thesis, except where otherwise indicated, is my original research.
2. This thesis has not been submitted for any degree or examination at any other university.
3. This thesis does not contain other person's data, pictures, graphs or other information, unless specifically acknowledged as being sourced from other persons.
4. This thesis does not contain other person's writing, unless specifically acknowledged as being sourced from other researchers. Where other written sources have been quoted, then:
   a. Their words have been re-written but the original information attributed to them has been referenced
   b. Where their exact words have been used, then their writing has been placed in italics and inside quotation marks, and referenced.
5. This thesis does not contain text, graphics or tables copied and pasted from internet, unless specifically acknowledge, and the source being detailed in the thesis and in the reference sections.

_____

Mohamed I. Fadlalla

Declaration 2

Publications and conference contributions

DETAILS OF CONTRIBUTION TO PUBLICATIONS that form part and/or include research presented in this thesis (include publications in preparation, submitted, in press and published and give details of the contributions of each author to the experimental and writing of each publication)

Publications

1.

Authors: Mohamed I. Fadlalla and Holger B. Friedrich

Title: Effect of molybdenum content on the activity and selectivity of magnesium molybdate in the oxidative dehydrogenation of *n*-octane.

Status: Submitted for publication to Applied Catalysis A: General

Contribution: I carried out all experimental work and manuscript preparation under the supervision of Prof. Holger B. Friedrich

2.

Authors: Mohamed I. Fadlalla and Holger B. Friedrich

Title: Effect of the carbon to oxygen ratio on the activity and the selectivity of magnesium molybdate in the oxidative dehydrogenation of *n*-octane

Status: Submitted for publication to Journal of Molecular Catalysis A. Chemical

Contribution: I carried out all experimental work and manuscript preparation under the supervision of Prof. Holger B. Friedrich.

3.

Authors: Mohamed I. Fadlalla and Holger B. Friedrich

Title: The effect of the oxidation environment on the activity and selectivity to aromatics and octenes over cobalt molybdate in the oxidative dehydrogenation of *n*-octane

Status: Published, *Catal. Sci. Technol.*, 2014, 4 (12), 4378 - 4385

Contribution: I carried out all experimental work and manuscript preparation under the supervision of Prof. Holger B. Friedrich.

4.

Authors: Mohamed I. Fadlalla and Holger B. Friedrich

Title: Effect of the cation in the molybdate structure: activity and selectivity in *n*-octane ODH

Status: Manuscript in preparation

Contribution: I carried out all experimental work and manuscript preparation under the supervision of Prof. Holger B. Friedrich.

Conference contribution

1.

Poster presentation, *Synthesis and characterization of molybdates with different cations and molybdenum content for n-octane activation*, CATSA conference, Langebaan, South Africa, 2012.

2.

Poster presentation, *n-Octane activation over magnesium molybdates; effect of C:O ratio*, Europacat conference, Lyon, France, 2013.

3.

Oral presentation, *Magnesium molybdate in ODH of n-octane; effect of C:O ratio and molybdenum content*, CATSA conference, Port Edward, South Africa, 2013.

Content overview

This thesis is formatted as a combination of four technical papers. Each paper consists of an abstract, introduction, experimental section, results and discussion section and a summary and conclusion sections, as well as figures, tables and schemes.

- Chapter one contains an introduction to catalysis, with the emphasis on different techniques for paraffin activation (mainly ODH). The most used catalysts and the properties that influence their activity and selectivity are discussed. Furthermore, this chapter also discusses the different approaches that researchers took to improve activity and selectivity of molybdate based catalysts. This chapter also includes the motivation for this study.
- Chapter two contains the first paper, which deals with the effect of the molybdenum content in magnesium molybdate catalysts in the conversion of *n*-octane and selectivity to value added products. It also discusses the stability of the catalysts under the reaction conditions.
- Chapter three contains the second paper, in which the effect of the carbon to oxygen ratio on the catalyst stability, activity and selectivity was investigated using a magnesium molybdate catalyst with a near stoichiometric ratio of Mg:Mo.
- Chapter four contains the third paper, where the effect of the carbon to oxygen ratio was investigated using a cobalt molybdate catalyst with a ratio of Co:Mo near the stoichiometric ratio, in terms of the catalyst activity, selectivity and stability.
- Chapter five contains the fourth paper (communication), where the effect of the cation in the molybdate was discussed in terms of the catalyst's chemical stability and catalytic performance (activity and selectivity).
- Chapter six provides an overall summary and conclusion of all the chapters.
- Appendix.

Table of content

Chapter one

Paraffin activation and molybdates

Chapter two

Effect of molybdenum content on the activity and selectivity of magnesium molybdate in the oxidative dehydrogenation of n-octane

Chapter three

Effect of the carbon to oxygen ratio on the activity and the selectivity of magnesium molybdate in the oxidative dehydrogenation of n-octane

Chapter four

The effect of the oxidation environment on the activity and selectivity to aromatics and octenes over cobalt molybdate in the oxidative dehydrogenation of n-octane

Chapter five

Effect of the cation in the molybdate structure: activity and selectivity in n-octane ODH

List of figures

(All figures reprinted with permission from the corresponding journals)

List of tables

List of schemes

Acknowledgements

First and foremost I thank god for his blessings, kindness and support throughout my life and in particular during this study. After god the thanks goes to my supervisor Professor Holger B. Friedrich for taking me into his research group, providing me with all I needed to carry out this work and in particular I'm grateful for the freedom he allowed me in designing the focus of this study, under this guidance and using his experience to help me throughout this work.

I'm thankful to the National Research Foundation (NRF), SASOL and THRIP (grant number TP1208035643) for their financial support throughout this study. I thank Mrs J. Govender, Ms C. Nkosi and Mrs C. Marnitz for all their help regarding ordering and payments for all chemicals and parts required for this work.

This work required the use of number of different instruments for different parts of the study. With that in mind I would like to thank the analytical laboratory staff in the Chemistry and Physics school in the University of KwaZulu Natal (Westville campus), with special thanks goes to Mrs A. Naidoo and Mr N. Broomhead for their assistance with ICP-OES and Raman analyses. I'm also thankful to the staff of the electron microscopy unit in the University of KwaZulu Natal (Westville campus), in particular Mr V. Bharart.

I would like to take this opportunity to thank the members of the Catalysis Research Group (CRG) in the University of Kwa-Zulu Natal (Westville campus) for the time and input during the group meetings. I especially thank Mr A. Golandaj and Dr V. Dasireddy for their help with the technical aspects and the scientific aspects of this study through countless fruitful discussions and planning.

To my friends (W. Shalan, A. Ismaeel, N. Osman, V. Duki, M. Pillay, V. Moodly, S. Moodly, L. Komarsamy and S. Sewpersad) thank you for all the support and encouragements.

There are no words to describe how thankful and grateful I'm for my family support. In particular my siblings (Omer, Dina, Razan and Yassin), my aunt (Eiman) and a heart filled thanks to my mother (Hanan). Without god blessing and you guys I will not be who I am, for that and way more please accept my humble thanks and appreciation.

List of abbreviations

BET-surface area measurements	Brunauer, Emmett and Teller-surface area measurements.
C:O ratio	Carbon to oxygen ratio.
GC	Gas chromatography
GJt^{-1}	Gigajouls per tone
CM	Cobalt molybdate.
DH	Dehydrogenation
GHSV	Gas hourly space velocity
HSAB	Hard soft acid base
ICP-OES	Inductively coupled plasma-optical emission spectroscopy.
MvK	Mars and van Kervlen.
MM	Magnesium molybdate.
ODH	Oxidative dehydrogenation.
PGM	Platinum group metals
SEM	Scanning electron microscopy.
STY	Space time yield
TEM	Transmission electron microscopy.
TPD	Temperature programmed desorption.
TPO	Temperature programmed oxidation.
TPR	Temperature programmed reduction.
XRD	X-Ray diffraction.

Chapter one

Paraffin activation and molybdates

1.1) Catalysis

Catalysis and catalysts play a major role in very many different types of industries (*e.g.* pharmaceutical, petrochemical, *etc.*). A catalyst is defined as a "substance that increases the rate at which a chemical system approaches equilibrium, without being consumed in the process" [1]. Any catalyst usually works by providing a new pathway to the products with a lower activation energy [1]. Consequently, there is a great amount of money and man-power focused on development and improvement of catalysts in industry and academia.

Catalysis plays an important role in the energy resources and chemical production fields. Around 75% of chemicals produced make use of catalysis, for example, in the production of intermediates in pharmaceuticals, fibers, dyes and they are also used in crude oil refining and chemical transformation. There are different types or branches of catalysis, which mainly differ is the number of physical states in the reaction or in the choice of catalyst used. The three main branches of catalysis are; heterogeneous, homogeneous and biological catalysis [2]. In heterogeneous catalysis the catalyst is typically a solid, while the reactants are either in a gas or a liquid phase. In homogeneous catalysis the catalyst is in the same physical state as the reactant. Biological catalysis includes the use of enzymes and biologically active catalysts in the laboratories. Each class or branch of catalysis has its advantages and disadvantages. Table 1.1 shows the main advantages and disadvantages between heterogeneous and homogeneous catalysis [3, 4]. The main advantage of heterogeneous catalysis is the fact that the catalyst can be recycled, making this type of catalysis desirable for industrial applications, especially when PGM metals are used. However, the main disadvantages of heterogeneous catalysis are the often harsh reaction conditions and the low selectivity to the target product. On the other hand,

homogeneous catalysis usually gives good selectivity to the target products and the reaction can be carried out under mild conditions. However, the main disadvantage of homogeneous catalysis is the fact that the catalyst cannot easily be recycled.

Table 1.1: Properties comparison between homogeneous and heterogeneous catalysis [5]

Properties	**Homogeneous catalyst**	**Heterogeneous catalyst**
Active centers	Most atoms are active	Only surface atoms are active
Concentration	Low	High
Selectivity	High	Lower
Diffusion problems	Practically absent	Present (mass-transfer-controlled reaction)
Reaction condition(s)	Mild (50-200 °C)	Severe (often > 250 °C)
Applicability	Limited	Wide
Activity loss	Irreversible reaction with the products (cluster formation), poisoning	Sintering of metal crystallites, poisoning
Structure/ stoichiometry	Defined	Undefined
Modification possibility	High	Low
Thermal stability	Low	High
Catalyst separation	Laborious	Simple
Catalyst recycling	Possible	Unnecessary
Cost of catalyst losses	High	Low

1.2) Methods of paraffin activation

There are number of different approaches to activating paraffins that have been developed and are in use since the first quarter of the last century. These processes include steam cracking, dehydrogenation, homogeneous C-H activation and lately oxidative dehydrogenation [6, 7]. This work will discuss steam cracking, dehydrogenation and oxidative dehydrogenation. For homogeneous C-H activation the reader is referred to the reviews by Crabtree [8] and Jun [9], where the thermodynamics and kinetics, organometallic complexes, co-oxidants and metal centers have been discussed among other factors.

1.2.1) Steam cracking

The steam cracking process for the activation of paraffins has been in practice for the past 50 years [6]. In this process paraffin activation takes place through pyrolysis, when the paraffin and steam are heated at high temperature (*e.g.* 800 °C). This method can be used for the activation of a large number of feeds as long as their boiling point is below 600 °C [6]. The steam cracking process can be divided into two parts, which are: part one; the feed and steam are preheated at the initial cracking temperature (*i.e.* 500 – 680 °C). Part two; the stream is fed into the high temperature reactor (*i.e.* 750 – 875 °C), where the steam pyrolysis takes place [10]. At this stage the contact time between the catalyst and feed is maintained at 0.1 to 0.5 seconds to control activity and selectivity. The selectivity in the steam cracking process is influenced by the partial pressure of the reactants as well as the ratio of feed to steam. The product profile in a steam cracking process is dominated by olefins and diolefins, which both are more reactive than the starting material (*i.e.* paraffin). To prevent subsequent reactions leading to a decrease in selectivity and yield of target products, the reactor efluent is quenched during 0.02 – 0.1 seconds [10]. Thereafter, the products are separated by a combination of distillation and absorption processes [6, 10].

There are different classes of catalyst used in the steam cracking process, however, zeolites have been extensively investigated due to their good activity, surface acidity and

shape selectivity (pore structure). There have been a number of modifications carried out on zeolites (mainly ZSM-5) to improve their selectivity and stability [11, 12]. One of the widely investigated modifications is by introduction of phosphorus into ZSM-5 [13, 14]. This modifications improved the selectivity to propylene and butene from *n*-decane cracking, also phosphorus stabilized the aluminum framework of ZSM-5 [14]. Another effect that was investigated is the introduction of iron in ZSM-5 in *iso*-butane cracking. The findings showed that low loading of iron improved activity and selectivity to total olefins formed compared to olefins obtained with high iron loading [12]. The effect of introduction of rare earth metals (*i.e*. La, Ce, Pr, Nd, Sm, Eu or Gd) in ZSM-5 improved the selectivity to olefins, however, the conversion was slightly influenced. Ce/ZSM-5 showed the highest selectivity to olefins, while Nd/ZSM-5 showed the highest selectivity to propene at 600 °C from propane [11].

Steam cracking is the main industrial process used for the production of ethene, however, there are a number of challenges or disadvantages associated with the process. For example, the high reaction temperature translates into high energy (*i.e*. heat) demand. The production of ethene from ethane requires 16 G J t^{-1} and 23 G J t^{-1} when naphtha is used as the feed. The second disadvantage is coke formation on the reactor tube walls, which is burned off by using air and steam. This process requires shut down of the reactor and that has economic implications for the process [6, 15].

1.2.2) Dehydrogenation

During World War II there was a great need for high octane content aviation fuel. That resulted in the use of the dehydrogenation process to take butane to butene over a chromia-alumina catalyst, then butenes were dimerized to octenes and then hydrogenated to octane [7, 16]. This process was developed and commercialized independently by Leuna in Germany and by Universal Oil Products in the USA [7, 17]. In the early 1940's two other plants came on line in England by Universal Oil Products for the same purpose of producing octane from butane, however, they used solid phosphoric acid developed by Schaad and Ipatieff rather than the chromium based catalyst [17]. The second phase of the development was carried out by Houdry where the dehydrogenation process was

carried out below atmospheric pressure with higher per-pass conversion [18]. This process became commercial for the production of butene by the end of World War II. Furthermore, Houdry developed and commercialized the use of a chromium alumimium catalyst for the production of butadiene (Catadiene™) [7, 19]. Due to those developments, a number of companies built dehydrogenation plants, such as: Gulf, DOW and Shell [7]. Houdry did not stop work on dehydrogenation over chromimum alumina catalysts and in the later part of the 1980's they developed and commercialized the dehydrogenation of propane to propylene and isobutene to isobutylene through a cyclic process similar to that in Catadiene™ [7, 19].

In the 1960's dehydrogenation found new horizons in the production of long chain mono-olefins from long chain paraffins. This work was initialized by Haensel [16] in the 1940's where he showed the platinum based catalysts are selective in the dehydrogenation of long chain paraffins. In the 1960's Bloch [20] further improved the selectivity of platinum based catalysts to internal mono-olefins from the dehydrogenation of long chain paraffins by lowering the selectivity to cracked products. Due to the importance of long chain olefins in the production of biodegradable detergents, a number of plants were build starting with the Universal Oil Products process called Pacol™ [21]. By the year 1999 there were 30 commercial platinum based catalyst dehydrogenation plants worldwide targeting the production of long chain olefins [7].

1.2.2.1) Advantages vs disadvantages of dehydrogenation

Dehydrogenation processes offer a number of important advantages that justify all the effort and investment focused on their development and commercialization. The main advantages that are associated with the dehydrogenation process are the high selectivity to target products, in addition, the hydrogen produced by the reaction (abstracted from paraffin) has economic value. However, the dehydrogenation process or reaction suffers from a number of drawbacks or disadvantages, such as those discussed in the following sections.

1.2.2.1.1) Thermodynamic limitation

The conversion in the dehydrogenation reaction is limited by the chemical equilibrium (Eq. 1), where X^2e is the equilibrium conversion, Kp is the equilibrium constant for the dehydrogenation reaction and P is the total absolute pressure. According to Le Chaterlier's equilibrium principle, to force the reaction in a specific direction (towards reactants or products), some reaction conditions must be altered, such as reaction temperature, pressure, concentration of starting material, *etc*. In the case of the dehydrogenation reaction both temperature and pressure can be manipulated to increase conversion [7]. Higher conversion of paraffins is usually achieved at high temperature and low pressure.

$$X_e^2 = \frac{Kp}{Kp+P} \longrightarrow \quad \text{(Eq. 1)}$$

The other point worth mentioning is the relationship between the length of the paraffin chain and the equilibrium constant in the dehydrogenation of those paraffins. Fig. 1.1 shows that the increase in the chain length is accompanied by an increase in the equilibrium constant for paraffins from C_1 to C_{16}. These findings indicate that dehydrogenation of short paraffins requires more energy (*i.e.* heat) than that of long chain paraffins. However, the increase in the equilibrium conversion at high temperatures brings on other limitations, such as deactivation of the catalyst, mainly through coking, and increase in selectivity to side reaction products leading to a decrease in the selectivity and yield of target products [6, 7].

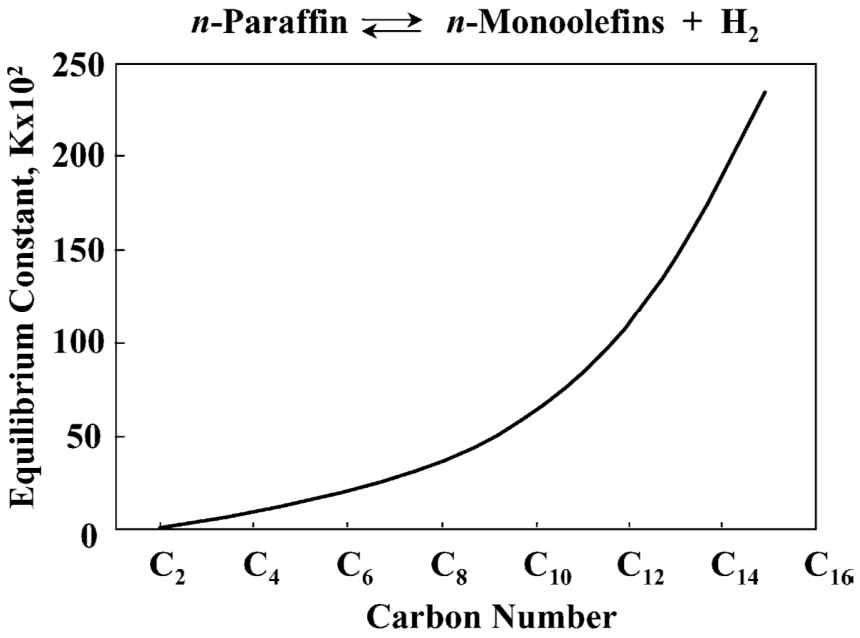

Figure 1.1: The relationship between the carbon number and equilibrium constant in the dehydrogenation process of paraffins at 500 °C. Reprinted from publication [7] with permission from Elsevier.

To improve the life time of the dehydrogenation process, in the early 1970's UOP introduced new technology, the continuous catalyst regeneration (CCR), that allowed continuous use of catalyst or limits shut down periods. This process was mainly used with noble metal based catalysts, because they can withstand harsh reaction conditions, and the use of CCR technology meant it was feasible to design and build large scale dehydrogenation units (UOP Oleflex^{TM}). Another approach or process was developed by Philips petroleum, where a multitubulular reactor design was used and with this system the shutdown period was reduced and there was also no need for a noble metal based catalyst. When the catalyst deactivated due to coking, then banks of the tubes can be removed and serviced while the others are still in place. This technology is known as STAR and now owned by Krupp-Uhde [7]. To overcome the equilibrium limitations of the dehydrogenation process an approach is the use of a selective extractor of the hydrogen produced, which is usually a membrane in what is known as membrane reactors. This technique allows achieving similar conversion and selectivity obtained with conventional reactor setups at lower reaction temperature [22].

1.2.2.1.2) Endothermic reaction

The dehydrogenation reaction is an endothermic reaction [6, 7, 23] and this introduces challenges in industrial applications. For example, the chromium alumina catalysts are heated in part by the heat that is stored in the catalyst during the regeneration step (through coke burn off). Further heat is also provided from the redox cycle of chromium in the catalyst. Due to this character of the dehydrogenation reaction a lot of heat must be provided. Furthermore, the total reactor cycle is as short as 10-20 min, this is mainly due to the availability of the required heat source(s) [7].

Due to the high need for heat and the use of the dehydrogenation reaction in non-cyclic mode, researchers have developed fluidized bed reactors. However, this approach results in a decrease in selectivity to target products due to what is known as a back mixing process that takes place in dense fluidized bed reactors [24].

1.2.2.2) Other approaches to dehydrogenation

There have been different approaches to the direct dehydrogenation of paraffins to olefins and diolefins, these approaches or methodologies are [7];

(1) Halogen assisted dehydrogenation.
(2) Oxidative dehydrogenation.

In the halogen assisted approach paraffins (mainly heavy) are first chlorinated and then dehydrochlorinated to produce olefins. This approach or process was carried out commercially in the past by Hüls and Shell [25]. The other example can be the pyrolysis of methane in the presence of chlorine to produce acetylene and ethylene. The disadvantages associated with this approach are the chemical properties of halogens (*e.g.* corrosion), in addition to the economic impact of the use of high quantities of halogens and the cost associated with recycle and/or disposal of halogens [7].

The second approach relies on the use of oxygen rather than halogens in the dehydrogenation of paraffins. The use of oxygen overcomes the main two disadvantages associated with the use of halogens.

1.2.3) Oxidative dehydrogenation

The oxidative dehydrogenation (ODH) process has gained a lot of interest in the last decade for the activation of paraffins to form olefins and aromatics. Although there are two established industrial processes for paraffin activation (*i.e.* steam cracking and dehydrogenation) to mainly olefins [26], there is still room or rather a need for improvement judging by the disadvantages or drawbacks associated with using those processes.

Oxidative dehydrogenation can be looked at from two points of view [6, 7], which are:

(1) The oxygen introduced into the reaction feed reacts with the hydrogen abstracted from paraffin in the first step of paraffin activation forming water. This shifts the equilibrium towards products formation as described by Le Chatelier's equilibrium principle. Therefore, the equilibrium constraint on the dehydrogenation is removed and higher conversion of paraffins can be achieved. This approach was used commercially in the UOP Styro-puls™ [27, 28] process for the production of styrene through dehydrogenation of ethylbenzene.

(2) Oxygen introduced in the reaction feed can re-oxidize the catalyst after it is reduced by the paraffin during the activation step by the lattice oxygen present in the catalyst. This will lead to the catalyst being stable for a longer period of time and prevent or limit carboneous material (coke) deposits on the catalyst. This method was successfully used for commercializing the production of dibutene from *n*-butenes (Oxo-D process) [6].

1.2.3.1) Advantages of oxidative dehydrogenation

Oxidative dehydrogenation has a number of advantages over the well-established processes (*i.e*. steam cracking and dehydrogenation), these advantages can be described as follows;

(1) Introduction of oxygen to the reaction feed removes the thermodynamic and equilibrium limitation associated with the direct dehydrogenation process [28, 29].
(2) The oxidative dehydrogenation reaction is exothermic, thus less energy is required to carry out the reaction [23], unlike steam cracking and dehydrogenation, where a lot of equipment and different sources of heat must be utilized in order to maintain the high reaction temperature. Thus, since the process is exothermic, the reaction can be carried out at lower temperatures [7, 23, 30].
(3) The presence of oxygen in the feed prevents or limits coke formation on the surface of the catalyst. Therefore, there are no needs for shut-down periods or regeneration steps to remove coke as is the case for steam cracking and dehydrogenation, respectively [31].
(4) The possibility of formation of oxygenated aromatics, which is not possible with steam cracking and dehydrogenation [31, 32].

1.2.3.2) Disadvantages of oxidative dehydrogenation

Oxidative dehydrogenation has a number of disadvantages or areas that require a substantial amount of research to improve the process, these areas are [31]:

(1) The selectivity to target products is lower than desired; this is due to secondary reactions and deep oxidation forming COx.
(2) The main by-product of ODH is COx which is economically less valuable than hydrogen that is produced from dehydrogenation [33].

(3) There are safety precautions that must be in place, since the oxygen-paraffin mixtures can be explosive if not maintained at the right hydrocarbon to oxygen ratios [7].

1.2.3.3) Considerations with oxidative dehydrogenation

Some of the main challenges facing commercializing of ODH are the selectivity to value added products (*e.g.* olefins). This is mainly due to the higher reactivity of paraffin ODH products in comparison to the paraffin. With that in mind, the major need for a selective catalyst in ODH arises to improve the yields of olefins in ODH to make the process economically valuable. Researchers have used or investigated different classes of catalysts, mainly in the ODH of short chain paraffins. However, before discussing the different classes of catalyst, one must consider the different pathways or general mechanisms that can be used to explain the ODH reaction and also what catalyst characteristics can influence catalyst activity and selectivity.

1.2.3.4) Mechanism considerations

There are a number of established and accepted mechanisms in the field of heterogeneous catalysis. The most discussed mechanism for oxidative dehydrogenation is the Mars and van Krevelen (MvK) mechanism, where the selectivity and activity of the catalyst relates to the catalyst reducibility [34, 35]. Paraffins (starting materials) reduce the catalyst and then the oxidant co-fed with the paraffin will re-oxidize the catalyst and the cycle carries on as shown in Fig. 1.2.

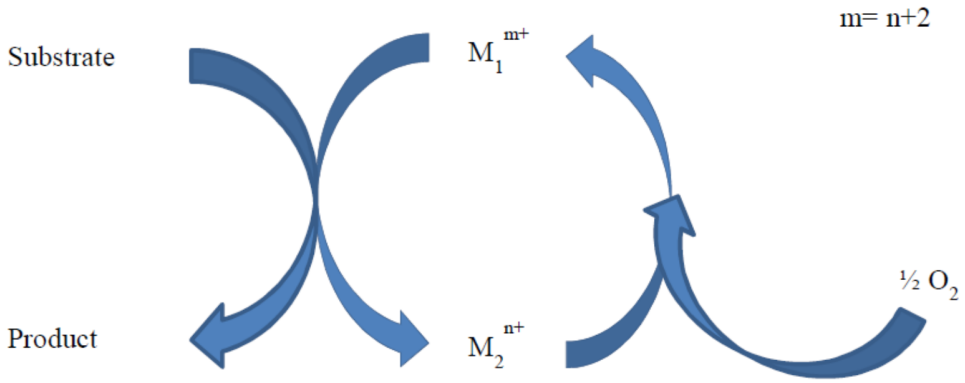

Figure 1.2: Systematic description of the MvK mechanism where oxygen is used as the oxidant in the reaction [34].

This redox mechanism requires a catalyst with high electrical conductivity and good oxygen storage capacity and mobility. The lattice oxygen greatly influences both activity and selectivity of the catalyst. The higher the oxygen storage capacity and mobility, the higher the activity and selectivity as shown in the ODH of propane [36].

Grasselli *et al.* [37, 38] proposed a mechanism (Fig. 1.3) for propane ODH over molybdate based catalysts. The rate-limiting step is the abstraction of the methylene hydrogen which is followed by abstraction of another hydrogen, after which the propylene molecule desorbs from the catalyst surface. The lattice oxygen that carries out the dehydrogenation is replaced by the oxygen in the feed and the catalytic cycle starts again. Therefore, lattice oxygen lability, reducability of the catalyst and electronic densities on the Mo-O bond are important.

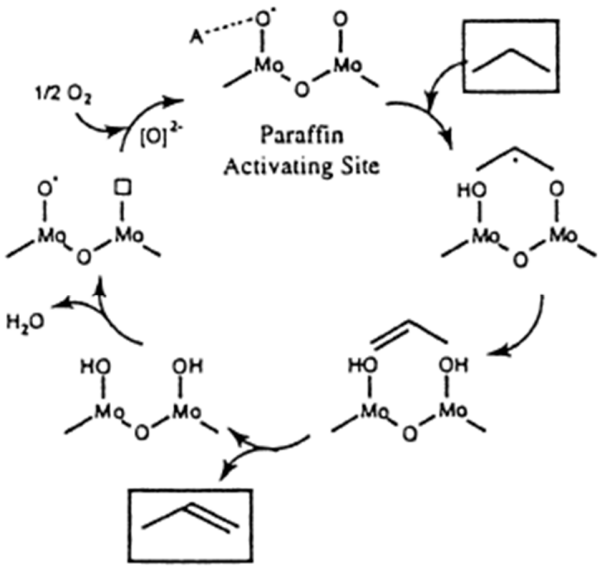

Figure 1.3: Proposed mechanism for the ODH of propane over a molybdate based catalyst. Reprinted from publication [37] with permission from Elsevier.

1.2.3.5) Factors influencing catalyst performance

Catalyst activity (in terms of paraffin conversion) and selectivity (to value added products) in ODH is influenced by a number of factors that differ from one catalyst to another. Some of these factors are: acid-base sites, surface defects, surface oxygen species, metal oxygen bond strength and functionality of the active sites and cooperation between phases. Here some of the main factors are discussed.

1.2.3.5.1) Acid-base character

Transition metals or cations can be classified into hard or soft acids and bases by following the Pearson's hard soft acid base theory (HSAB theory) [39, 40]. Interactions between a soft acid and a soft base are stronger than the interaction between a soft acid and a hard base or *vice versa*. Considering paraffins and olefins, in general, as soft bases, therefore, to increase the desorption rate of the olefin from the catalyst surface, the catalyst must be considered to be a hard acid, in order to prevent deep oxidation of the primary products of ODH to COx. According to HSAB theory, cations in the d^1 group

are hard acids, while cations with empty or full *d* orbitals are considered as soft acids. For example, the selectivity to benzene from propylene increased over metal oxides possessing weak basic or weak acid sites [40]. The acid-base character influences the selectivity of the catalyst through the adsorption/desorption rate. The slower the desorption rate of the primary products, the longer time it spent on the catalyst surface, which could lead to deep oxidation or a sequential reaction to form a secondary product. Similar observations were made by Pillay *et al.* [23] showing that an increase in the molybdenum content in nickel molybdate resulted in an increase in surface acidity and thereafter the COx selectivity increased [23].

1.2.3.5.2) Oxygen-metal bond

The strength of the oxygen-metal bond varies with the different oxidation states of the metal and the degree of reduction of the catalyst. This affects the catalyst activity and selectivity, particularly for a redox active catalyst [6, 41]. The strength of the oxygen-metal bond can be correlated to the activity and selectivity as a volcano plot [41]. For example, taking into consideration the supported vanadium catalyst, when the vanadium loading increases in the support, it becomes more dense and that weakens the oxygen-metal bond and increases activity, however, the selectivity of the catalyst decreases [42, 43]. On the other hand, when vanadium loading is low the oxygen-metal bond becomes stronger and the selectivity of the catalyst to value added products increased. For this reason, silica supported vanadium shows high selectivity because no polymeric vanadium species are present.

Another aspect of the oxygen present in the reaction, in general, is the nature of the oxygen species. Oxygen species that could be present in the ODH reaction can be grouped into two main types, which are: electrophilic and nucleophilic oxygen species. They determine whether activation will be through nucleophilic attack or electrophilic attack. The presence of these species depends on two factors, the oxidation state of the cation and its environment, that in turn influences the polarization strength of the M=O bond. In the case of nucleophilic oxygen species (*i.e.* $\overset{\delta^+}{M}=\overset{\delta^-}{O}$), deprotonation of the paraffin will be favored which will lead to ODH product formation. In the case of weakly

polarized M=O bonds (*i.e.* $\overset{\delta^+}{M}=\overset{\delta^-}{O}$), they will favor homolytic reactions as in the allylic olefin dehydrogenation. The third case is the electrophilic $\overset{\delta^-}{M}=\overset{\delta^+}{O}$ bond and this will lead to attack on conjugated bonds (*i.e.* double bond or aromatic ring) [39].

The choice of oxidant in ODH also influences the activity and selectivity of the catalyst. When CO_2 is used rather than O_2, the activity of the catalyst decreases because the former re-oxidize the reduced catalyst at a much slower rate than the latter. However, the selectivity of the catalyst improved, which could be a result of the mild oxidant that limits deep oxidation and by that improving the overall selectivity [44].

1.2.3.5.3) Surface defects

The presence of surface defects in terms of steps, kinks and/or corners, improves the selectivity and activity of the catalyst compared to a catalyst with no surface defects [45, 46]. This could be due to the cation having vacant coordination positions which can be considered as preferential adsorption sites or Lewis acid sites. For example, the oxidation of *n*-butane to maleic anhydride over $(VO)_2P_2O_7$ shows better activity over less crystalline $(VO)_2P_2O_7$ than over the well crystalline $(VO)_2P_2O_7$ catalyst. Zeng [47] modified and manipulated the surface of molybdenum oxide through chemical etching, but the effect of this treatment was not catalytically investigated. Ressler *et al.* [48-51] investigated the dynamic change on MoO_3 under propane oxidation, showing the structural and chemical changes that took place. Lee *et al.* [52] showed that crystalline molybdenum oxide on the surface of magnesium molybdate decreased the activity of the catalyst in the oxidative dehydrogenation of propane [52].

1.2.3.6) Catalyst classes in oxidative dehydrogenation

With the aim of addressing the selectivity challenge with the ODH of paraffins, researchers have worked with different classes or types of catalyst. Those catalysts vary in both chemical and physical properties.

1.2.3.6.1) Metal oxides

Mixed metal oxides from a catalytic point of view are oxygen containing compounds and materials that contain two or more metallic ions, the ratio of these ions can be varied to obtain specific properties. These materials are widely used in catalysis mainly for their redox behavior and acid base character [53]. Mixed metal oxides are widely used in different catalysis fields; such as, organic synthesis [53], hydrogenation reactions [54], CO oxidation [55], water gas shift reactions [56], steam cracking [57], dehydrogenation and oxidative dehydrogenation [7, 58, 59], to name few. However, when considering industrial implemented catalyst, they usually tend to have more than metals in the catalyst. This is mainly to tailor specific character(s) of the catalyst that may lead to improvement in the activity, selectivity and/or stability. Considering the Pt-Sn/support catalyst that is commercially used for dehydrogenation of light to C_{14} paraffins as an example, the addition of tin is believed to improve activity, selectivity and stability by neutralizing the acidity of the support (usually Al_2O_4, $ZnAl_2O_4$ or $MgAl_2O_4$). Tin also interacts electronically with platinum and that reduces the ensemble effect that favour coke formation. Furthermore, this catalyst is usually promoted with alkali metals and other metals to further modify the surface acidity, morphology and activity with certain percentage of a coke formation on the surface of the catalyst. The support is there to improve the surface area of the catalyst and reduce sintering [60].

Transition metal oxides have been extensively investigated or explored for paraffin activation through ODH. The main advantage of transition metals is that they have different numbers of stable oxidation states that make them ideal in ODH, since they can carry on in a redox cycle [6].

Two metals have been widely investigated in the activation of short chain and, to a lesser extent, medium chain paraffins. These two metals are vanadium and molybdenum.

1.2.3.6.2) Vanadium oxide

The vanadium cation can be in the +3, +4 and +5 oxidation state, which makes it a potential catalyst for ODH due to its redox property. Due to this, among other reasons,

there is a vast number of reports for vanadium-based catalysts in the ODH of paraffins [6, 29, 58, 61-70]. The activity and selectivity of supported vanadium oxide can be influenced and/or tailored by a number of factors, such as:

(1) Vanadium loading on the support.
(2) Choice of support
(3) Dopants

1.2.3.6.2.1) Vanadium loading on the support

To understand the effect of vanadium loading, researchers opted to establish the active site, to determine if it is the V=O bond or the bridging V-O-support bond. Martinez-Huerta *et al.* [71] investigated the activity and selectivity of vanadium on γ-Al_2O_3. Three different catalysts were synthesized (*i.e.* isolated vanadium species, polymeric and V_2O_5 nanoparticles) and extensively characterized. The effect of vanadium loading was mainly on the vanadium species present on the support. At low loading a monolayer of vanadium species or a sub-monolayer is present that is dominated by V-O-support species and there are few terminal V=O species. Increase in vanadium loading results in the catalyst becoming dominated by V-O-V bridging bonds and few terminal V=O and V-O-support species [72]. As the loading of vanadium increases the reduction temperature of the catalyst decreases. In the case of V_2O_5 nanoparticles or isolated vanadium species, the reduction temperature increases due to the difficulty of reducing the vanadium species. Since the high loaded vanadium catalyst is dominated by V-O-V species and that these did not influence the activity, it was concluded that V-O-V is not catalytically active or it is not the active site in the ODH of ethane. Furthermore, since V=O species did not influence the catalyst reduction, it was also ruled out as the active site [72-74]. Thus, the active site was said to be the V-O-support species since it's the only possible species [6].

Elkalifa and Friedrich [58] and Dasireddy *et al.* [75] found a similar effect of vanadium loading where an increase in the vanadium loading resulted in an increase in the conversion of *n*-octane, when vanadium was supported on MgO [58] and hydroxyapatite [75, 76]. Martinez-Huerta *et al.* [71] showed a similar trend in the ODH of ethane over

vanadium on γ-Al_2O_3 and they concluded that this could be due to the vanadium free γ-Al_2O_3 acidic sites at low vanadium loading which promotes deep oxidation to mainly CO. At high vanadium loading, vanadium is responsible for the overall acidity of the catalyst. It's noteworthy that there are still debates and conflicts between theoretical and experimental data on the active site in the vanadium based systems.

1.2.3.6.2.2) Choice of support

The choice of the support plays an important role in the activity and selectivity of vanadium based catalysts. Support type influences the acidity of the catalyst and the interaction between vanadium and support. The structure of the support also plays a role, as do the vanadium species present.

Some of the widely used and investigated supports for vanadium are; γ-Al_2O_3 [77], SiO [78], MgO [58], however, some other supports have been reported such as hydroxyapatite [61, 75, 76] with different cations [76]. Le Bars *et al.* [77] compared the activity and selectivity of vanadium supported on γ-Al_2O_3 and SiO_2. There results showed that vanadium supported on the former shows better activity and selectivity than on the latter. This could be due to better dispersion of vanadium on γ-Al_2O_3 rather than on SiO_2; this makes the vanadium more easily reduced by ethane leading to better activity. The other support that is widely used is MgO, which is basic, stable and inexpensive. On MgO there are various vanadium phases that can exist. Those phases are the metavanadate (MgV_2O_6), pyrovanadate ($Mg_2V_2O_7$) and orthovanadate ($Mg_3V_2O_8$). Those different phases have different selectivity to different products as shown by Elkalifa and Friedrich [58] in the ODH of *n*-octane.

1.2.3.6.3) Molybdenum oxide and molybdate based catalysts

There are many similarities between molybdenum and vanadium based catalysts, therefore they been extensively used in the ODH of mainly light paraffins, with few examples of their use for medium chain paraffins. However, when considering the ODH of light paraffins, vanadium based catalysts tend to show better activity than molybdenum based catalysts [79].

Researchers have found number of factors that can be used to tailor and improve the activity and selectivity of the molybdenum based catalysts, in particular in the ODH of light paraffins. The loading of molybdenum oxide on the support has a great effect on activity and selectivity. Chang *et al.* [80] showed activity increased in propane ODH with increase in the loading, indicating that the surface molybdenum species are active and better than a monolayer dispersion of molybdenum oxide on the surface. However, after a particular molybdenum oxide loading, further increase actually negatively impacted activity which correlated to one or many reasons; the increase in molybdenum content led to the formation of crystalline molybdenum trioxide that hinders the interaction between the paraffin and active phase, in addition to the increase in the size of the molybdenum trioxide crystallite which increased the strength of the Mo=O bond, therefore the reducibility of MoO_3 decreased as did the activity of the catalyst [81, 82]. Another factor that can be considered is that the high loading of molybdenum will result in increased interaction with the support, for example, in the case of the alumina support, the Al_2MoO_4 phase will form which is catalytically less active [83].

Another approach that was taken to improve activity and selectivity of molybdenum oxide catalysts was by doping the catalyst with alkali metals to alter the catalyst's electronic properties [84]. An increase in both loading and basicity of the dopant resulted in decreasing the reducibility of molybdenum trioxide, therefore, the activity of the catalyst decreased. However, the selectivity increased, since the dopant limited or reduced the acidity of MoO_3 [85]. On the opposite end, doping the catalyst with chlorine ions improved the activity of the catalyst by lowering the redox potential of Mo^{4+} making more selective lattice oxygens available for the reaction [6, 86-88].

Since attaining promising results with room for improvement, researchers started introducing cations with molybdenum to form molybdates. Molybdates with different cations gained a great deal of interest in different fields, such as in the battery industry, where they are used as anode material [89], in the coating industry, where they are used on steel [90] and in catalysis, in particular heterogeneous catalysis. For example, iron molybdate is commercially used in the production of formaldehyde from methanol.

One of the important properties of molybdates that gained these materials considerable interest is their structural polymorphism. Considering the two phases of molybdates (α and β-phases) in nickel molybdates and cobalt molybdate (both *iso*-structural) [91]. In the α-phase of cobalt molybdate, both cobalt and molybdenum occupy octahedral geometry that are linked in the corners by oxygen atoms (Fig. 1.4 a). However, in the β-phase molybdenum takes a distorted tetrahedral coordination (Fig. 1.4 b), while cobalt remains in the octahedral geometry. The change from α to β, or *vice versa*, mainly depends on the cation in the molybdate structure. Ehrenberg *et al.* [92] showed the α-$NiMoO_4$ to belong to the monoclinic space group *C2/m*, where both nickel and molybdenum have an octahedral geometry with the oxygen atoms occupying the corners of that octahedral geometry. Smith and Ibers [93] showed the existence of a filled octahedral metal chain and octahedral holes along the *c* axis. In the case of nickel molybdate, the change from α to β takes place at ~750 °C at atmospheric pressure and from β to α from 350 °C upon cooling [23]. In the case of both cobalt molybdate and magnesium molybdate both phases coexists at room temperature and atmospheric pressure. However, careful control of the synthesis conditions (mainly pH and calcination temperature) will favour dominance of a specific phase over the other [94]. Chang *et al.* [80] showed the effect of the pH in the synthesis of magnesium molybdate (Fig. 1.5).

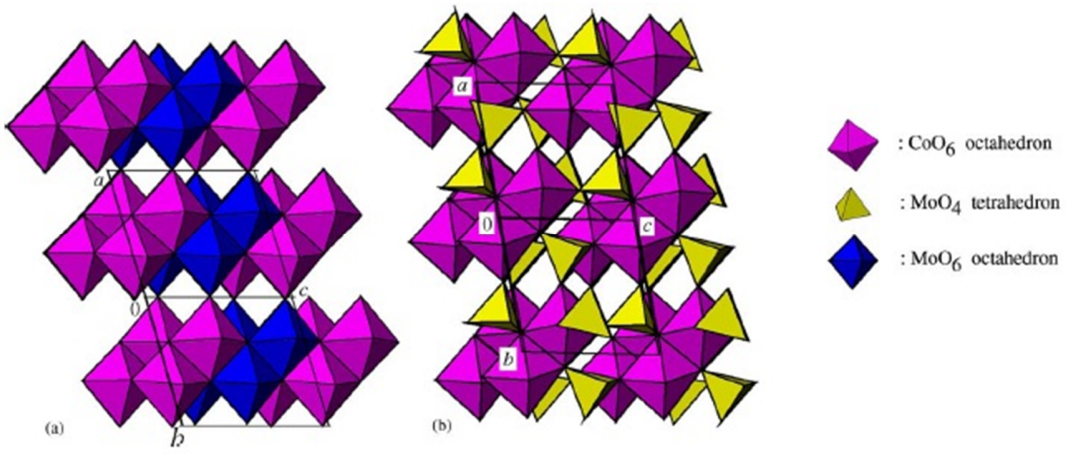

Figure 1.4: The different coordination of molybdenum atoms in the α-phase (a) and β-phase (b) in cobalt molybdate structure. Reprinted (adapted) with permission from [95]. Copyright (1992) American Chemical Society.

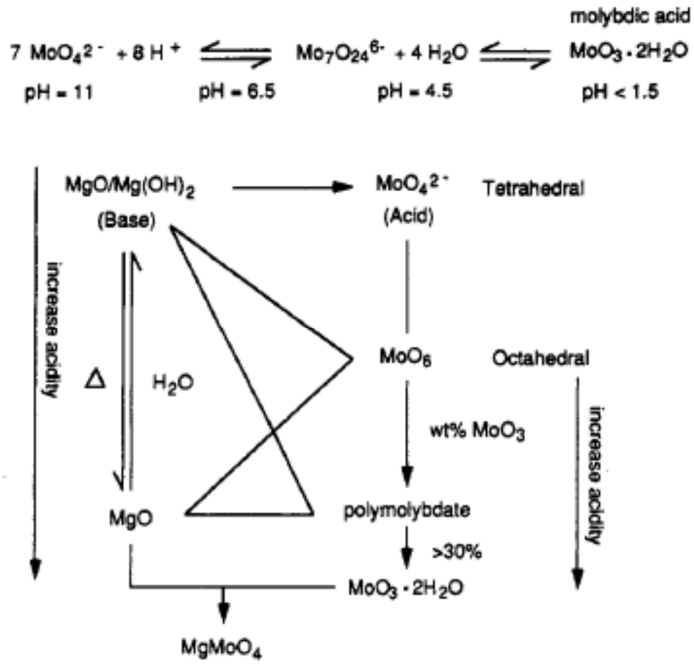

Figure 1.5: Effect of the pH in magnesium molybdate formation and acidity. Reprinted from publication [80] with permission from Elsevier.

In the β-phase of cobalt or nickel molybdate, the geometry of molybdenum is distorted tetrahedral. However, the transformation between α → β is greatly influenced by the

cation. β-Cobalt molybdate can exists at room temperature. The change in the co-ordination of molybdenum usually is accompanied by a change in the physical appearance of the material (*e.g.* α-cobalt molybdate is purple in colour, while β-cobalt molybdate is green). Furthermore, the cation in the molybdate also influences the geometry around molybdenum. In the case of magnesium molybdate, molybdenum occupies a distorted tetrahedral coordination site (isotopic to $ZnMoO_4$) in the α-phase and tetrahedral geometry in the β-phase (isotopic to α-$MnMoO_4$) [96].

In terms of magnesium molybdate structural polymorphisms, Sleight *et al.* [97] showed that molybdenum in $MgMoO_4$ will favour the tetrahedral geometry due to the very close cell dimension in the $MgMoO_4$, compared to $CoMoO_4$ and $NiMoO_4$ where molybdenum can be in octahedral geometry.

1.2.3.6.3.1) Factors influencing activity of molybdates

Molybdate's activity and selectivity can be tailored or altered using different approaches, such as: changing the cation in the molybdates [98], changing the molybdates phase (*i.e.* α and/or β) [23, 99-102], varying the amount of molybdenum in the molybdate and/or doping of the molybdates (mainly with alkaline promoters) [32, 102-104]. Before elaborating further on those approaches, it is important to mention why molybdates are good catalysts, this is mainly due to their lattice oxygen mobility, thermal stability and structure defects [35].

Yoon *et al.* [98] studied a range of molybdates (differing in the choice of cation) in the ODH of propane (Table 1.2). They reported that at low conversion over all molybdates high selectivity to propene was obtained (up to 80%), however, an increase in conversion resulted in an increase in the selectivity to over-oxidation products *(i.e.* COx and acrolein). The effect of the cation was clear in terms of activity and selectivity, where cobalt molybdates showed the highest activity and selectivity, together with magnesium molybdate. On the other hand, nickel molybdate and chromium molybdate are active but not selective. The opposite trend was observed with $MnMoO_4$ where high selectivity and low activity was obtained [98].

Table 1.2: Effect of the cation in molybdates in terms of activity and selectivity in the ODH of propane [98]

Catalyst	**Reaction temperature (°C)**	**Conversion of propane (%)**	**Selectivity of propene (%)**
$MgMoO_4$	500	8.9	67
$CaMoO_4$	500	5.3	83
$SrMoO_4$	500	1.1	62
$BaMoO_4$	500	1.5	78
$ZnMoO_4$	500	0.2	100
$CoMoO_4$	500	10.9	63
$NiMoO_4$	432	12.4	35
$MnMoO_4$	500	1.4	49
$CuMoO_4$	500	3.9	17
$Fe_2MO_3O_{12}$	500	1.3	83

The effect of molybdate polymorphs was showed by Pillay *et al*. [23, 100] where the β-nickel molybdate showed reduced activity but higher selectivity to hexenes in the ODH of *n*-hexane. Indeed, a lot of effort has been focused on stabilizing the β-nickel molybdate at room temperature [105]. Some researchers used excess nickel oxide, some used oxalate precursors and supporting the nickel molybdate on different supports such as silica [105-107]. Zhang *et al.* [108] showed the effect of the synthesis method on the activity and selectivity of $MgMoO_4$. The catalyst prepared by the co-precipitation method showed better activity (conversion of isobutane) and selectivity to isobutene, while the catalyst prepared by a solid state reaction gave high selectivity to cracked products.

The other approach to improve activity and selectivity of molybdates is through dopants and in particular alkali promoters, mainly because molybdates are acidic in general. Use of promoters such as Li, Na, K and Cs improved selectivity to olefins by modifying the surface acidity of the catalyst, making it less acidic or more basic, therefore reducing the

interaction between the primary products and catalyst, which limits over oxidation of those products [32, 85, 109].

Another factor that was studied is the amount of molybdenum trioxide in the molybdate which was also shown to influence both activity and selectivity. In the case of the commercial iron molybdate catalyst in the oxidation of methanol to formaldehyde the Mo:Fe ratio exceeds 5 [110-112]. The "excess" molybdenum trioxide slows down the deactivation of the catalyst, since the catalyst deactivates through molybdenum leaching. In the case of the ODH of light paraffins this effect was extensively investigated with magnesium molybdates [52, 94, 113-115] and to a lesser extent with cadmium molybdate [116] and manganese molybdate [96]. The surface molybdenum trioxide clusters are reported to be necessary for activation of both the hydrocarbon and the oxygen molecule [52, 114]. Ozkan *et al.* [96, 116] attribute the improvement in molybdate based catalyst performance to oxygen spillover between the molybdate phase and the surface molybdenum trioxide phase. Guerrero-Ruiz *et al.* [117] showed that the mobility of oxygen is also influenced by the crystalline structure of the molybdenum trioxide clusters, where the (010) is easier to reduce. The effect of excess molybdenum trioxide in improving the activity and selectivity could be due to a change in the catalyst acidity and/or a molybdenum trioxide monolayer coverage that improves activity [52, 94, 99], where the activity of the catalyst increased with increase in the acidity of the catalyst brought on by increasing the molybdenum content. A further reason could be the improved redox cycle between Mo^{5+} and Mo^{6+} that improves activity and selectivity of the catalyst. Zhang *et al.* [108] reported that isobutane oxidation over magnesium molybdate seems to require surface tetrahedral Mo^{6+} sites, where there is MoO_3 or octahedral Mo^{6+}; probably Mo^{5+} or coordinately unsaturated surface sites could be the reason for the activity of the catalyst. It is important to note that after a certain ratio of cation to molybdenum the catalyst activity decreases, mainly due to the formation of molybdenum trioxide crystallites that are inactive and coverage of the catalyst surface with molybdenum dioxide that is catalytically inactive [52, 113].

1.4) Motivation for this study

Lately there has been an increase in the number of gas to liquid (GTL) and coal to liquid (CTL) plants worldwide [23] and more are being planned. This is expected to be accompanied by an increase in the already abundant linear paraffins (especially medium chain length paraffins). Therefore, there have been reports emerging in the literature for the ODH of medium chain paraffins, like *n*-hexane [23, 69, 100], *n*-octane [29, 58, 61, 62, 75, 76, 118] and *n*-decane [119, 120]. However, no reports were found dealing with the use of molybdates in the activation of *n*-octane through ODH.

Molybdates are known to be active catalysts in the ODH of short chain paraffins and *n*-hexane as shown by Yoon *et al.* [94, 98, 99, 121] and Pillay *et al.*[23, 100], respectively. Both authors showed that molybdates can be selective to value-added products, mainly olefins, of the corresponding paraffin. This work focuses on investigating the activity and selectivity of molybdates in the ODH of *n*-octane. Yoon *et al.* [98] demonstrated the effect of the cation in the molybdate structure in its activity, along with selectivity, in the ODH of short chain paraffins. Therefore, different molybdates with different cations are the subject of this study. These are: magnesium molybdate and cobalt molybdate. Magnesium molybdate and cobalt molybdates were shown by Yoon *et al.* [121] and Lee *et al.* [52] to have good activity and selectivity to olefins in the ODH of short chain paraffins, thus, they are investigated in the ODH of *n*-octane. Another focus point of this work is to investigate the effect of the molybdenum content on the catalyst performance. This effect was investigated in the ODH of short chain paraffins [114] and in iron molybdate catalysts for methanol oxidation [111]. These studies showed that there is a point after which the excess molybdenum content negatively impacts the catalyst. Magnesium molybdate catalysts with different molybdenum content were used to investigate this effect and to determine the ideal ratio of Mg:Mo in the ODH of *n*-octane. Elkalifa and Friedrich [62] and Pillay *et al.* [100] showed that the carbon to oxygen ratio has a great influence of the activity and selectivity of the catalyst in the ODH of *n*-octane and *n*-hexane, respectively. Thus, great effort is focused on investigating this effect over both molybdates, using oxygen environments ranging from oxygen lean to oxygen rich and accordingly studying the activity and selectivity of the catalysts to value-added

products (*i.e.* octenes and C8 aromatics). This study will also focus on comparing the effect of the cation in the molybdate structure in terms of activity and selectivity at *iso*-thermal and *iso*-conversion conditions.

This study also focused on characterization of the used catalysts in order to have a better understanding of the effect of the carbon to oxygen ratio on the catalysts chemical stability.

1.5) References

[1] G.C. Bond, Heterogeneous Catalysis: principles and applications, Oxford University Press, London, 1974.
[2] J.T. Richardon, Principle of catalyst development, Plenum Press, New York, 1989.
[3] D. Shriver, P. Atkins, Inorganic chemistry, Oxford University Press, London, 1999.
[4] G.C. Bond, Principle of catalysis, The Chemical Society, London, 1972.
[5] J. Hagen, Industrial catalysis: A practical approach, second ed., Wiley-VCH, Weinheim, 2006.
[6] C.A. Gärtner, A.C. van Veen, J.A. Lercher, ChemCatChem., 5 (2013) 3196-3217.
[7] M.M. Bhasin, J.H. McCain, B.V. Vora, T. Imai, P.R. Pujadó, Appl. Catal., A: Gen., 221 (2001) 397-419.
[8] R.H. Crabtree, Dalton Trans., (2001) 2437-2450.
[9] C.-H. Jun, Chem. Soc. Rev., 33 (2004) 610-618.
[10] H. Zimmermann, R. Walzl, Ullmann's Encyclopedia of Industrial Chemistry, Weinheim, Wiley-VCH, 2000.
[11] W. Xiaoning, Z. Zhen, X. Chunming, D. Aijun, Z. Li, J. Guiyuan, J. Rare Earths, 25 (2007) 321-328.
[12] J. Lu, Z. Zhao, C. Xu, P. Zhang, A. Duan, Catal. Commun., 7 (2006) 199-203.
[13] G. Zhao, J. Teng, Z. Xie, W. Jin, W. Yang, Q. Chen, Y. Tang, J. Catal., 248 (2007) 29-37.
[14] G. Jiang, L. Zhang, Z. Zhao, X. Zhou, A. Duan, C. Xu, J. Gao, Appl. Catal., A: Gen., 340 (2008) 176-182.
[15] A.S. Bodke, D.A. Olschki, L.D. Shmidt, E. Ranzi, Science, 285 (1999) 712-715.
[16] G.F. Hornaday, F.M. Ferrell, G.A. Mills, Manufacture of mono- and diolefins from paraffins by catalytic dehydrogenation, in: Advances in petroleum Chemistry and Refining,Vol. 4, Interscience, Pans, 1961.
[17] V.N. Ipatieff, R.E. Schaad, Ind. Eng. Chem., 30 (1938) 596-599.
[18] R.G. Craig, D.C. Spence, in: R.A. Meyers (Ed.), Handbook of Petroleum Processes, McGraw-Hill, New York, 1986.
[19] A.L. Waddams, Chemicals from Petroleum, Gulf Publishing Company, Houston, 1978.

[20] H.S. Bloch, Catalytic dehydrogenation of paraffinic hydrocarbons, U.S. Patent number 3,448,165, 1969.
[21] R.C. Berg, B.V. Vora, Detergent alkylate, in: Encyclopedia of chemical processing and Design, Marcel Dekker, New York, 1982.
[22] P. Ciavarella, D. Casanave, H. Moueddeb, S. Miachon, K. Fiaty, J.A. Dalmon, Catal. Today 67 (2001) 177-184.
[23] B. Pillay, M.R. Mathebula, H.B. Friedrich, Appl. Catal., A: Gen., 361 (2009) 57-64.
[24] D. Sanfilippo, F. Buonomo, G. Fusco, I. Miracca, S. Spa, V. Maritano, G. R.Kotelnikov, Yarsintez, P. Oktyabrya, Stud. Surf. Sci. Catal., Elsevier, 1998.
[25] S.W. Benson, Conversion of methane, U.S. Patent number 4,199,533, 1980.
[26] F. Cavani, F. Trifirò, Appl. Catal., A: Gen., 88 (1992) 115-135.
[27] R. Lodeng, P. Soraker, Reactor for catalytic dehydrogenation of hydrocarbons with selective oxidation of hydrogen, U.S. Patents number 5,997,826A, 1999.
[28] J.G. Tsikoyiannis, D.L. Stern, R.K. Grasselli, J. Catal., 184 (1999) 77-86.
[29] H.B. Friedrich, A.S. Mahomed, Appl. Catal., A: Gen., 347 (2008) 11-22.
[30] G. Centi, F. Cavani, F. Trifiro, Selectivity Oxidation by Heterogeneous Catalysis, Kluwer Academic/Plenum publishers, New York, 2001.
[31] J. Vila, F. Sapina, E. Martinez, V. Cortes, J. Podobinski, Contrib. Sci., 4 (2008) 223-229.
[32] J. Barrault, C. Batiot, L. Magaud, M. Ganne, Selective oxidation of propane into oxygenated compounds over promoted nickel-molybdenum catalysts, in: R. K. Grasselli, S. T. Oyama, A. M. Gaffney and J. E. Lyons (Eds), Stud. Surf. Sci. Catal., Elsevier, 1997.
[33] F. Cavani, F. Trifirò, Catal. Today, 24 (1995) 307-313.
[34] P. Mars, D.W. van Krevelen, Chem. Eng. Sci. 3, Supplement 1 (1954) 41-59.
[35] A. Kaddouri, R. Del Rosso, C. Mazzocchia, P. Gronchi, D. Fumagalli, J. Therm. Anal. Calorim., 66 (2001) 63-78.
[36] R. Del Rosso, A. Kaddouri, R. Anouchinsky, C. Mazzocchia, P. Gronchi, P. Centola, J. Mol. Catal. A: Chem., 135 (1998) 181-186.
[37] R.K. Grasselli, Catal. Today, 49 (1999) 141-153.
[38] D.L. Stern, R.K. Grasselli, J. Catal., 167 (1997) 550-559.
[39] G.E. Vrieland, C.B. Murchison, Appl. Catal., A: Gen., 134 (1996) 101-121.
[40] T. Seiyama, M. Egashira, T. Sakamoto, I. Aso, J. Catal., 24 (1972) 76-81.
[41] R. Grasselli, Top. Catal., 21 (2002) 79-88.
[42] P. Concepción, A. Galli, J.M.L. Nieto, A. Dejoz, M.I. Vazquez, Top. Catal., 3 (1996) 451-460.
[43] O.R. Evans, A.T. Bell, T.D. Tilley, J. Catal., 226 (2004) 292-300.
[44] S. Wang, Z.H. Zhu, Energy & Fuels, 18 (2004) 1126-1139.
[45] F. Cavani, F. Trifirò, Catal. Today, 51 (1999) 561-580.
[46] L.-T. Weng, B. Delmon, Appl. Catal., A: Gen., 81 (1992) 141-213.
[47] H.C. Zeng, Inorg. Chem., 37 (1998) 1967-1973.
[48] T. Ressler, O. Timpe, T. Neisius, J. Find, G. Mestl, M. Dieterle, R. Schlögl, J. Catal., 191 (2000) 75-85.
[49] T. Ressler, A. Walter, J. Scholz, J.P. Tessonnier, D.S. Su, J. Catal., 271 (2010) 305-314.

[50] T. Ressler, J. Wienold, R. E. Jentoft, F. Girgsdies, Eur. J. Inorg. Chem., 2003 (2003) 301-312.
[51] T. Ressler, J. Wienold, R.E. Jentoft, T. Neisius, J. Catal., 210 (2002) 67-83.
[52] K.H. Lee, Y.S. Yoon, W. Ueda, Y. Moro-oka, Catal. Lett. 46 (1997) 267-271.
[53] M.B. Gawande, R.K. Pandey, R.V. Jayaram, Catal. Sci. Tech., 2 (2012) 1113-1125.
[54] S.U. Sonavane, R.V. Jayaram, Synth. Commun., 33 (2003) 843-849.
[55] G. Avgouropoulos, T. Ioannides, H. Matralis, J. Batista, S. Hocevar, Catal. Lett., 73 (2001) 33-40.
[56] Y. Li, Q. Fu, M. Flytzani-Stephanopoulos, Appl. Catal. B, 27 (2000) 179-191.
[57] H. Noichi, A. Uddin, E. Sasaoka, Fuel Process. Technol., 91 (2010) 1609-1616.
[58] E.A. Elkhalifa, H.B. Friedrich, Appl. Catal., A: Gen., 373 (2010) 122-131.
[59] L.M. Madeira, M.F. Portela, Appl. Catal., A: Gen., 281 (2005) 179-189.
[60] D. Sanfilippo, I. Miracca, Catal. Today, 111 (2006) 133-139.
[61] V.D.B.C. Dasireddy, H.B. Friedrich, S. Singh, Appl. Catal., A: Gen., 467 (2013) 142-153.
[62] E. A. Elkhalifa, H. B. Friedrich, Catal. Lett., 141 (2011) 554-564.
[63] N. Ballarini, F. Cavani, C. Cortelli, S. Ligi, F. Pierelli, F. Trifirò, C. Fumagalli, G. Mazzoni, T. Monti, Top. Catal., 38 (2006) 147-156.
[64] T. Blasco, J.M.L. Nieto, Appl. Catal., A: Gen., 157 (1997) 117-142.
[65] T. Blasco, J.M.L. Nieto, A. Dejoz, M.I. Vazquez, J. Catal., 157 (1995) 271-282.
[66] S.R.G. Carrazán, C. Peres, J.P. Bernard, M. Ruwet, R. Ruiz, B. Delmon, J. Catal., 158 (1996) 452-476.
[67] M.A. Chaar, D. Patel, M.C. Kung, H.H. Kung, J. Catal., 105 (1987) 483-498.
[68] K. Chen, A.T. Bell, E. Iglesia, J. Phys. Chem. B, 104 (2000) 1292-1299.
[69] H.B. Friedrich, N. Govender, M.R. Mathebula, Appl. Catal., A: Gen., 297 (2006) 81-89.
[70] C. Téllez, M. Abon, J.A. Dalmon, C. Mirodatos, J. Santamarí a, J. Catal, 195 (2000) 113-124.
[71] M.V. Martínez-Huerta, X. Gao, H. Tian, I.E. Wachs, J.L.G. Fierro, M.A. Bañares, Catal. Today, 118 (2006) 279-287.
[72] H. Tian, E.I. Ross, I.E. Wachs, J. Phys. Chem. B, 110 (2006) 9593-9600.
[73] X. Gao, M.A. Bañares, I.E. Wachs, J. Catal., 188 (1999) 325-331.
[74] Z. Zhao, X. Gao, I.E. Wachs, J. Phys. Chem. B, 107 (2003) 6333-6342.
[75] V.D.B.C. Dasireddy, S. Singh, H.B. Friedrich, Appl. Catal., A: Gen., 421–422 (2012) 58-69.
[76] V.D.B.C. Dasireddy, S. Singh, H.B. Friedrich, Appl. Catal., A: Gen., 456 (2013) 105-117.
[77] J. Le Bars, A. Auroux, M. Forissier, J.C. Vedrine, J. Catal., 162 (1996) 250-259.
[78] P. Knotek, L. Čapek, R. Bulánek, J. Adam, Top. Catal., 45 (2007) 51-55.
[79] E. Heracleous, M. Machli, A.A. Lemonidou, I.A. Vasalos, J. Mol. Catal. A: Chem., 232 (2005) 29-39.
[80] S.C. Chang, M.A. Leugers, S.R. Bare, J. Phys. Chem., 96 (1992) 10358-10365.
[81] K. Chen, S. Xie, A.T. Bell, E. Iglesia, J. Catal., 198 (2001) 232-242.
[82] K. Chen, S. Xie, E. Iglesia, A.T. Bell, J. Catal., 189 (2000) 421-430.

[83] E. Heracleous, A.F. Lee, I.A. Vasalos, A.A. Lemonidou, Catal. Lett., 88 (2003) 47-53.
[84] F. Cavani, N. Ballarini, A. Cericola, Catal. Today, 127 (2007) 113-131.
[85] S.N. Koc, G. Gurdag, S. Geissler, M. Guraya, M. Orbay, M. Muhler, J. Mol. Catal. A: Chem., 225 (2005) 197-202.
[86] R.B. Watson, S.L. Lashbrook, U.S. Ozkan, J. Mol. Catal. A: Chem., 208 (2004) 233-244.
[87] C. Liu, U.S. Ozkan, J. Mol. Catal. A: Chem., 220 (2004) 53-65.
[88] C. Liu, U.S. Ozkan, J. Phys. Chem. A, 109 (2005) 1260-1268.
[89] M. Wakihara, H. Ikuta, Y. Uchimoto, in: W. Schalkwijk, B. Scrosati (Eds.), Advances in Lithium-Ion Batteries, Springer US, 2002.
[90] V. Karpakam, K. Kamaraj, S. Sathiyanarayanan, G. Venkatachari, S. Ramu, Electrochimica Acta 56 (2011) 2165-2173.
[91] A. Kaddouri, E. Tempesti, C. Mazzocchia, Mater. Res. Bull., 39 (2004) 695-706.
[92] H. Ehrenberg, I. Svoboda, G. Wltschek, M. Wiesmann, F. Trouw, H. Weitzel, H. Fuess, J. Magn. Magn. Mater., 150 (1995) 371-376.
[93] G.W. Smith, J.A. Ibers, Acta Crystallog., 19 (1965) 269-275.
[94] Y.S. Yoon, K. Suzuki, T. Hayakawa, S. Hamakawa, T. Shishido, K. Takehira, Catal. Lett., 59 (1999) 165-172.
[95] K. Eda, Y. Uno, N. Nagai, N. Sotani, M. Stanley Whittingham, J. Solid State Chem., 178 (2005) 2791-2797.
[96] U.S. Ozkan, M.R. Smith, S.A. Driscoll, J. Catal., 134 (1992) 24-35.
[97] A.W. Sleight, B.L. Chamberland, J.F. Weiher, Inorg. Chem., 7 (1968) 1093-1098.
[98] Y.S. Yoon, N. Fujikawa, W. Ueda, Y. Moro-oka, K.W. Lee, Catal. Today, 24 (1995) 327-333.
[99] Y.S. Yoon, W. Ueda, Y. Moro-oka, Catal. Lett., 35 (1995) 57-64.
[100] B. Pillay, M.R. Mathebula, H.B. Friedrich, Catal. Lett., 141 (2011) 1297-1304.
[101] J. L. Brito, A. L. Barbosa, J. Catal., 171 (1997) 467-475.
[102] A. Calafat, F. Vivas, J.n.L. Brito, Appl. Catal., A: Gen., 172 (1998) 217-224.
[103] S.N. Koc, G. Gurdag, S. Geissler, M. Muhler, Ind. Eng. Chem.Res., 43 (2004) 2376-2381.
[104] F. Cavani, M. Koutyrev, F. Trifirò, Catal. Today, 28 (1996) 319-333.
[105] C. Mazzocchia, F. Di Renzo, C. Aboumrad, G. Thomas, Solid State Ionics, 32–33, Part 1 (1989) 228-233.
[106] C.R. Dias, R. Zãvoianu, M. Farinha Portela, Catal. Commun., 3 (2002) 85-90.
[107] C. Mazzocchia, A. Kaddouri, R. Anouchinsky, M. Sautel, G. Thomas, Solid State Ionics 63–65 (1993) 731-735.
[108] Y.J. Zhang, I. Rodríguez-Ramos, A. Guerrero-Ruiz, Catal. Today, 61 (2000) 377-382.
[109] L. Leveles, S. Fuchs, K. Seshan, J.A. Lercher, L. Lefferts, Appl. Catal., A: Gen., 227 (2002) 287-297.
[110] A.P.V. Soares, M.F. Portela, A. Kiennemann, Catal. Rev., 47 (2005) 125-174.
[111] A.P.V. Soares, M. Farinha Portela, A. Kiennemann, L. Hilaire, J.M.M. Millet, Appl. Catal., A: Gen., 206 (2001) 221-229.
[112] M.P. House, A.F. Carley, M. Bowker, J. Catal., 252 (2007) 88-96.

[113] J. Miller, N. Jackson, L. Evans, A. Sault, M. Gonzales, Catal. Lett., 58 (1999) 147-152.
[114] W. Ueda, K. H. Lee, Y. S. Yoon, Y. Moro-oka, Catal. Today, 44 (1998) 199-203.
[115] L.E. Cadus, M.F. Gomez, M.C. Abello, Catal. Lett., 43 (1997) 229-233.
[116] U.S. Ozkan, R.C. Gill, M.R. Smith, Appl. Catal. A: Gen., 62 (1990) 105-117.
[117] A. Guerrero-Ruiz, I. Rodriguez-Ramos, P. Ferreira-Aparicio, M. Abon, J.C. Volta, Catal. Today, 32 (1996) 223-227.
[118] M. Narayanappa, V.D.B.C. Dasireddy, H.B. Friedrich, Appl. Catal., A: Gen., 447–448 (2012) 135-143.
[119] S. Pradhan, J.K. Bartley, D. Bethell, A.F. Carley, M. Conte, S. Golunski, M.P. House, R.L. Jenkins, R. Lloyd, G.J. Hutchings, Nat. Chem., 4 (2012) 134-139.
[120] S. Pradhan, R. Lloyd, J.K. Bartley, D. Bethell, S. Golunski, R.L. Jenkins, G.J. Hutchings, Chem. Sci., 3 (2012) 2958-2964.
[121] Y. Yoon, W. Ueda, Y. Moro-oka, Top. Catal., 3 (1996) 265-275.

Chapter two

Effect of molybdenum content on the activity and selectivity of magnesium molybdate in the oxidative dehydrogenation of n-octane

Abstract

The oxidative dehydrogenation of *n*-octane was investigated using magnesium molybdate catalysts in a continuous flow fixed bed reactor at a carbon : oxygen ratio of 8:3 in a temperature range from 350 to 500 °C. Four magnesium molybdate catalysts with different molybdenum content were synthesised by the co-precipitation method (Mg:Mo, coded MM0.87, MM0.98, MM1.06 and MM1.25). The catalysts were characterized by XRD, BET-surface area measurements, ICP-OES, SEM, IR, Raman spectroscopy and temperature programmed reduction and oxidation analysis. The excess molybdenum in the catalyst was in the MoO_3 phase as determined by XRD and Raman spectroscopy. The surface morphology of the catalyst changed with increase in the molybdenum content and the surface area also increased (slightly) with molybdenum content. The excess molybdenum improved the activity of the catalyst (*i.e. n*-octane conversion), especially at lower temperatures (below 450 °C), due to the lower reduction temperature of MoO_3 compared to the magnesium molybdate phase. The main effect of molybdenum content was determined to be altering the acidity of the catalyst and that in turn affected the selectivity of the catalyst. The *iso*-conversion (~24%) results at 500 °C showed that the highest C8 value added products (*i.e.* octenes and aromatics) selectivity was obtained over MM0.98 and MM1.06, amounting to 64% and 66%, respectively. Highest selectivity to COx was obtained over MM0.87 and MM1.25. Characterization of the used catalysts by Raman spectroscopy showed that the catalysts undergo a degree of reduction, mainly the MoO_3 phase.

Keywords: Magnesium molybdate, n-octane ODH, molybdenum trioxide, octenes selectivity.

2.1) Introduction

Activation of medium chain length (C_6 - C_{12}) *n*-paraffins is becoming an interesting topic both academically and industrially, due to mainly; (1) the increase in the number of gas to liquid (GTL) and coal to liquid (CTL) plants worldwide, which causes the amount of *n*-

paraffins to increase and (2) paraffins can be used as a starting materials for the production of economically and industrially important feed-stocks, such as olefins and aromatics [1-4].

In the past years activation of paraffins to products of equal chain length was mainly carried out by dehydrogenation: for example butane to butene [5-7]. However, this process suffers from two main disadvantages, firstly the reaction is endothermic requiring high reaction temperatures, which in turn promotes thermal cracking of the paraffins to lighter paraffins [3, 5] and requires a frequent regeneration step due to the catalyst being deactivated by coke formation [3, 5, 8]. Oxidative dehydrogenation (ODH) is an alternate route for paraffin activation that can overcome the two disadvantages of the dehydrogenation route. Introduction of oxygen in the reaction mixture leads the reaction to become exothermic (lowering the reaction temperature) and there is no need for a regeneration step, since the oxygen in the feed is removing or limiting coke formation [9-11]. However, the main challenge in ODH is the fact that the products of paraffin activation (such as olefin and aromatics) in an oxidative environment are more reactive than the starting material [3]. Thus, these primary products can react further to yield undesired products (*i.e.* cracked products and COx). However, depending on the catalyst choice, ODH can produce oxygenated products [12] unlike dehydrogenation.

Different groups of catalysts have been extensively investigated for the activation of hydrocarbons through dehydrogenation and partial oxidation reactions [1, 2, 10, 13-17]. Molybdate based catalysts with different cations have also been extensively explored for short chain paraffin activation [18]. Thus, magnesium molybdate has been investigated for the activation of light hydrocarbons, such as propane [14-24] and butane [25-27]. The dominant product from both C_3 and C_4 activation is the corresponding olefin. In addition, magnesium molybdate was also used in the activation of ethylbenzene [14, 28, 29]. Furthermore, Yoon *et al.* [18] compared the activity of different cations in the molybdates structure in the oxidative dehydrogenation of propane, where the most activity and highest selective (to propene) was found over the magnesium and cobalt molybdate.

The presence of excess molybdenum in the magnesium molybdate catalyst for the activation of propane gave higher activity, while maintaining the selectivity to propene [24]. Similar observations were made with $MnMoO_4$-MoO_3 [30] and $CdMoO_4$-MoO_3 [31] in the oxidation of butane. The effect of excess of molybdenum was extensively investigated to understand how excess molybdenum improves the catalytic activity [14-16, 22, 24]. There are different

reasons in literature to explain the effect of excess MoO_3. Ozkan *et al.* [30, 31] attributed the improved catalytic performance to oxygenspill over mechanism between the two phases (molybdate and molybdenum trioxide). Guerrero-Ruiz *et al.*[32] showed that the oxygen mobility associated with the MoO_3 was effected by the different faces present, where the (010) face gave the highest oxygen mobility. In contrast, Moro-oka and co-workers [16, 33] and Yoon *et al.* [15] believe the activity resulted from change in the catalyst acidity and/or the formation of a molybdenum trioxide monolayer covering the magnesium molybdate promoting higher activity [16]. Catalyst treatment resulted in a magnesium rich surface that showed lower activity, and the molybdenum rich surface improved the activity. However, high molybdenum concentration on the surface results in crystalline molybdenum trioxide, which is catalytically inactive [16]. The catalyst treatment (basic and acidic) was believed to change the catalyst phase composition, which could also have an effect on the catalyst activity [16, 33]. Furthermore, Lee *et al.* [16] believe that the catalyst undergoes surface reduction, which increases the Lewis acid sites, increasing the rate of reaction of the methylene C-H bond, which is the rate determining step. On the other hand, Cadus *et al.* [24] and Miller *et al.* [14] believe that a synergetic effect is resultant from a redox cycle between the Mo^{5+} and Mo^{6+} ions. The modification in the redox cycle was confirmed by EPR analysis where Mo^{5+} was detected in the used catalyst. Zhang *et al.* [26] indicated that the Mo^{5+} improves the activity since its coordinately unsaturated. Due to the high selectivity to olefins shown by magnesium molybdate in the ODH of light paraffins, we focused on using magnesium molybdate in the ODH of *n*-octane (which was not reported previously to the best of our knowledge). In addition, the effect of excess molybdenum was investigated by preparing four catalysts with different molybdenum content. Moreover, the used catalysts were characterized to understand the effect of the reaction conditions on the catalyst phase composition and textural characteristics.

2.2) Experimental

2.2.1) Catalyst preparation

Four magnesium molybdate (MM) catalysts with different molybdenum content were prepared by a co-precipitation method adopted from literature [26]. Two separate solutions of magnesium nitrate (Sigma-Aldrich) (0.5 M) and ammonia heptamolybdenum nitrate (Merck) solution (0.5 M) were prepared in de-ionized water. The pH of the molybdenum solution was adjusted to pH 6 using aqueous ammonia (Saarchem) under continuous stirring. The

magnesium nitrate was added drop-wise at room temperature. After complete addition of the magnesium nitrate solution, the mixture was heated to 90 °C and maintained until a white slurry was formed. The slurry was then dried in the oven at 110 °C for 12 h to yield the magnesium molybdate precursor. The precursor was then calcined at 550 °C for 2 h to yield the magnesium molybdate catalyst. The different ratios of Mg:Mo were prepared by varying the concentration of the initial molybdenum solution.

2.2.2) Catalyst characterization

The phase(s) present in the different catalysts were analysed by X-Ray diffraction (XRD) utilizing a Bruker D8 Advance diffractometer equipped with an Anton Paar XRK 900 sample chamber. The analyses were carried out at 2θangle window from 10 – 70θ, 40 kV and 40 mA and a Cu radiation source. The surface areas of the catalysts were determined by BET surface area measurements. All samples were degassed in a Micromeritics Sample Prep 060 under nitrogen flow at 200 °C overnight. The samples were then analysed using a Micromeritics Tristar II. Infra-red (IR) spectra of the catalysts were obtained utilizing a PerkinElmer Precisely spectrometer equipped with a universal attenuance total reflection (ATR) sample holder. Raman analyses were carried out using an Advantage 532 series spectrometer with Nuspec software.

The molar ratios of magnesium to molybdenum were determined by inductively coupled plasma-optical emission spectroscopy (ICP-OES) using a PerkinElmer Precisely Optima 5300 DV. The surface morphology of the catalysts was viewed using a Zeiss ultra plus scanning electron microscope (SEM). Samples were carbon coated prior to imaging. Temperature programmed reduction (TPR) oxidation (TPO) and NH_3 desorption (TPD) were carried out using a Micromeritics AutoChem II. The TPR/TPO/TPR analysis was carried out by heating the catalyst under argon flow at 400 ^{O}C for 80 min and thereafter reduction analysis started by using 5% H_2 in argon as a reducing gas with flow rate of 30 mL/min. The TPO analysis was carried over the same sample by cooling it down to 80 ^{O}C and a similar method (as for TPR) was followed, the only difference was the analysis gas which is 5% O_2 in argon. After that another TPR (as details above) was carried out. The deconvolution of the TPR/TPO profile was done by the method illustrated by Webster [34] . The NH_3-TPD analysis method was identical to a method reported previously [9]. To calibrate the TPR profile, a gas mixture of 5 % H_2 was passed through the TCD detector with a difference flow rate of 10 % to the reference gas varying the flow rates from 50 mL to 5 mL. The signal in

the thermal conductivity detector (TCD) was recorded, and the graph was drawn between the TCD Signal *vs* the amount of gas passed through the TCD detector. The calibration factor was calculated as described by Blass and Halsey [35]. To avoid negative signals, the TCD signal was set at 5.0. The amount of gas consumed to give a particular peak was calculated with respect the peak area in the TPR profile by using the calibration factor obtained.

2.2.3) Catalytic testing

All catalytic testing was carried out in the temperature range 350-500 °C in 50 °C intervals. The reactor used was a continuous flow fixed bed reactor operated in vertical mode. The catalyst (1 mL (~0.8 g) with a particle size between 600-1000 µm) was placed in a stainless steel tube at the hot spot of the reactor. The temperature of the catalyst bed was monitored by a thermocouple that was placed in the vertical axis. *n*-Octane (99%, Merck) was introduced into the reactor lines (pre-heated to 200 °C) utilising a HPLC pump. The gas eluent from the reactor was measured by a Ritter drum-type gas flow meter. The liquid eluent was collected in a catch pot pre-cooled to 2 °C, the carbon to oxygen (C:O) ratio was maintained at 8:3 (using air as source of oxygen) and the GHSV usually at 4000 h^{-1} (total flow of 67 mL/min of gases). All gaseous samples were analysed using a PerkinElmer Clarus 400 gas chromatography (GC) equipped with (FID) detector and a PerkinElmer Clarus 400 GC equipped with TCD detector. The liquid samples were analysed by GC-FID. The *n*-octane conversion and product selectivity were calculated as shown in equations 1 and 2 respectively. All reactions reported had a carbon balance between 95-103% and values were obtained at least in duplicates (±3 %). The homogenous reaction contribution (carborundum packed reactor) was small at all reactions temperatures (the highest conversion was 9% at 500 °C, with high selectivity to cracked and COx products).

$$\text{Conversion} = \left(\frac{mole\ of\ octane\ in - mole\ octane\ out}{mole\ of\ octane\ in}\right) X\ 100 \qquad \text{(Eq. 1)}$$

$$\text{Selectivity} = \left(\frac{Moles\ of\ carbon\ in\ \ selected\ product}{Total\ moles\ of\ carbon\ in\ all\ products}\right)\ X\ 100 \qquad \text{(Eq. 2)}$$

2.2.4) Used catalyst characterization

After the reaction the catalyst was kept under N_2 to avoid any reoxidation that might occur after the reaction and the catalyst were characterized by XRD, Raman spectroscopy (within 3 hours after the reaction) and SEM as described above.

2.3) Results and discussion

2.3.1) Catalyst characterization

The XRD (Fig. 2.1) patterns revealed the formation of the $MgMoO_4$ phase accompanied by the presence of MoO_3. Comparison between the 021 (β-$MgMoO_4$) and the 201 (α-$MgMoO_4$) planes, showed that the dominant phase in the magnesium molybdate is the β-$MgMoO_4$. This is due to maintaining the pH at 6 during the synthesis and calcining the catalysts at 550 °C, since Yoon *et al.* [15] showed that the synthesis pH and calcination temperature affect the ratio of the α-$MgMoO_4$ to β-$MgMoO_4$ phases. Synthesis at low pH (*i.e.* below 3) and low calcination temperature (*i.e.* below 550 °C) results in the α-$MgMoO_4$ being the dominant phase. The coordination around the molybdenum centre in the α-$MgMoO_4$ is distorted tetrahedral that is isotopic to α-$ZnMoO_4$ [36], while the coordination around the molybdenum centre in the β-$MgMoO_4$ phase is tetrahedral that is isotopic to the α-$MnMoO_4$ phase [37]. The ICP-OES results and the BET-surface area measurements (Table 2.1) show that as the molybdenum content increases in the catalysts, the surface area increases (to a small degree). This observation was also noted for magnesium molybdate and cobalt molybdate catalysts reported by Yoon *et al.* [17].

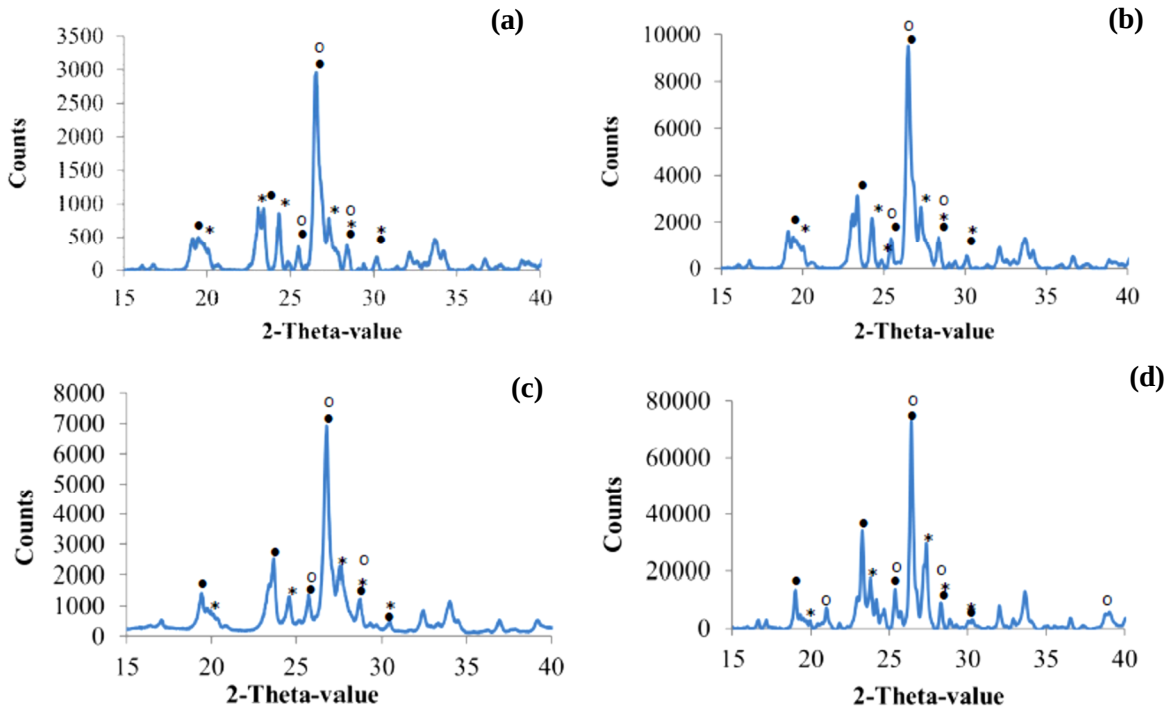

Figure 2.1: XRD patterns of magnesium molybdate synthesised by the co-precipitation method catalyst (a) MM0.87 (b) MM0.98 (c) MM1.06 and (d) MM1.25. $MgMoO_4$ phase assignment: α-$MgMoO_4$ (*), β-$MgMoO_4$ (•) and MoO_3 (O).

Table 2.1: Molar ratio and BET surface area measurements for catalysts

Catalyst	ICP-OES ratio (Mg:Mo)	BET-surface area m^2g^{-1}	Used catalyst BET-surface area m^2g^{-1}
MM0.87	1:0.87	3.2	12
MM0.98	1:0.98	3.8	23
MM1.06	1:1.06	4.2	3
MM1.25	1:1.25	4.7	4

IR spectra of the different catalysts (Appendix 2.1) showed the bands for $MgMoO_4$ at 935 cm^{-1} (shoulder) corresponding to the V_{as} (MoOMo), 885 cm^{-1} (strong) also corresponding to V_{as} (MoOMo), in addition to bands at 811 cm^{-1} and 725 cm^{-1} corresponding to V_{as} (MoOMo). These bands were observed together with two bands for the terminal Mo=O in MoO_3 at 767 and 409 cm^{-1} [15]. The Raman spectra show the Mo-O bending at ~ 346 cm^{-1} in all catalysts. The characteristic band of molybdenum trioxide was observed in all catalysts at ~ 815 cm^{-1} (Fig. 2.2, Table 2.2). The presence of the $MgMoO_4$ was confirmed by the bands at ~ 852, 903 (asymmetric Mo-O) and 959 cm^{-1} (symmetric Mo-O). The ratio in intensity between the

characteristic band for molybdenum trioxide (~ 815 cm^{-1}) and that of magnesium molybdate (~ 959 cm^{-1}) gave an indication of the ratio in which the two phases are present in the catalyst. The increase in the molybdenum content in the catalyst (determined by ICP-OES) leads to an increase in the I_{815}/I_{959}, showing that the excess molybdenum in the magnesium molybdate catalyst is present in the molybdenum trioxide phase.

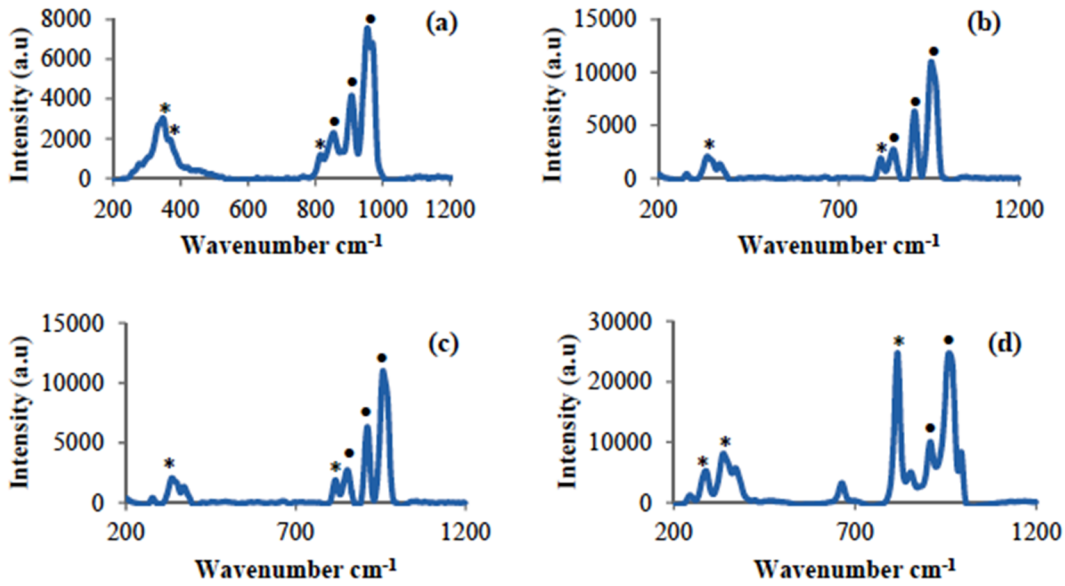

Figure 2.2: Raman spectra of all four catalysts with different molybdenum content (a) MM0.87 (a) MM0.98 (b), MM1.06 (c) and MM1.25 (d) showing both phases (*) MoO_3 and (•) $MgMoO_4$.

Table 2.2: Raman spectroscopy different modes for MoO_3 and $MgMoO_4$ in the magnesium molybdate catalysts with different molybdenum content

Phase	Wavenumber (cm^{-1})	Raman mode
MoO_3	346	Mo-O bending
	815	Mo-O asymmetric stretching
$MgMoO_4$	959	Mo-O symmetric stretching
	852, 903	Mo-O asymmetric stretching

The TPR profiles for the different catalysts (Fig. 2.3 a-d) all showed two peaks, the first peak at around 650 °C and the second peak at around 900-950°C (depending on the catalyst). The first peak intensity increases as the molybdenum content increases in the catalyst (Fig. 2.3 a-d), resulting in higher hydrogen consumption (Table 2.3) to reduce the molybdenum trioxide phase to the molybdenum dioxide phase. Moreover, the hydrogen consumption for the second peak also increased as the molybdenum content increased, this could be a subsequent reduction of the products from the first reduction. Miller *et al.* studied the activity and selectivity of the magnesium molybdate catalyst in the oxidative dehydrogenation of propane, where the catalyst possessing a reduction peak at 650 °C showed high activity and selectivity, while catalysts that do not have that reduction peak showed no activity in propane ODH [14]. The second reduction peak is due to the reduction of the magnesium molybdate phase. Furthermore, the different composition of the catalysts resulted in shifts in the second peak to a lower onset reduction temperature as the amount of MoO_3 increased in the catalyst (Table 2.3). TPR-O-R analyses of catalysts MM0.98 and MM1.25 (Fig. 2.3 e and f, respectively) showed that in the reduction cycle after oxidation only one peak is observed, the peak that is believed to be due to MoO_3 was no longer present. This is because the reduction of molybdenum trioxide to molybdenum dioxide is not reversible under these conditions. However, the magnesium molybdate phase undergoes reversible reduction, oxidation and reduction, unlike the molybdenum trioxide phase.

The SEM imaging (Appendix 2.2) showed the plate-like particles associated with MoO_3 and the size of these plates increases as the Mo content in the catalyst increases, supporting the increase in MoO_3 content observed in the Raman results, ICP-OES and TPR results.

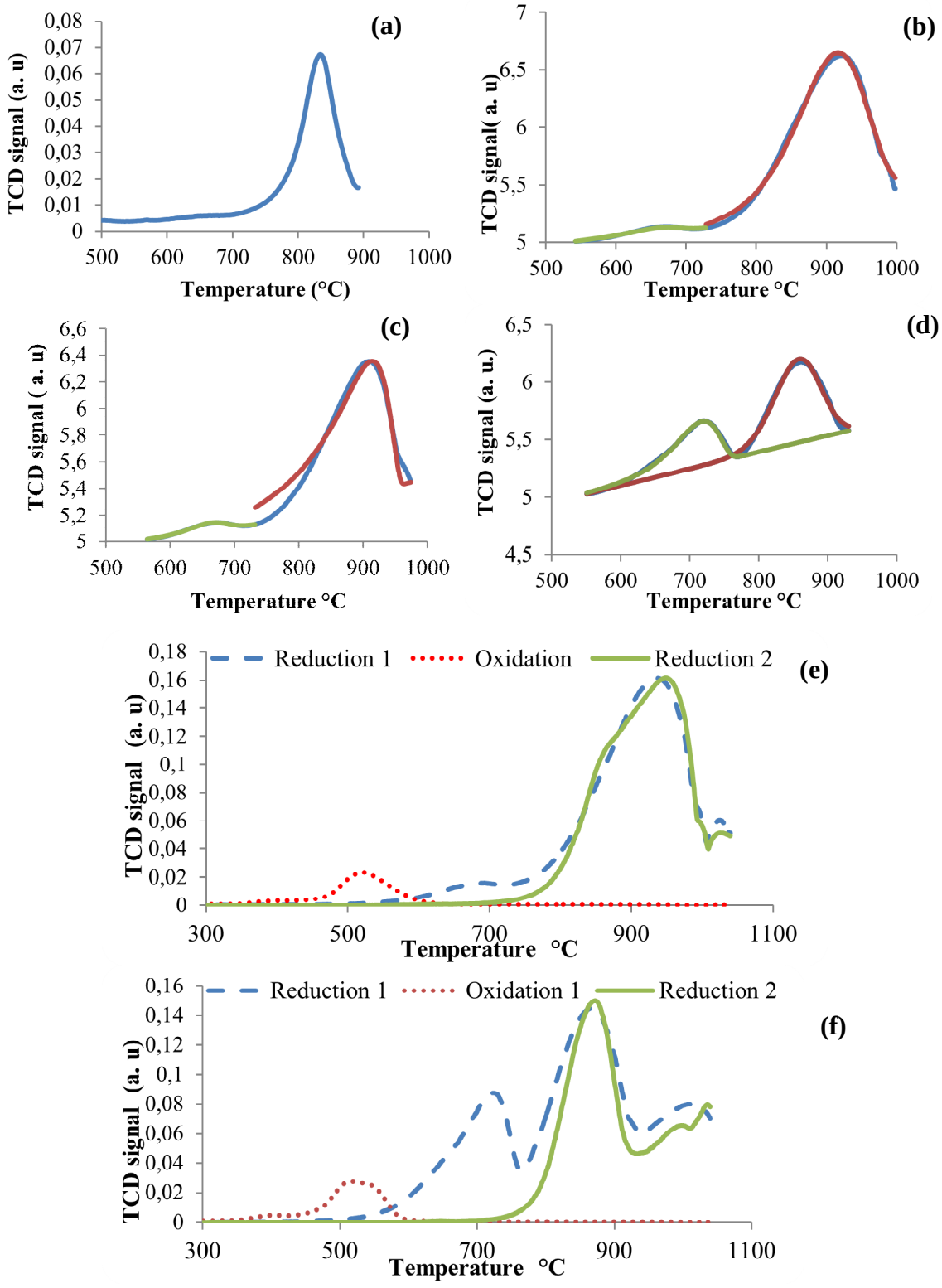

Figure 2.3: TPR profile (blue) and deconvolution (green and red) for MM0.87 (a), MM0.98 (b), MM1.06 (c) and MM1.25 (d), obtained using 5% hydrogen as the reducing gas, TPR-TPO-TPR cycle for MM0.98 (e) and MM1.25, (f) using air as the oxidizing gas.

Table 2.3: TPR analysis including onset temperature, maximum temperature and H_2 consumption for magnesium molybdates catalyst with different molybdenum content

Catalyst	Onset temperature (^{O}C)	Maximum temperature (^{O}C)		H_2 consumption (mL/g)	
		Peak 1	Peak 2	Peak 1	Peak 2
MM0.87	701	-	834	-	66
MM0.98	558	658	924	1.31	70
MM1.06	547	658	921	2.82	76
MM1.25	535	718	857	18.9	31

The total acidity of MM0.87 and MM1.25 was determined by NH_3-TPD (Appendix 2.3). The increase in the total acidity of the catalyst could be attributed to the increase in the amount of molybdenum trioxide in the catalyst. This is expected since molybdenum trioxide is acidic in nature. The strength of the acid site is documented to influence both activity and selectivity in isomerization of *n*-butane [38], furthermore, Elkhalifa and Friedrich [39] showed the effect of the total acidity in the ODH of *n*-octane over VMgO system to promote consecutive reactions to form aromatics from octenes through different cyclization modes, also Dasireddy *et al.* [12] showed the same effects.

2.3.2) Catalytic testing

The catalytic testing was focused on examining the effect of the molybdenum content in the magnesium molybdate catalysts in terms of their selectivity (in particular to value added products, which are octenes and aromatics) and activity in the ODH of *n*-octane at a carbon to oxygen ratio of 8:3 and a 4000 h^{-1} GHSV. The dominant products observed throughout the temperature range over the different catalysts are octenes (dominanted by the 2-octene isomer among 1-octene, 3-octene and 4-octene), aromatics (the dominant aromatic is ethylbenzene among xylene and styrene), cracked products and carbon oxides.

The effect of temperature and molybdenum content on the conversion of *n*-octane and oxygen is shown in Fig. 2.4. The catalysts with the highest molybdenum content (*i.e.* MM1.25) showed higher conversion at lower temperature (below 450 °C) than the catalysts with lower molybdenum content. This could be explained by the onset reduction temperature from TPR analysis (Table 2.3), where the onset temperature decreased as the molybdenum content increased resulting in the catalyst being more active as the molybdenum content

increased, especially at low temperatures. This could be due to the molybdenum trioxide on the surface of magnesium molybdate, which is supported by the TPR results (Fig. 2.3). The catalyst with the lowest molybdenum content (*i.e.* MM0.87) showed low conversion (Fig. 2.4 a) at lower temperatures and this is due to absence of the MoO_3 phase that reduces at low temperature, hence no synergistic interaction is possible between MoO_3 and $MgMoO_4$. At higher temperature MM0.98 and MM1.06 showed to be the most active catalysts, while the other catalysts (*i.e.* MM0.87 and MM1.25) showed a lower conversion especially at high reaction temperature (Fig. 2.4 a). This could be due to the surface MoO_3 being reduced to MoO_2, which is catalytically inactive and partially blocking *n*-octane from reacting with the $MgMoO_4$ phase. This explanation is supported by the oxygen conversion data which is always below 100% and, indeed, lower than 60% for MM0.87 and MM1.25. For the catalysts with lower molybdenum content (*i.e.* MM0.87 and MM0.98) conversion of *n*-octane increased with increase in temperature. In the case of MM0.87 the conversion increased significantly after 450 °C. This is in correlation with the TPR results of the onset temperature for the reduction of the $MgMoO_4$, therefore, the *n*-octane is being oxidatively dehydrogenated as the $MgMoO_4$ is being reduced. Similar observations were made with the MM0.98 and MM1.06 catalysts, with higher conversion of *n*-octane at higher temperature due to the synergistic effect of the two molybdenum species at the near stoichiometric ratio, and the presence of mainly the $MgMoO_4$ phase.

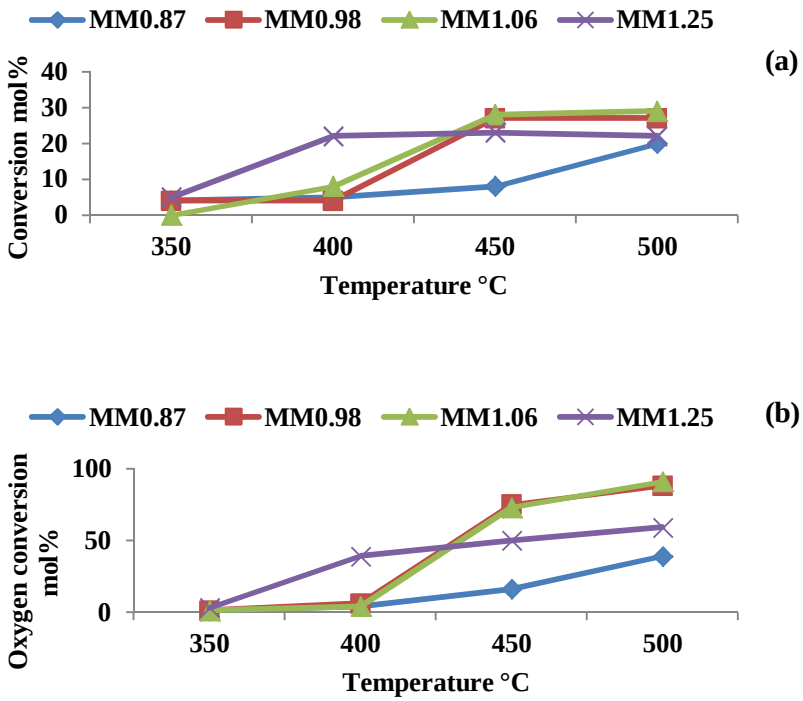

Figure 2.4: Conversion of *n*-octane (a) and oxygen conversion (b) as function of temperature and the molybdenum content in the magnesium molybdate catalysts, at 8:3 C:O ratio and GHSV of 4000 h^{-1}.

Selectivity to different products over the magnesium molybdate catalyst is greatly influenced by the surface acidity of the catalyst, as was shown by the reaction of *iso*-propyl alcohol (IPA) over magnesium molybdate catalyst [15, 16, 23]. The selectivity to octenes (Fig. 2.5 a) was highest at low temperatures with MM0.87, MM0.98 and MM1.06 (*i.e.* catalysts with low MoO_3 content), the opposite was observed for MM1.25 (*i.e.* catalyst with highest molybdenum content). The high selectivity to octenes at low temperature could be due to the catalyst surface acidity character [2]. Furthermore, the high selectivity to octene (> 85%) at this low conversion indicates that they are the primary reaction products. The increase in a acidity of the catalyst introduced by excess molybdenum content, resulted in the drop of the selectivity to octenes. As the temperature of the reaction increased the selectivity of octenes decreased and the selectivity to secondary reaction products (*i.e.* aromatics, cracked products and COx) increased. The highest selectivity above 450 °C for octenes was obtained over the MM0.87 catalyst. This was due to the excess MgO modifying the catalyst surface, making it less acidic and limiting and/or reducing the consecutive reaction forming secondary products to which octenes act as a precursor [2] (Scheme 2.1).

The selectivity of aromatics, shown in Fig. 2.5 b, increased with the increase in the reaction temperature. The lowest selectivity to aromatics was obtained over MM0.87 as a result of low molybdenum content, thus, the catalyst is less acidic (compared to MM0.98, MM1.06 and MM1.25) and, therefore, not promoting the consecutive reaction of octenes to aromatics (Scheme 2.1). The highest selectivity to aromatics was obtained over MM1.06 at higher temperature (>400 °C), where the surface acidity/basicity is balanced promoting secondary reactions of the octenes to form aromatics, but limiting over-oxidation of aromatics to the thermally stable COx products. There was thus a correlation in the selectivity to aromatics and the molybdenum content in the catalyst. The catalyst with the highest molybdenum content (*i.e.* MM1.25) resulted in aromatic formation from 400 °C, while the catalyst with lower molybdenum content resulted in aromatic formation at higher temperatures. This emphasises the correlation between the surface acidity/basicity and, hence, the nature of the active site, and the selectivity to different products. It has previously been shown that as the acidity of the catalyst increase the selectivity to secondary products (mainly aromatics) over vanadium based catalyst in the ODH of *n*-octane [12, 39]. Furthermore, Santos *et al.* [40] showed that the strength of the catalyst acidity plays a major role in the isomerization of *n*-octane in terms of conversion and selectivity, where high acidity leads to better activity of HY zeolite based catalysts.

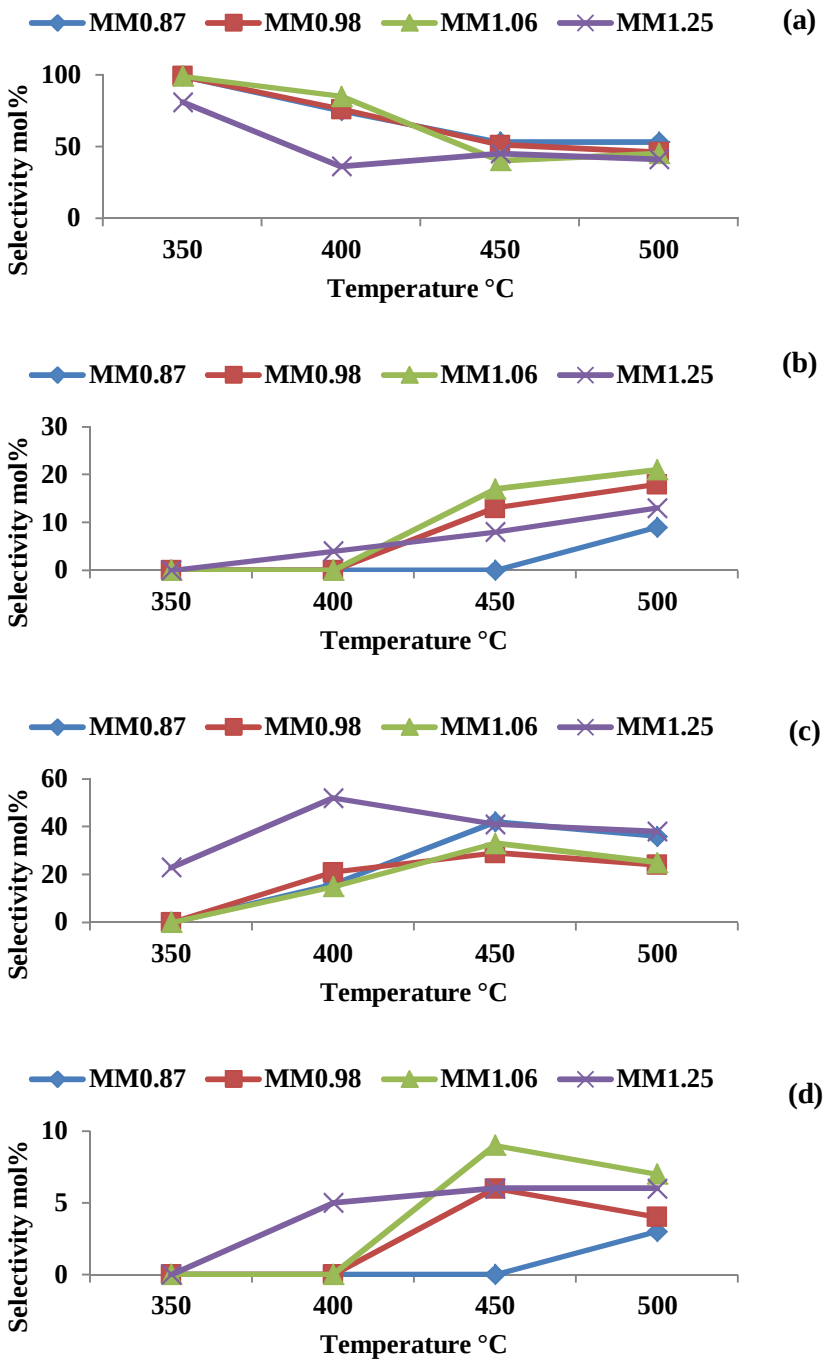

Figure 2.5: Effect of temperature and molybdenum content on the selectivity to octenes (a), aromatics (b), COx (c) and cracked (d) in the ODH reaction of *n*-octane at C:O ratio of 8:3 and GHSV of 4000 h^{-1}.

n-octane → octenes/octadi(tri)enes → aromatics → cracked → COx

Scheme 2.1: Possible reaction sequence for the ODH of *n*-octane based on literature [39, 41, 42].

The breakdown of the selectivity to different C8 aromatics (*i.e.* ethylbenzene, styrene and xylene) (Fig. 2.6), showed that C_1-C_6 is the favoured aromatization or cyclization mode, indicated by the greater selectivity to ethylbenzene and styrene in contrast with *o*-xylene. Furthermore, the amount of excess MoO_3 plays a role in the aromatics formation temperature (Fig. 2.5 b), where increase in the molybdenum content results in aromatics formation at lower temperature, and this could be due to it promoting of consecutive reactions of octenes. Moreover, the selectivity to styrene in general increased with increase in the reaction temperature and molybdenum content in contrast to ethylbenzene. It could be that both factors promote the ODH of ethylbenzene to styrene.

The selectivity to COx (Fig. 2.5 c) was highest with the high molybdenum content catalyst (*i.e.* MM1.25). The high selectivity to COx could be due to high acidity in this catalysts introduced by the excess molybdenum (MoO_3) present in the catalyst [1]. The general trend is that the selectivity to COx over all catalysts decreased with increase in the reaction temperature. This is likely due to the activation energy required for aromatics formation being overcome, leading to the increase in the aromatic selectivity [2]. The lowest COx selectivity was obtained over the MM0.98 and MM1.06 catalysts. This is in agreement with the increase in the aromatic selectivity over the same catalysts, which further emphasis the reaction sequence (Scheme 2.1) where usually high selectivity to aromatics in accompanied by low selectivity to cracked and COx products.

The selectivity to the cracked products (Fig. 2.5 d) was low for all catalysts and temperatures. The trend observed was that the selectivity to cracked products increased as the molybdenum content increased in the catalysts with the exception of MM1.06. This is a further general correlation between the surface acidity/basicity and the product distribution.

Oxygen conversion analysis (Fig. 2.4 b) showed the highest oxygen conversion obtained was ~90% at 500 °C over both MM0.98 and MM1.06. This indicates the reaction is not oxygen starved, however, further increase in the oxygen concentration in the reaction mixture would likely lead to a decrease selectivity to value added products. The increase in the conversion over MM0.98 and MM1.06 from 450 °C is likely due to the reduction of the magnesium molybdate phase in the catalyst and the lattice oxygen being replaced by the oxygen in the feed. This increase in oxygen consumption is accompanied by increase in the selectivity to aromatics (since aromatics formation requires oxygen). The breakdown of COx (*i.e.* CO and CO_2) (Appendix 2.4) was not influenced by the oxygen conversion, however, only CO_2 was

formed below 450 °C, except over MM1.25 where CO was also detected at 400 ^{O}C. This could indicate that CO_2 is a primary product, since its observed at low temperatures and low conversion, this correlation was also made by Maderia and Portela [43] where at low temperatures or contact time CO was not observed in the ODH of *n*-butane. The ratio of CO_2/CO was unaffected by both temperature and oxygen conversion, which could indicate CO does not undergo deep oxidation to CO_2. Similar results were obtained over a Ni-W-O system in the ODH of ethane as reported by Solsona *et al.* [44].

2.3.3) Product distribution at iso-conversion

Selectivities of the different products at *iso*-conversion (~24%) (*iso*-conversion was obtained by changing the GHSV to obtain the desired conversion) at 500 °C (Fig. 2.7 a) showed that the selectivity to octenes decreased with increase in the molybdenum content in the catalyst. This decrease in the octene selectivity could be explained by the change in the catalyst acidity upon introduction of molybdenum. The catalyst with highest acidity (*i.e.* MM1.25) showed the lowest selectivity due to octenes undergoing secondary reactions on the catalyst resulting in the formation of mostly COx, which is evident by the high selectivity to COx over MM1.25. The highest selectivity to octenes was obtained over MM0.87. This could be a result of the excess magnesium oxide, which is basic in nature, and hence, octenes do not undergo secondary reactions. However, MM0.87 also showed high selectivity to CO_2 (Appendix 2.4) which indicates some combustion of *n*-octane. This was also observed in the ODH of *n*-octane over VMgO, likely due to the MgO phase [2, 45].

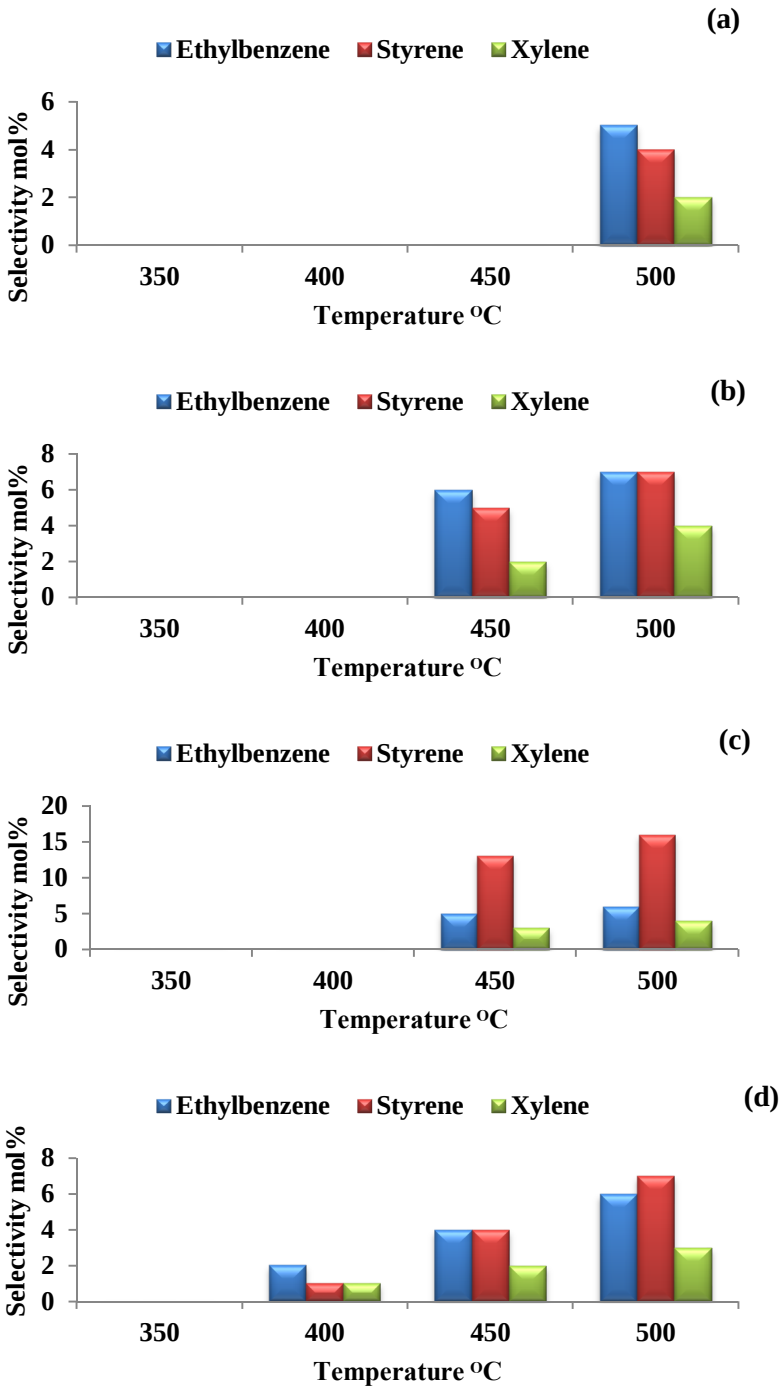

Figure 2.6: Breakdown of the C8 aromatics in the ODH of *n*-octane at C:O 8:3 and 4000 h^{-1} GHSV over magnesium molybdate with different molybdenum content, MM0.87 (a), MM0.98 (b), MM 1.06 (c) and MM1.25 (d).

The selectivity to aromatic products (*i.e.* ethylbenzene, styrene and xylene) was highest over MM1.06 and MM0.98. This could be explained considering the total acidity of the catalyst promoting consecutive reaction of the octenes (which can be considered as the precursors) to form aromatics COx. Thus comparing the total acidity of the MM0.98 and MM1.25, over the most acidic catalyst (*i.e.* MM1.25) the consecutive reactions were promoted up to COx formation and over the less acidic catalyst (*i.e.* MM0.98) the consecutive reactions stopped at the aromatics formation stage [2, 9, 39] (Scheme 2.1). In the case of MM0.87, the excess MgO decreased the strength of the acidity of the catalyst and this resulted in limiting the consecutive reactions of octenes (Fig. 2.7 a) relatively to the other catalysts [46]. This is evident by the low selectivity to aromatics obtained over MM0.87. The selectivity to aromatics over MM0.98 improved, relative to MM0.87, which was expected, since the catalyst is more acidic due to the near stoichiometric ratio of Mg:Mo. Thus, octenes undergo secondary reaction to form aromatics. The slight excess molybdenum in MM1.06 increased the consecutive reactions of octenes over the catalyst, leading to a further increase in the selectivity to aromatics. Furthermore, MM1.25 shows the highest selectivity to CO (Appendix 2.4) indicating further or consecutive reactions of octenes/aromatics to CO, since Madeira and Portela [43] showed that CO is produced from the over oxidation of the primary products of butane ODH over cesium doped nickel molybdate catalyst.

The breakdown of the octenes isomers (Fig. 2.7 b) at *iso*-conversion (~24%) showed that the *n*-octane activation occurs at all positions (C_1-C_4). The dominant octene isomer formed is the 2-octene isomer, which is the most thermodynamically stable octene [2]. Furthermore, the fact that the 4-octene isomer is formed indicates that there are no significant steric effects playing a role in determining the selectivity to a specific isomer over another. Also *trans*-isomers dominant over *cis*-isomers, likely because *trans* isomers are more thermodynamically stable compared to the *cis* isomers. That *trans*-2-octene dominantes over the catalyst, might also indicate that all catalysts posses similar or identical active sites that are responsible for octene formation. Since octene formation takes place through the homolytic cleavage of a C-H bond, followed by fast abstraction of a neighbouring hydrogen resulting in the formation of octene [46], all catalysts have similar active sites where the first C-H abstraction takes place.

The selectivity to C8 aromatics (ethylbenzene, styrene and xylene) at *iso*-conversion (~24%) (Fig. 2.7 c) showed that ethylbenzene is the dominant aromatic isomer over all four catalysts. The aromatic formation from *n*-octane takes place *via* one of two routes (Scheme 2.2),

namely; C_1-C_6 cyclization which produces ethylbenzene and styrene, or C_2-C_7 cyclization producing xylene [2, 39, 47, 48]. Molybdenum content in the catalyst did not influence the cyclization mode, since all catalysts showed high selectivity to the C_1-C_6 cyclization mode products. However, styrene selectivity increased over both MM0.98 and MM1.06, this could be related to the acidity of the catalyst surface. Furthermore, the selectivity of styrene was higher over the MM1.06 catalyst in comparison to MM0.98, which could also be due to the acidity of the catalyst promoting further ODH of ethylbenzene to styrene. This agrees with the aromatics selectivity over MM0.87 and MM1.25, where ethylbenzene is the dominant aromatic isomer.

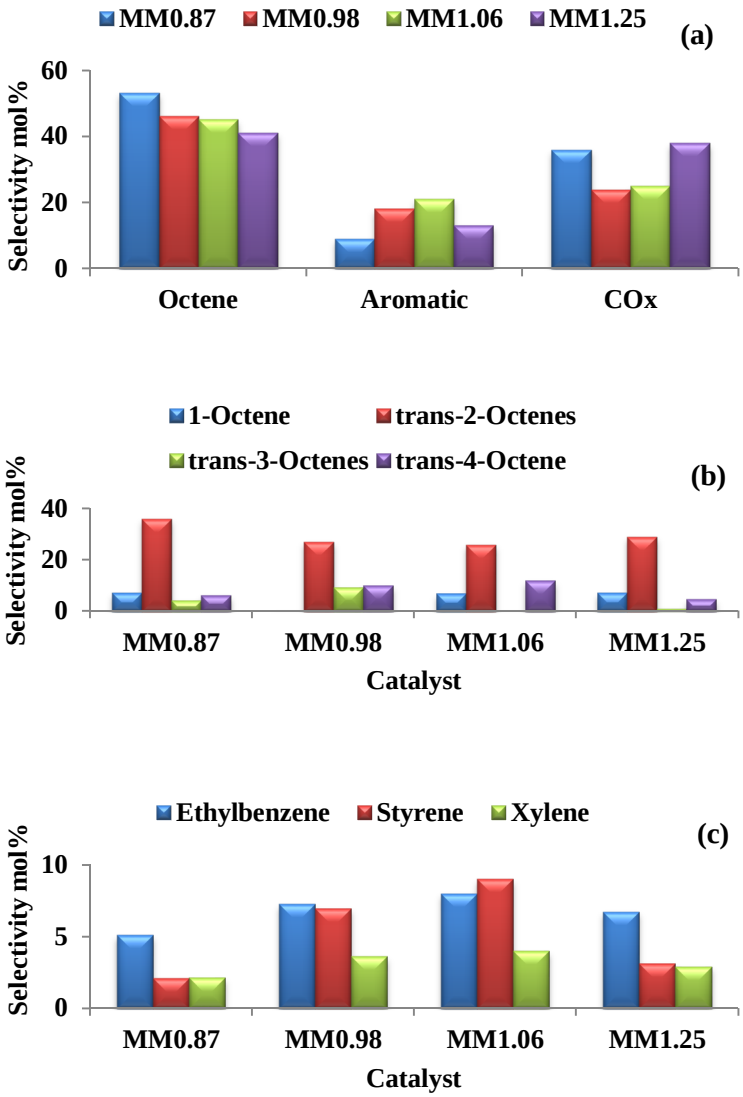

Figure 2.7: Selectivity profile of octenes, aromatics and COx (a) Selectivity breakdown of octene isomers (b) and aromatics (c) over MM0.87, MM0.98, MM1.06 and MM1.25 at *iso*-conversion of ~24% at 500 ^{O}C.

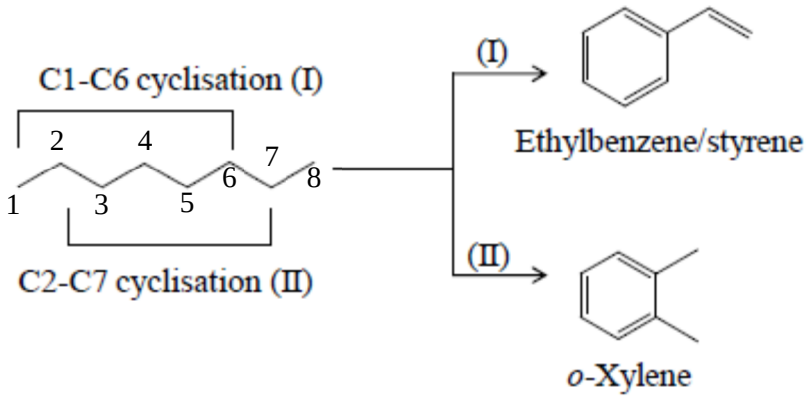

Scheme 2.2: The cyclisation mode of *n*-octane to produce C8 aromatics based on literature [39].

Another explanation to the change in the selectivity could be due to change in the content of α and β-$MgMoO_4$ in the catalyst. MM0.87 showed comparable α and β-$MgMoO_4$ content (judging by the intensity of the α-201 and β-021peaks), all other catalyst are dominanted by the β-$MgMoO_4$ phase. Yoon *et al.* [15] showed that when the magnesium molybdate is dominanted by the β-$MgMoO_4$, lower conversion of propane and *iso*-butane is obtained in comparison to a catalyst dominanted by the α-$MgMoO_4$, due to α-$MgMoO_4$ being more acidic [15]. However, in this study the phase composition will likely not play a major role, since the acidity was altered by the molybdenum content rather than the phase composition of the catalyst. However, MM1.25 has crystalline MoO_3 (Appendix 2.2) which is reported by Lee *et al.* [16] and Ueda *et al.* [33] to be inactive in the ODH of light alkanes.

2.3.4) Used catalyst characterization

The catalyst after each reaction was characterized by XRD and Raman spectroscopy (to investigate any phase change that may have taken place during the reaction) and SEM (to see if the surface morphology of the catalyst was altered). The XRD patterns (not shown here) of the used catalysts showed that all of the catalysts maintained the initial phases. However, the Raman spectroscopy analyses (Fig. 2.8) showed that the catalysts underwent some degree of reduction. This was observed by a decrease in the intensity of the molybdenum trioxide phase in relation to the magnesium molybdate phase, likely due to reduction of MoO_3 to

MoO_2 (Raman inactive). Furthermore, the catalyst colour changed from white to grey, further indicating reduction of the catalyst. The BET surface area measurement of the used catalysts (Table 2.1) showed that the surface areas of the catalysts with less molybdenum (*i.e.* MM0.87 and MM0.98) increased after the reaction, while the opposite was observed with the catalyst rich in molybdenum trioxide. A similar trend was observed for nickel molybdate with molybdenum trioxide [1].

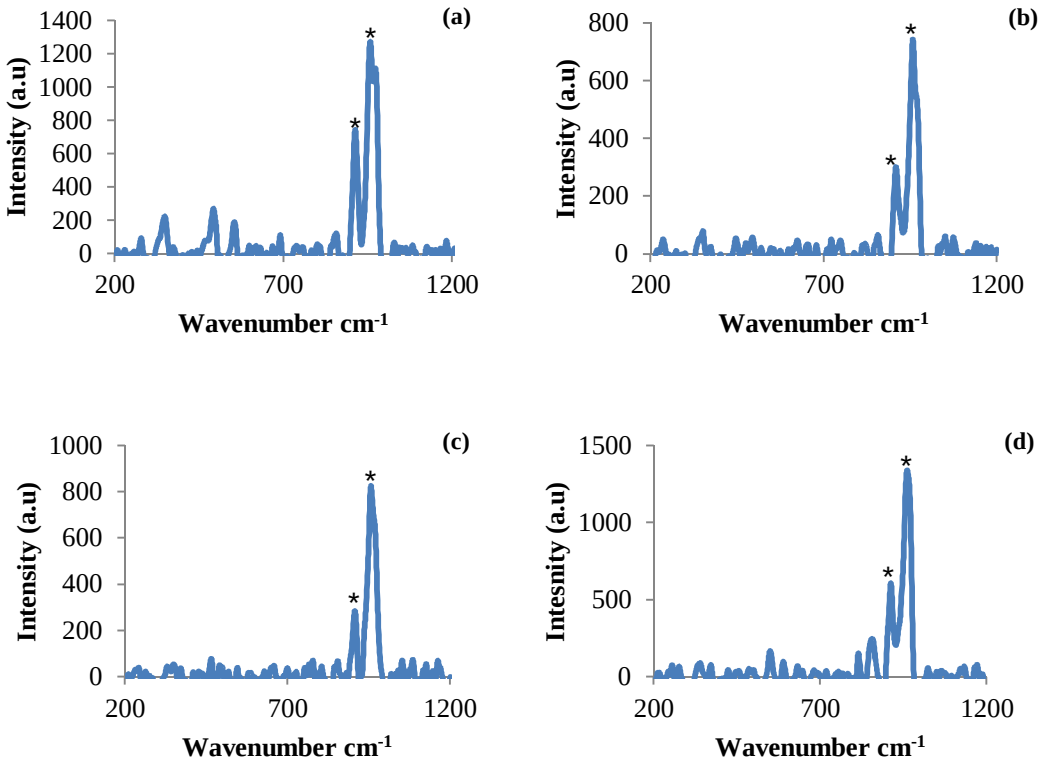

Figure 2.8: Raman spectra of the used catalysts MM0.87 (a), MM0.98 (b), MM1.06 (c) and MM1.25 (d), at carbon to oxygen ratio of 8:3 and 4000 h^{-1} GHSV , $MgMoO_4$ (*).

SEM analysis of the used catalysts (Appendix 2.5) showed that all catalysts have a slightly altered surface morphology by appearance of more plate-like structures. This could be as a result of partial reduction that took place under the reaction conditions. However, all catalyst surface morphologies are still very similar to the initial surface morphology, showing both the round shaped particles and the plate-like structure.

2.4) Conclusion

The ODH of *n*-octane is affected by the amount of molybdenum in the catalyst in terms of activity and selectivity. Four catalysts were investigated with varying molybdenum content (*i.e.* MM0.87, MM0.98, MM1.06 and MM1.25). The main effect introduced by the molybdenum content is the alteration of catalyst surface acidity, which in turn influenced the selectivity of the catalysts. The selectivity to octenes increased over the catalysts in the order MM0.87>MM0.98~MM1.06>MM1.25, the increase in the strength of the acidity was in the same order. In terms of the selectivity to aromatics, the most selective catalyst was MM0.98~MM1.06>MM1.25>MM0.87, while the opposite order was observed for the selectivity to COx indicating over oxidation. The highest selectivity to C8 products (octenes and aromatics) was obtained over MM0.98 and MM1.06 based on the *iso*-conversion results (~ 24%) at 500 °C. Used catalyst characterization showed that the catalysts undergo reduction dominanted by the decrease in the molybdenum trioxide peak in the Raman spectra.

2.5) Acknowledgements

The authors thanks SASOL, NRF and THRIP (grant number TP 1208035643) for financial support, the UKZN Westville campus EM unit staff for their help with imaging.

2.6) References

[1] B. Pillay, M.R. Mathebula, H.B. Friedrich, Appl. Catal., A: Gen., 361 (2009) 57-64.
[2] E.A. Elkhalifa, H.B. Friedrich, Appl. Catal., A: Gen., 373 (2010) 122-131.
[3] H.B. Friedrich, A.S. Mahomed, Appl. Catal., A: Gen., 347 (2008) 11-22.
[4] B. Pillay, M.R. Mathebula, H.B. Friedrich, Catal. Lett., 141 (2011) 1297-1304.
[5] B.M. Weckhuysen, R.A. Schoonheydt, Catal. Today, 51 (1999) 223-232.
[6] U. Illgen, R. Schäfer, M. Noack, P. Kölsch, A. Kühnle, J. Caro, Catal. Commun., 2 (2001) 339-345.
[7] J. Happel, H. Blanck, T.D. Hamill, Ind. Eng. Chem. Fundam., 5 (1966) 289-294.
[8] J. Vila, F. Sapina, E. Martinez, V. Cortes, J. Podobinski, Contrib. Sci., 4 (2008) 223-229.
[9] V.D.B.C. Dasireddy, S. Singh, H.B. Friedrich, Appl. Catal., A: Gen., 421–422 (2012) 58-69.
[10] V. Cortés Corberán, Top. Catal., 52 (2009) 962-969.
[11] M.M. Bettahar, G. Costentin, L. Savary, J.C. Lavalley, Appl. Catal., A: Gen., 145 (1996) 1-48.
[12] V.D.B.C. Dasireddy, S. Singh, H.B. Friedrich, Appl. Catal., A: Gen., 456 (2013) 105-117.
[13] F. Cavani, F. Trifirò, Catal. Today, 51 (1999) 561-580.
[14] J. Miller, N. Jackson, L. Evans, A. Sault, M. Gonzales, Catal. Lett., 58 (1999) 147-152.
[15] Y. S. Yoon, K. Suzuki, T. Hayakawa, S. Hamakawa, T. Shishido, K. Takehira, Catal. Lett., 59 (1999) 165-172.
[16] K. H. Lee, Y. S. Yoon, W. Ueda, Y. Moro-oka, Catal. Lett., 46 (1997) 267-271.
[17] Y. Yoon, W. Ueda, Y. Moro-oka, Top. Catal., 3 (1996) 265-275.
[18] Y. S. Yoon, N. Fujikawa, W. Ueda, Y. Moro-oka, K.W. Lee, Catal. Today, 24 (1995) 327-333.
[19] S.N. Koc, G. Gurdag, S. Geissler, M. Muhler, Ind. Eng. Chem.Res., 43 (2004) 2376-2381.
[20] L.E. Cadus, M.C. Abello, M.F. Gomez, J.B. Rivarola, Ind. Eng. Chem.Res., 35 (1996) 14-18.
[21] M.C. Abello, M.F. Gomez, L.E. Cadús, Ind. Eng. Chem.Res., 35 (1996) 2137-2143.
[22] K. H. Lee. W. Ueda, Y. S. Yoon, Y. Moro-oka, Catal. Today, 24 (1998) 327-333.
[23] Y.S. Yoon, W. Ueda, Y. Moro-oka, Catal. Lett., 35 (1995) 57-64.
[24] L.E. Cadus, M.F. Gomez, M.C. Abello, Catal. Lett., 43 (1997) 229-233.
[25] G.E. Vrieland, C.B. Murchison, Appl. Catal., A: Gen., 134 (1996) 101-121.
[26] Y.J. Zhang, I. Rodríguez-Ramos, A. Guerrero-Ruiz, Catal. Today, 61 (2000) 377-382.
[27] J.Soler. M. L. Pacheco, A. Dejoz, J. M. Lopez Nieto, J. Herguido, M. Menedez, J. Santamaria, Catal. Today, 61 (2000) 101-107.
[28] J. Hanuza. W. Oganowski, B. Jezowska-Trzebiatowska, J. Wrzyszcz, J. Catal., 39 (1975).
[29] J. Hanuza, B. Jezowska-Trzebiatowska, J. Wrzyszcz, J. Mol. Catal. A: Chem., 4 (1978) 271-278.
[30] U.S. Ozkan, M.R. Smith, S.A. Driscoll, J. Catal., 134 (1992) 24-35.
[31] U.S. Ozkan, R.C. Gill, M.R. Smith, Appl. Catal. A: Gen., 62 (1990) 105-117.

[32] A. Guerrero-Ruiz, I. Rodriguez-Ramos, P. Ferreira-Aparicio, M. Abon, J.C. Volta, Catal. Today, 32 (1996) 223-227.
[33] W. Ueda, K.H. Lee, Y.S. Yoon, Y. Moro-oka, Catal. Today, 44 (1998) 199-203.
[34] G.M. Webster, Socity of Exploration Geophysicists 2, Tusla, OK, 1978.
[35] W.E. Blass, G.W. Halsey, Deconvolution of absorption spectra, Academic Press, New York 1981.
[36] S.C. Abrahams, J. Chem. Phys., 46 (1967).
[37] P.P. Cord, P. Courtines, G. Pannetier, J. Guillermett, Spectrochim. Acta Pt A. 28 (1972) 1601-1613.
[38] A.C. Oliveira, N. Essayem, A. Tuel, J.-M. Clacens, Y.B. Tâarit, J. Mol. Catal. A: Chem., 293 (2008) 31-38.
[39] E.A. Elkhalifa, H.B. Friedrich, J. Mol. Catal. A: Chem., 392 (2014) 22-30.
[40] R.C.R. Santos, A. Valentini, C.L. Lima, J.M. Filho, A.C. Oliveira, Appl. Catal., A: Gen., 403 (2011) 65-74.
[41] E. Elkhalifa, H. Friedrich, Catal. Lett., 141 (2011) 554-564.
[42] V.D.B.C. Dasireddy, H.B. Friedrich, S. Singh, Appl. Catal., A: Gen., 467 (2013) 142-153.
[43] L.M. Madeira, M.F. Portela, Appl. Catal., A: Gen., 281 (2005) 179-189.
[44] B. Solsona, J.M. López Nieto, P. Concepción, A. Dejoz, F. Ivars, M.I. Vázquez, J. Catal., 280 (2011) 28-39.
[45] E.A. Elkhalifa, H.B. Friedrich, Arab. J. Chem.DOI: 10.1016/j.arabjc.2014.10.002..
[46] R. Burch, M.J. Hayes, J. Mol. Catal. A: Chem., 100 (1995) 13-33.
[47] P. Meriaudeau, A. Thangaraj, C. Naccache, S. Narayanan, J. Catal., 146 (1994) 579-582.
[48] B.C. Shi, B.H. Davis, J. Catal., 157 (1995) 626-630.

Chapter three

Effect of the carbon to oxygen ratio on the activity and the selectivity of magnesium molybdate in the oxidative dehydrogenation of n-octane

Abstract

A magnesium molybdate catalyst was synthesised by the co-precipitation method and was tested in the oxidative dehydrogenation of *n*-octane. The catalyst was characterized by *in situ* X-Ray diffraction under reducing and oxidising environments (using 5% hydrogen in nitrogen and air, respectively), transmission electron microscopy, ICP-OES, BET-surface area measurements and Raman spectroscopy. The *in situ* results showed that the catalyst is stable under reduction and oxidation environments up to 600 °C. The effect of the carbon to oxygen ratio on the activity (*n*-octane conversion) and selectivity of the magnesium molybdate catalyst in the ODH of *n*-octane was investigated under four different C:O ratios ranging from oxygen lean to oxygen rich environments (*i.e.* 8:0, 8:1, 8:2 and 8:4). The conversion of *n*-octane is directly proportional to the oxygen content in the reaction feed, with highest conversion (37 %) at a C:O ratio of 8:4 and temperature of 500 °C. The selectivity to octenes, aromatics and COx was greatly influenced by the C:O ratio. The selectivity at *iso*-conversion (~26 %) showed that the octenes selectivity decreases while selectivity to aromatics and COx increases with increase in the oxygen content in the reaction mixture. The characterization of the used catalyst by XRD showed that the catalyst maintained the initial phase (*i.e.* magnesium molybdate), however, the Raman results showed that the partial reduction of the magnesium molybdate took place under oxygen lean environments (*i.e.* 8:0 and 8:1).

Keywords: Magnesium molybdate; oxygen concentration; n-octane; C8 products.

3.1) Introduction

Activation of *n*-paraffins is currently an important field of research for academic and industrial reasons. This interest has arisen, in part, due to the increase in the number of coal and gas to liquids plants that also produce linear paraffins [1, 2]. Medium chain length paraffins (C_6-C_{12}) are hence abundant, but of low value. Thus, paraffins can be considered a

cheap and increasingly available starting material for products with higher economic value (*e.g.* olefins and aromatics) [3]. Oxidative dehydrogenation (ODH) is one of the means for activating paraffins, among others (*e.g.* dehydrogenation). The advantages of ODH are the low operational cost and that it is more environmentally friendly than competitive processes. However, the disadvantage of ODH is that the products are more reactive than the starting material (*i.e.* paraffin) [3, 4]. The main challenge in ODH is tailoring a selective catalyst to the target product with minimum production of COx.

Molybdates based materials gained a lot of attention due to their structural chemistry, such as oxygen mobility, thermal stability and structural defects. All these properties play a major role in the activity and selectivity of the molybdate catalyst to the target product [5]. Due to this, molybdates have been widely used in the oxidation of olefins and ethylbenzene [6, 7]. Molybdates based catalysts with different cations (*e.g.* Mg, Co, Zn, Mn and Ni) have been extensively investigated in the activation of shorter chain paraffins (*e.g.* propane and butane). The main products obtained with those paraffins are propene and butadiene in the activation of propane and butane, respectively. Yoon *et al*. [6] reported the effect of the magnesium to molybdenum ratio, and the results showed that a slight excess of molybdenum resulted in an increase in the conversion of propane to propene. This observation was also made by Cadus *et al*. [8] where they also showed similar behaviour when the magnesium molybdate catalyst was physically mixed with molybdenum trioxide. Ueda *et al.* [9] studied the effect of surface enriched molybdenum by washing the catalyst with organic and inorganic acids to remove magnesium from the surface of the catalyst. Pre-treatment of the catalyst with ascorbic acid increased the conversion of propane from 2 to 12%, with an increase in the selectivity to propene from 76 to 81%. Moreover, the ODH of *n*-hexane over nickel molybdate showed good activity and selectivity to hexenes. Nickel molybdate catalysts demonstrated enhanced activity and selectivity to olefins compared to the nickel oxide and the molybdenum oxide, separately [3]. This phenomenon is well documented in literature where two inactive phases mixed together result in better catalytic activity and selectivity. This effect can be influenced by the synthesis method, which determines if the interaction between the different phases is chemical or physical [10]. Furthermore, the two phases of nickel molybdate (α and β-$NiMoO_4$) showed different activity and selectivity to hexenes. This is related to the fact that in the β-phase molybdenum is octahedrally coordinated and in the α-phase molybdenum is tetrahedrally coordinated [3, 11].

The focus of this study is to investigate the activity of the magnesium molybdate catalyst in the oxidative dehydrogenation of *n*-octane to value added products. Furthermore, the effect of the carbon to oxygen ratio on the catalyst activity and selectivity was also investigated.

3.2) Experimental

3.2.1) Catalyst synthesis

The magnesium molybdate catalyst ($MgMoO_4$) was synthesised following a previously reported method [12]. The reagents used in the synthesis were ammonium heptamolybdatetetrahydrate (≥ 99%, Merck), magnesium nitrate hexahydrate (min. 97%, Sigma-Aldrich) and ammonia solution (Saarchem). Molybdenum solution (0.5 M) was stirred and the pH was maintained at 6 by the addition of ammonia solution. Thereafter, 0.5 M magnesium solution was added drop-wise to the molybdenum solution. After complete addition of the magnesium solution, the mixture was heated to 100 °C. The dry precursor was calcined at 550 °C for two hours, resulting in the magnesium molybdate catalyst.

3.2.2) Catalyst characterization

The phase(s) presence in the magnesium molybdate catalyst ($MgMoO_4$) bulk were determined by X-Ray diffraction (XRD), using a Bruker D8 diffractometer equipped with a VANTEC detector with a current and voltage of 40 mA and 40 kV, respectively. The redox behaviour of the catalyst was investigated by *in situ* XRD (Anton Paar XRK 900 reaction chamber) under a reducing environment (5% H_2 in nitrogen) and an oxidising environment (air), in the temperature range of 100 to 600 °C at 50 °C intervals. The Catalyst structure was viewed on a JOEL 1010 transmission electron microscopy (TEM) equipped with megaView software. The catalyst morphology was viewed using a Zeiss ultra plus scanning electron microscopy (SEM) The bulk composition was determined by inductively coupled plasma-optical emission spectroscopy (ICP-OES) using a PerkinElmer Optima 5300 DV. The surface area of the catalyst was determined by BET-surface area measurements using a Micromeritics Tristar II. Raman spectra were obtained using an Advantage 532 series spectrometer equipped with Nuspec software.

3.2.3) Catalytic testing

The catalytic investigations were carried out using a continuous flow reactor. The catalyst (1 mL (~ 0.8g) and particle size between 1000-600 μm) was placed in a stainless steel tube (230 x 15 mm) positioned in a copper heating block. The catalyst bed temperature was monitored and controlled by a movable coaxially centred thermocouple. The reactor tube was filled with silicon carbide (24 gritt) above and below the catalyst bed. *n*-Octane (99%, Merck) was introduced using an HPLC pump as a liquid which was then vapourised at 200 °C, so that it interacted with the catalyst in the gas phase. The products were collected in a catch pot that was cooled to ≤2 °C. The gaseous products were identified and quantified by a PerkinElmer Clarus 400 gas chromatograph (GC) equipped with both flame ionization detector (FID) (for hydrocarbons) and thermal conductivity detector (TCD) (for COx). The products collected from the catch pot were also analysed by a PerkinElmer Clarus 400 GC equipped with an FID detector.

All catalytic testing was carried out at atmospheric pressure. The carbon to oxygen ratio was controlled by varying the amount of air (oxygen source), and nitrogen was used as a diluent gas at 4000 h^{-1} GHSV. All reactions were carried out in a temperature range of 350-500 °C at 50 °C intervals. All reactions had a carbon balance of 100% ±5% and all data points represent an average of 2 runs (±3% error).

3.2.4) Used catalyst characterization

Used catalysts were characterised after the reaction, without any pre-treatment (kept under nitrogen after the reaction), by XRD and Raman spectroscopy.

3.3) Results and discussion

3.3.1) Catalyst characterization

The *in situ* XRD results under reducing and oxidizing environments (Fig. 3.1 a and b, respectively) showed that the catalyst did not undergo thermal lattice expansion, since there was no shift in the d-spacing of the peaks as a function of increase in the temperature. In addition, the catalyst was also stable since no reduction was observed (Fig. 3.1 a). These results differ from those observed with other molybdates [13]. Therefore, the cation balancing the charge in the molybdate structure also influences the reduction and oxidation of the molybdate catalyst, apart from influencing the coordination of molybdenum (tetrahedral

vs octahedral) at different temperatures. For instance, in the nickel molybdate catalyst only the α-phase is stable at room temperature and ambient pressure, whereas the β-phase is stable at high temperature and pressure [3]. In the case of magnesium molybdate, both phases (*i.e.* α and β) co-exist at low temperature [7, 12, 14] and both the α- and β-$MgMoO_4$ phases where detected (Fig. 3.1). However, the catalyst was dominated by the β-phase at all temperatures and also under reducing and oxidising environments. This was expected since the phase composition is mainly determined during the synthesis step and the conditions used in this work (*i.e.* pH of 6 and calcination temperature of 550 °C) favour the β-phase [14]. The bulk chemical composition of the catalyst was determined by ICP-OES and gave a Mo/Mg ratio of 1.06 and the surface area of the catalyst was determined to be 4.2 m^2/g.

The Raman spectroscopy results (Fig. 3.2) showed the presence of both the magnesium molybdate and molybdenum trioxide phases. The asymmetric Mo-O stretching in the $MgMoO_4$ was indicated by the peaks at 852 and 903 cm^{-1}, with the symmetric stretching at 959 cm^{-1}. The ICP-OES results implied the presence of a slight excess of molybdenum and the Raman spectroscopy showed it to be in the MoO_3 phase as indicted by the peak at 815 cm^{-1}. The analysis of the catalyst structure by TEM showed (Fig. 3.3 a) that the catalyst consists of round particles and plate-like structures. The round particles are likely due to the magnesium molybdate phase, while the plate-like structure is due to the molybdenum trioxide phase that is present in the catalyst as indicated by the Raman spectroscopy and SEM analysis (Appendix 2.2). To further confirm that the plate-like structure is the molybdenum trioxide phase, electron diffraction on the plate-like structure was carried (Fig. 3.3 b and c) and it matches that of molybdenum trioxide reported in literature [15]. This serves as a further indication that the excess molybdenum in the catalyst is present as the molybdenum trioxide phase.

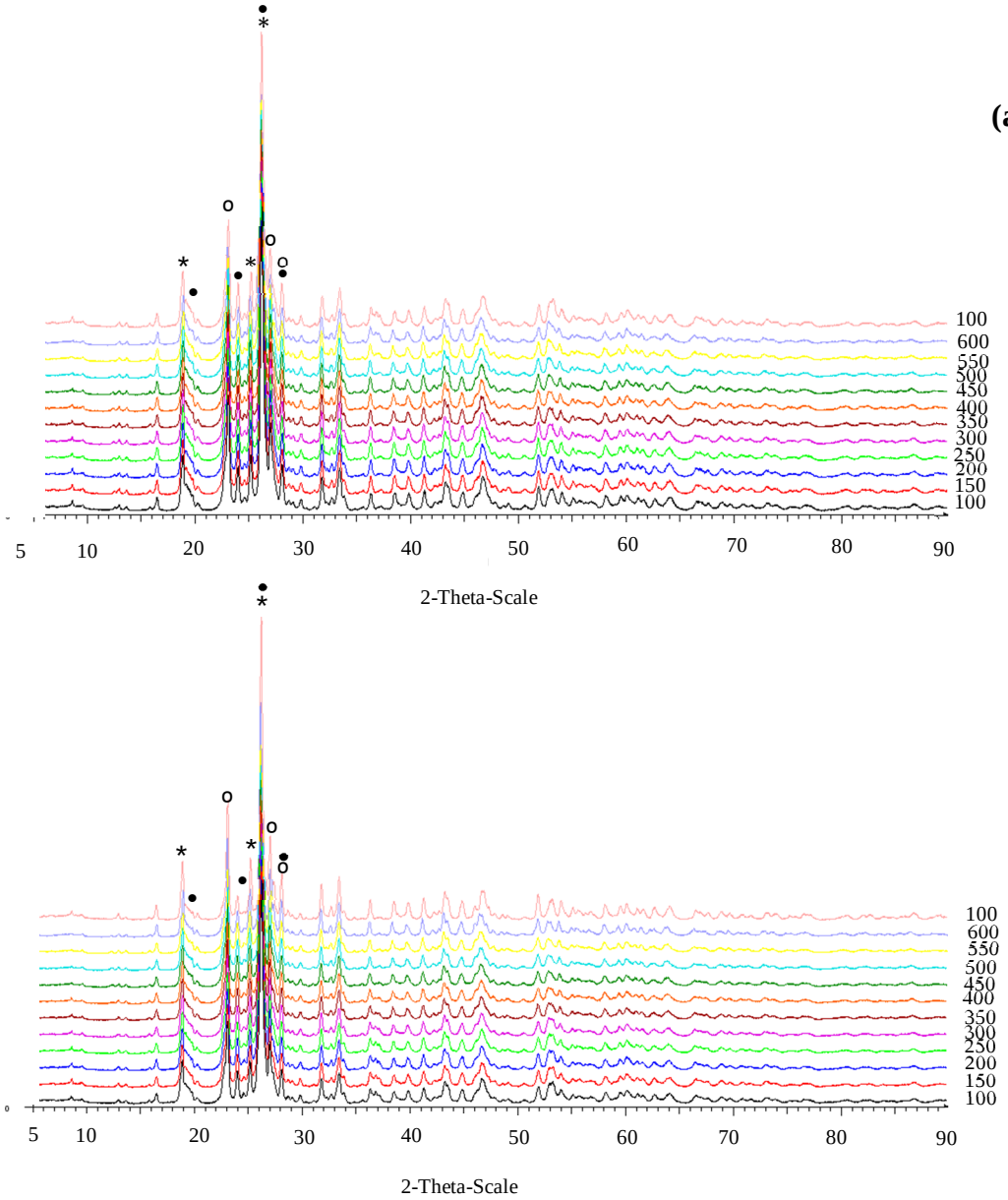

Figure 3.1: *in* situ XRD patterns of the $MgMoO_4$ catalyst in the temperature range of 100 to 600 °C under reduction environment (a) and oxidation environment (b). β-$MgMoO_4$ (*), α-$MgMoO_4$ (^{O}) and MoO_3 (•).

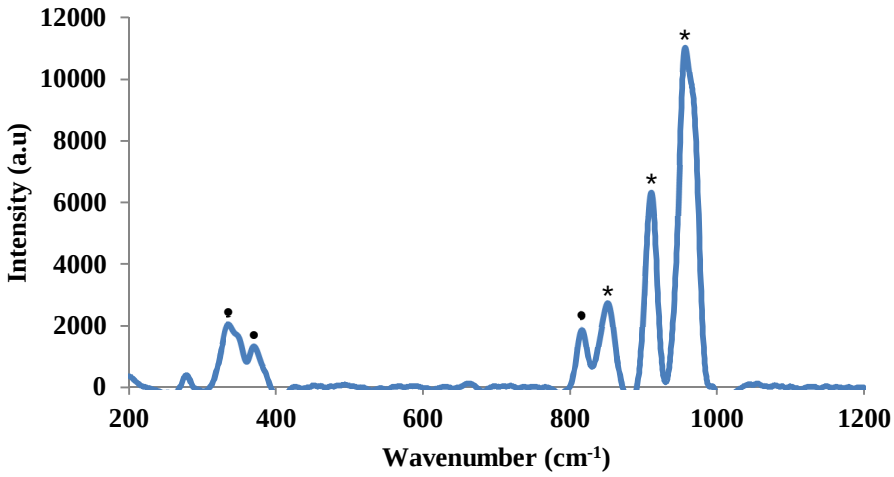

Figure 3.2: Raman spectrum of magnesium molybdate catalyst prepared by the co-precipitation method, magnesium molybdate (*) and molybdenum trioxide (•)

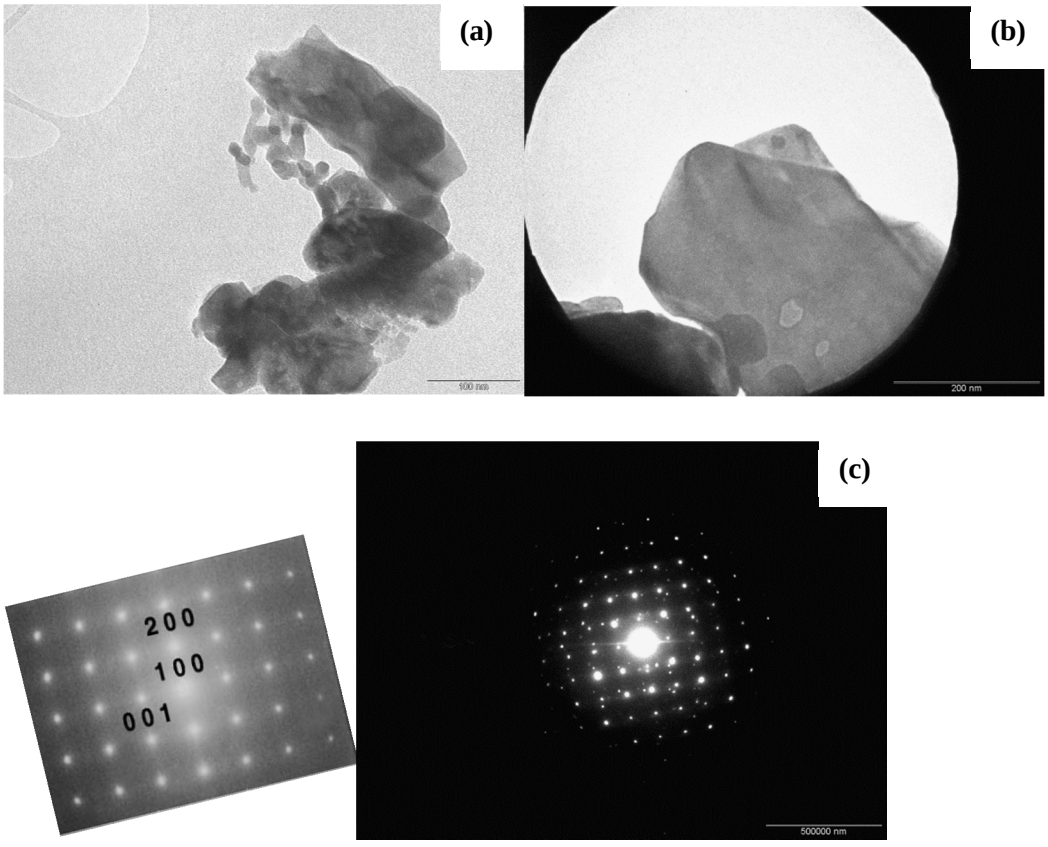

Figure 3.3: TEM image of magnesium molybdate catalyst (a) and selected area showing the plate like structure (b) and electron diffraction (c).

3.3.2) Catalytic results

This study focused at establishing the effect of carbon to oxygen ratio for the activation of *n*-octane over magnesium molybdate catalyst. The influence of oxygen concentration in the feed on the selectivity is illustrated in the equations below [16]. The carbon to oxygen (C:O) ratios studied were 8:0 (dehydrogenation), 8:1, 8:2 and 8:4. All the catalytic tests now reported were carried out at a GHSV of 4000 h^{-1}. The *n*-octane content in the feed was maintained at around 11% in the total gaseous mixture at different flow rates of air to obtain the different carbon to oxygen ratios and the balance to the 67 mL/min flow was made up with nitrogen (as a diluent).

$C_8H_{18} \longrightarrow C_8H_{16}+H_2$ (dehydrogenation) (Eq.1)

$C_8H_{18} + 0.5O_2 \longrightarrow C_8H_{16} + H_2O$ (Eq.2)

$C_8H_{18} + O_2 \longrightarrow C_8H_{14}+2H_2O$ (Eq.3)

$C_8H_{18} + 2O_2 \longrightarrow C_8H_{10} + H_2+ 4H_2O$ (Eq.4)

$C_8H_{18} + 12.5O_2 \longrightarrow 8CO_2+ 9H_2O$ (Eq.5)

3.3.2.1) n-Octane activation without fed oxygen (C:O =8:0)

The catalyst under dehydrogenation conditions (no oxygen) showed low conversion of *n*-octane. The low conversion is likely mostly due to the thermodynamic limitation caused by the presence of the abstracted hydrogen from the *n*-octane molecule [4]. The conversion of *n*-octane was below 1% at low temperatures (up to 400 °C), however, the increase in the reaction temperature beyond this resulted in a significant increase in the conversion of *n*-octane (Fig. 3.4) and also the reduction of the magnesium molybdate catalyst, which has an onset temperature of ~550 ^{O}C under 5% H_2 as shown in TPR results (Chapter two). The dominant product at all temperatures is 2-octene, which is considered the primary dehydrogenation product, as a result of the abstraction of hydrogen from *n*-octane. The position of the abstraction affects which octene isomer is formed, in addition to which octene isomer is the more stable [17-19]. The breakdown of octenes (Fig. 3.4) demonstrated that only one octene isomer, 2-octene, is formed at all temperatures. In comparison with the other octene isomers, 2-octene is the most thermodynamically stable octene isomer, thus it is expected to have high selectivity [17]. However, at 550 °C aromatics formation was detected

(selectivity of 55%), in particular C8 aromatics (*i.e.* ethylbenzene (25%), styrene (12%) and xylene (18%)). This indicates that the catalyst favours the 1,6-cyclization mode that leads to the formation of ethylbenzene that then can undergo dehydrogenation to form styrene [20-22], rather than the 2,7-cyclization that results in xylene formation.

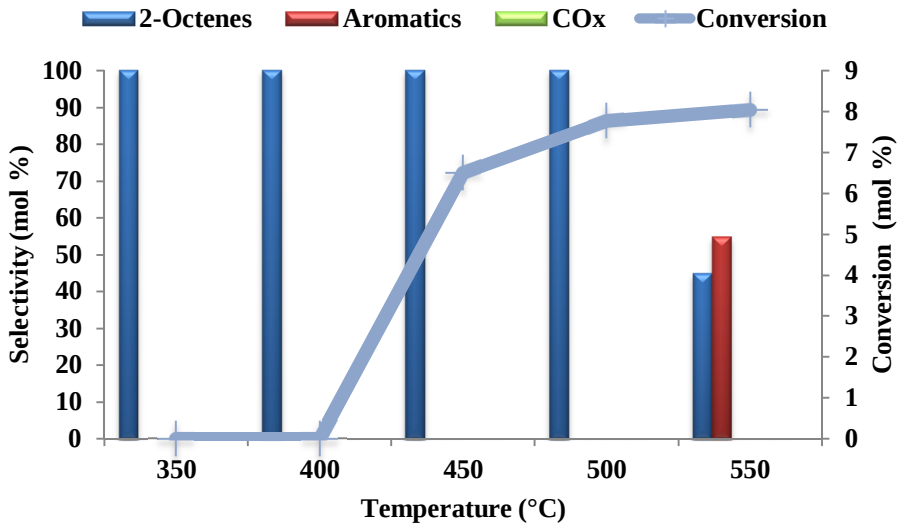

Figure 3.4: *n*-Octane conversion and selectivity patterns over the magnesium molybdate at 4000 h^{-1} and C:O (8:0) as a function of temperature.

The stability of the catalyst was examined in a time on line experiment where the temperature was maintained at 550 °C (Fig. 3.5). The conversion decreased with increase in the reaction time. The decreased in the conversion could be due the stripping of the lattice oxygen from the magnesium molybdate catalyst. The selectivity of aromatics decreased with increasing reaction time, while the octenes selectivity increased. This could also be due to the stripping of the lattice oxygen which is required for the cyclization of octenes to aromatic (*i.e.* ethylbenzene, styrene and xylene). Thus, initially the reaction likely takes place through the Mars and van Krevelen (MvK) mechanism (lattice oxygen removal) producing octenes and aromatics. As the concentration of the lattice oxygen decreases the selectivity to aromatics decreases (oxygen consuming steps) and selectivity to octenes increase (because the sequential reaction to form aromatics stops).

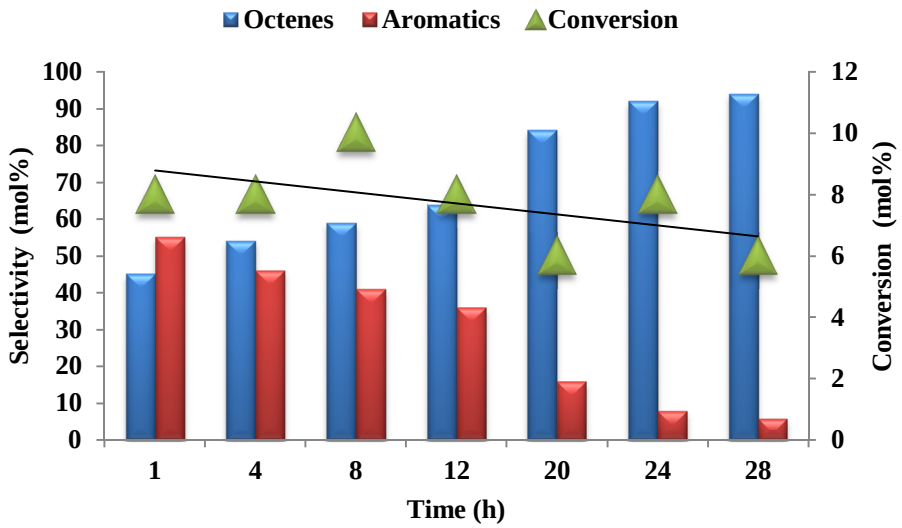

Figure 3.5: Time on stream of *n*-octane over the magnesium molybdate catalyst under dehydrogenation conditions and GHSV of 4000 h^{-1}at 550 ^{O}C.

3.3.2.2) Effect of carbon to oxygen ratio on activity and selectivity

Three different C:O ratios (*i.e.* 8:1, 8:2 and 8:4) were tested in order to understand the catalyst stability and activity under oxygen lean and oxygen rich environments. The conversion of *n*-octane (Fig. 3.6 a) increased with increase in the oxygen content in the reaction mixture. This is due to the oxygen in the reaction feed reacting with the abstracted hydrogen from *n*-octane (forming H_2O) and thus shifting the equilibrium to higher conversion [4] and eliminating the thermodynamic limitation that is associated with the dehydrogenation reaction. Another influence could be the increase in the (MvK) mechanism rate leading to an increase in conversion of *n*-octane. Furthermore, the shift in the equilibrium to higher conversion could be due to the formation of the thermodynamically stable COx product [17]. This trend was also observed in the ODH of *n*-octane over a ceria based catalyst [23] and vanadium based catalysts [17]. The conversion of n-octane significantly increased from 450 ^{O}C under all C:O ratios; this could be as a result of the reduction of the magnesium molybdate catalyst which corresponds to the onset reduction temperature (~550 ^{O}C) under 5% H_2 observed in TPR analysis (Chapter 2).

The selectivity profile to octenes under different C:O ratios (Fig. 3.6 b) showed the opposite trend to that of the conversion of *n*-octane. Thus, the selectivity to octenes decreased as the oxygen content in the reaction mixture increased and as the reaction temperature increased. These two factors likely promoted sequential reactions where octenes produce aromatics,

COx and cracked products either directly or *via* multi-step reactions. The most dominant octene isomer under the different C:O ratio is 2-octene, since this isomer is the most thermodynamically stable octene isomer [17]. These findings correlate well with those observed in the ODH of *n*-octane over ceria [23] and vanadium [17] based catalysts. However, at high temperatures and under oxygen rich environments the selectivity to 2-octene decreased. This could be due to 2-octene reacting further to form aromatics, since 2-octene possess 5 adjacent sp^3 carbon atoms that can rotate freely to cyclize and react further to form aromatics, while 3-octene and 4-octene have a more rigid structure that limits them from reacting further to form aromatics [17, 24].

The effect of C:O ratio on the selectivity of C8 aromatics (*i.e.* ethylbenzene, styrene and xylene) was investigated. The selectivity to aromatics increased with increase in the oxygen content and reaction temperature (Fig. 3.6 c). Furthermore, under the oxygen richest environment (8:4 C:O ratio) the initial aromatics formation temperature was 400 °C, rather than 450 °C under the other C:O ratios (*i.e.* 8:1 and 8:2 C:O ratio). Considering the selectivity of both octenes and aromatics suggests that there is a close relationship between them, where the octenes selectivities decrease the aromatics selectivities increase, indicating the possibility that octenes are precursors to aromatics. The highest selectivity to aromatics was for ethylbenzene, followed by styrene and then xylene. Therefore, the catalyst favours 1,6-cyclization (forming ethylbenzene and styrene) rather than 2,7-cyclization (forming xylene). A similar observation was made under the dehydrogenation condition, however, introduction of oxygen in the reaction mixture improved the selectivity to aromatics, as well as lowering the formation temperature.

One of the disadvantages of ODH is the decrease in the selectivity to target products due to the formation of the thermodynamically stable COx [4]. The selectivity to COx (*i.e.* CO and CO_2) (Fig. 3.6 d) increases with increase in the oxygen content in the reaction mixture. This could be as a result of the physisorbed oxygen promoting secondary or combustion reactions of the primary ODH products (mainly octenes) [25], this was supported by increase in the formation of CO (indicating oxidation of primary products) and CO_2 (indicating combustion of *n*-octane) [26], furthermore, the ratio of CO to CO_2 (Appendix 3.1) was not influenced by the reaction temperature which could indicate that CO does not undergo oxidation to CO_2 [27]. The selectivity of COx peaked at 450 °C, which is the reduction temperature of the magnesium molybdate catalyst. A correlation between the aromatic selectivities and COx can be seen, since above 450 °C the selectivity to aromatics increase and selectivity to COx

decreased. This trend was also observed in other work with *n*-octane ODH [16, 17, 23, 28]. Thus, from *ca.* 450 °C sufficient energy is supplied for the aromatics formation, making it a competitive reaction to deep oxidation.

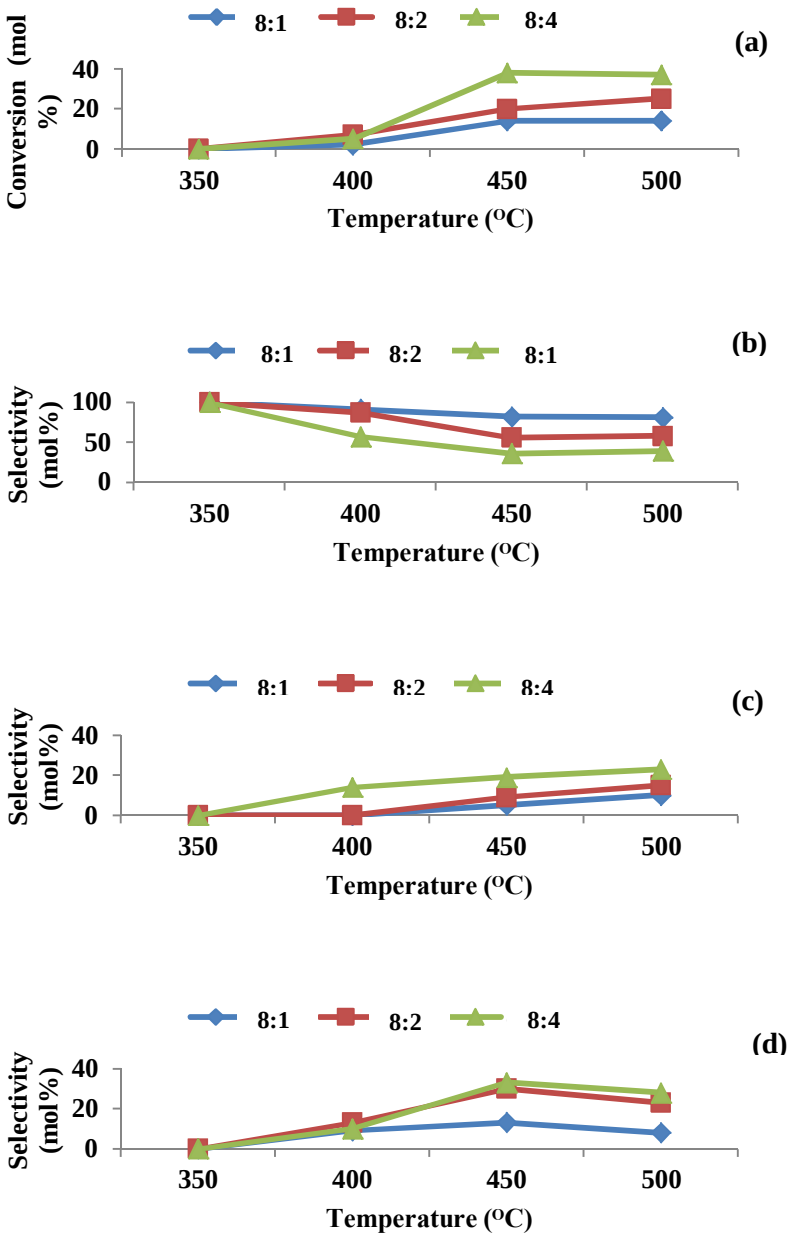

Figure 3.6: Effect of the C:O ratio on the ODH of *n*-octane in terms of conversion (a), selectivity to octenes (b), selectivity to aromatics (c) and selectivity to COx (d) as function of temperature at 4000 h^{-1} GHSV.

The oxygen conversion (Fig. 3.7) increased with increase in both reaction temperature and oxygen concentration in the reaction mixture. The oxygen conversion increase was

accompanied by increase in the conversion of *n*-octane and selectivity to COx, likely due to the manipulation of the reaction equilibrium (towards product formation) [17], the increase in the selectivity to COx could be as a result of the physisorbed oxygen on the surface of the catalyst. Furthermore, the selectivity to aromatics increased with increase in oxygen concentration and conversion. This might be due to the presence of sufficient amount of oxygen for cyclization of octenes and dehydrogenation of those cyclic products to aromatics (mainly ethylbenzene and styrene) [25]. At low temperatures (*i.e.* 350 and 400 °C) the oxygen conversion is very low, however, from 450 °C the conversion significantly increased, this could be due to the oxygen replacing the lattice oxygen in the catalyst, since this corresponds to the reduction temperature of the magnesium molybdate phase.

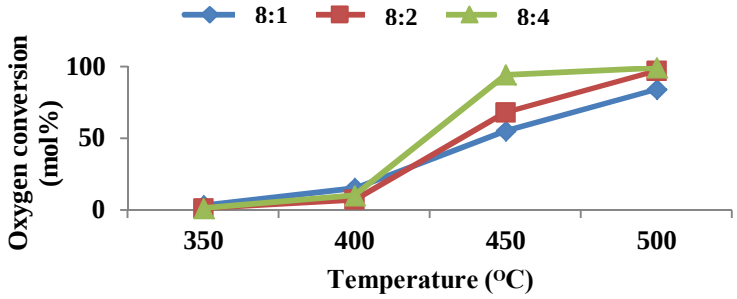

Figure 3.7: Oxygen conversion in the ODH of *n*-octane over the magnesium molybdate catalyst as a function of temperature and oxygen concentration in the reaction mixture at 4000 h^{-1} GHSV.

The space time yield (STY) [27] of octenes (STY($g_{octenes}$ g_{cat}^{-1} s^{-1})) (Fig. 3.8 a), emphasises the importance of oxygen in the feed in increasing the STY of octene. The general trend that was observed is as the oxygen concentration in the feed and reaction temperature increases the STY of octenes increases. This trend was stronger with the STY of aromatics (Fig. 3.8 b), indicating the need for oxygen in the reaction and the higher reaction temperature to produce C8 aromatics. This could be explained by considering that aromatic formation takes place through subsequent reaction of octenes to aromatics through cyclization and dehydrogenation steps [25]. All these steps require oxygen to be present [29], therefore, the STY increased with increase in oxygen concentration. The increase in the STY for these two classes of products (*i.e.* octenes and aromatics) with increase in temperature is a consequence of crossing the activation barrier. Similar observations were made with the ODH of *n*-octane over vanadium based catalyst [17, 19] .

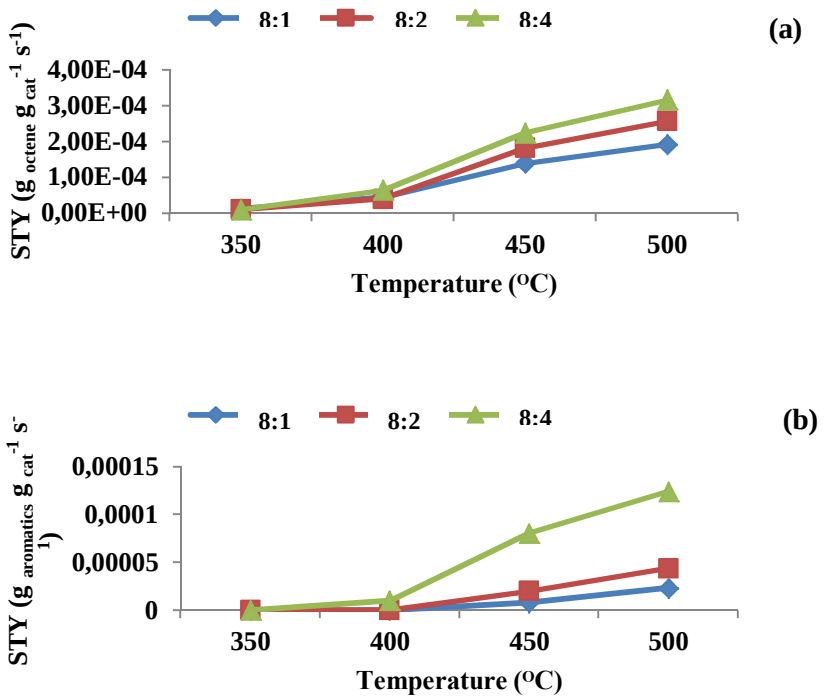

Figure 3.8: Space time yield of octenes (a) and aromatics (b) over the magnesium molybdate catalyst in the ODH of *n*-octane, as a function of oxygen concentration and reaction temperature at 4000 h^{-1} GHSV.

3.3.2.3) iso-Conversion with the different C:O ratios at 500 °C

In order to compare and determine the most selective or optimum conditions among the different C:O ratios, *iso*-conversion (~26%) data was obtained for the reactions at 8:2 and 8:4 C:O ratios by changing the GHSV to obtain similar conversion under the different carbon to oxygen ration. The results obtained (Fig. 3.9) showed that the ratio of 8:2 (C:O) shows best selectivity towards octenes and aromatics combined, among the two ratios. The highest selectivity towards aromatics was obtained under the 8:4 C:O conditions. This could be due to the available oxygen required for the formation of the aromatic molecules, assuming their formation takes place through oxidative dehydrogenation, cyclization and aromatization. The *iso*-conversion results also showed that the increase in the oxygen content in the reaction mixture promoted deep oxidation or combustion of the primary products of *n*-octane activation.

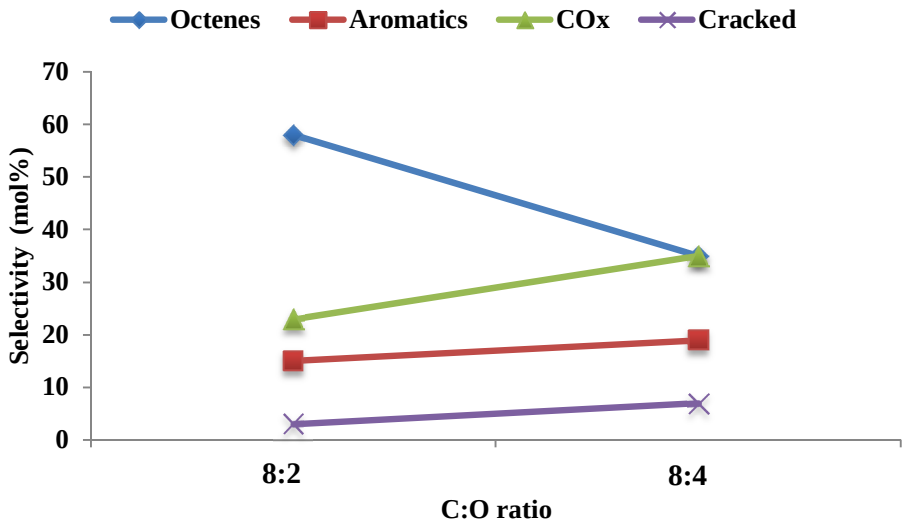

Figure 3.9: Selectivity profile at different C:O ratios at *iso*-conversion of ~26 at 500 °C, for the ODH of *n*-octane over magnesium molybdate catalyst.

The breakdown of the selectivity to the different octene isomers at *iso*-conversion (Fig. 3.10 a) shows that the selectivity to both 1-octene and 2-octene decreased with increase in the oxygen content in the reaction. It is likely that these two octene isomers undergo cyclization and dehydrogenation to form the aromatic products, which is supported by the increase in the aromatics selectivity. Ethylbenzene and styrene are likely be the product of 1,6 cyclization while xylene would be formed through the 2,7-cyclization [24]. The selectivity to different aromatics at *iso*-conversion (Fig. 3.10 b) shows an increase with increase in the oxygen concentration in the reaction mixture. Also seen is the increase in the selectivity to styrene as the oxygen content increase in the reaction mixture. This could be due to the availability of oxygen to carry out the further oxidative dehydrogenation step of ethylbenzene to styrene. The selectivity to xylene was not greatly affected by the oxygen content in the reaction mixture, which could be because the formation of xylene requires less oxygen in comparison to styrene.

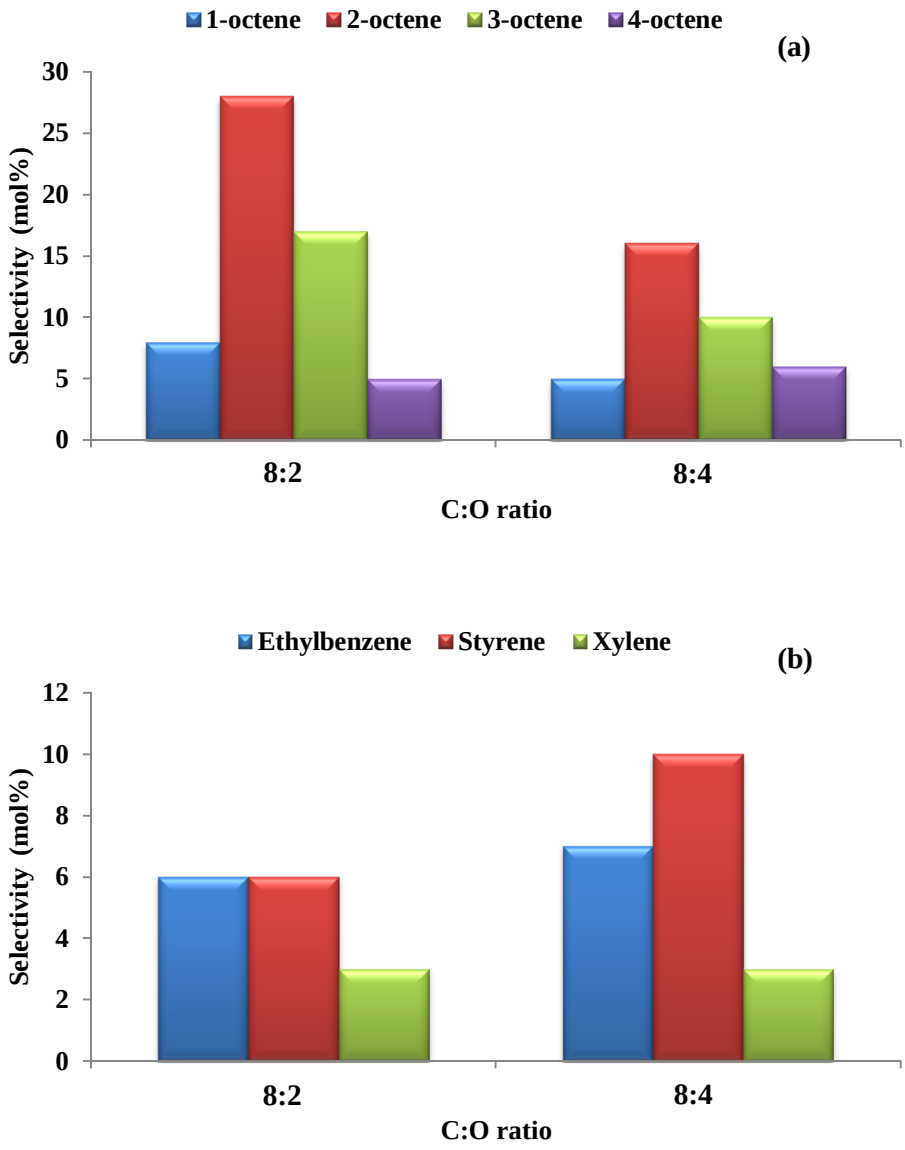

Figure 3.10: Octenes isomers (a) and aromatics (b) breakdown at *iso*-conversion of different C:O ratio at 500 °C, over the magnesium molybdate catalyst.

3.3.3) Used catalyst characterization

The used catalysts after each run were kept under nitrogen and characterized by XRD and Raman spectroscopy in order to understand the effect of the oxygen content in the reaction mixture on the catalyst structure. The XRD results (Fig. 3.11) indicate that the catalyst did not undergo structural changes under the different oxygen concentration in the reaction mixture. All the phases observed in the fresh catalyst are present in the used catalyst.

Furthermore, the ratio of α- to β-$MgMoO_4$ seems to be unaffected by the oxygen content. However, the Raman results (Fig. 3.12) show that some of the catalysts did undergo partial reduction which was influenced by the oxygen content in the reaction mixture. The Raman spectra (Fig. 3.12 a and b) of the catalysts that were used under oxygen lean environments (*i.e.* 8:0 and 8:1 C:O) showed that both catalysts underwent partial reduction, as indicated by the formation of MoO_3 shown by the peak at ~ 815 cm^{-1}. The intensity of the MoO_3 peak in comparison to the intensity of the $MgMoO_4$ can indicate the level of reduction. As expected the catalyst used under dehydrogenation conditions showed the highest level of reduction, since there is no oxygen in the feed to reoxidize the catalyst. The reduction level decreased with increase in the oxygen content, due to the oxygen in the feed reoxidizing the catalyst.

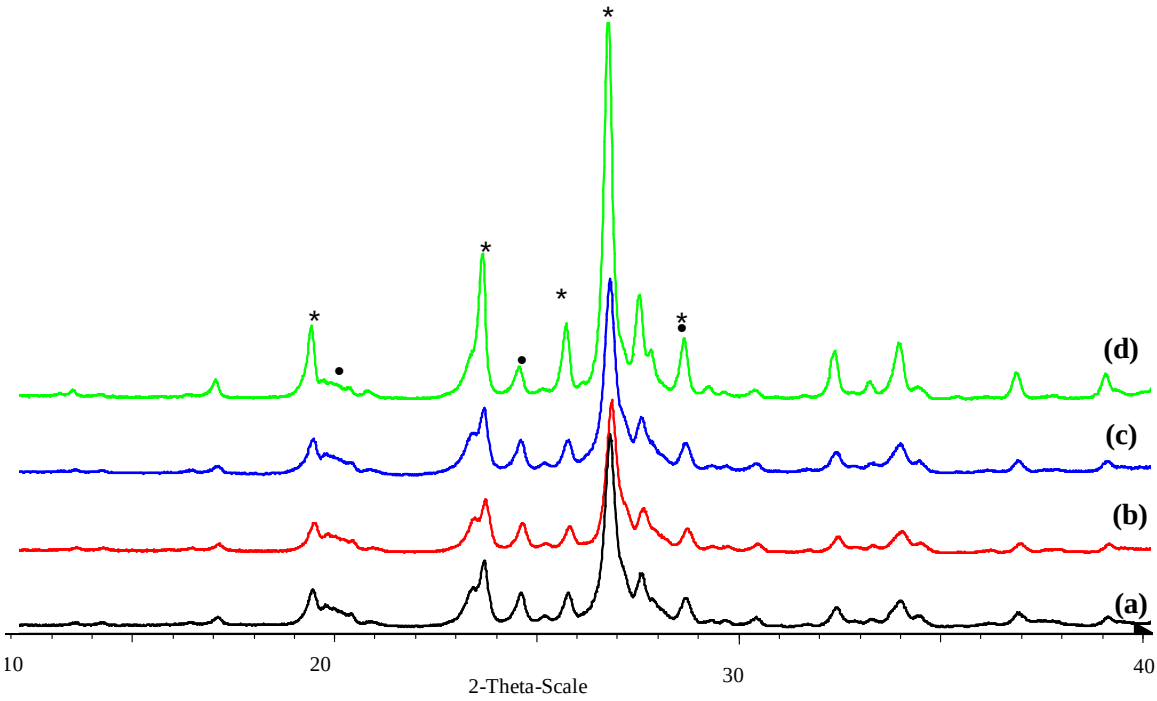

Figure 3.11: XRD patterns of the used magnesium molybdate catalyst in the activation of *n*-octane at 4000 h^{-1} under different C:O ratios: 8:0 (a), 8:1 (b), 8:2 (c), and 8:4 (d) magnesium molybdate (*) and molybdenum trioxide (•).

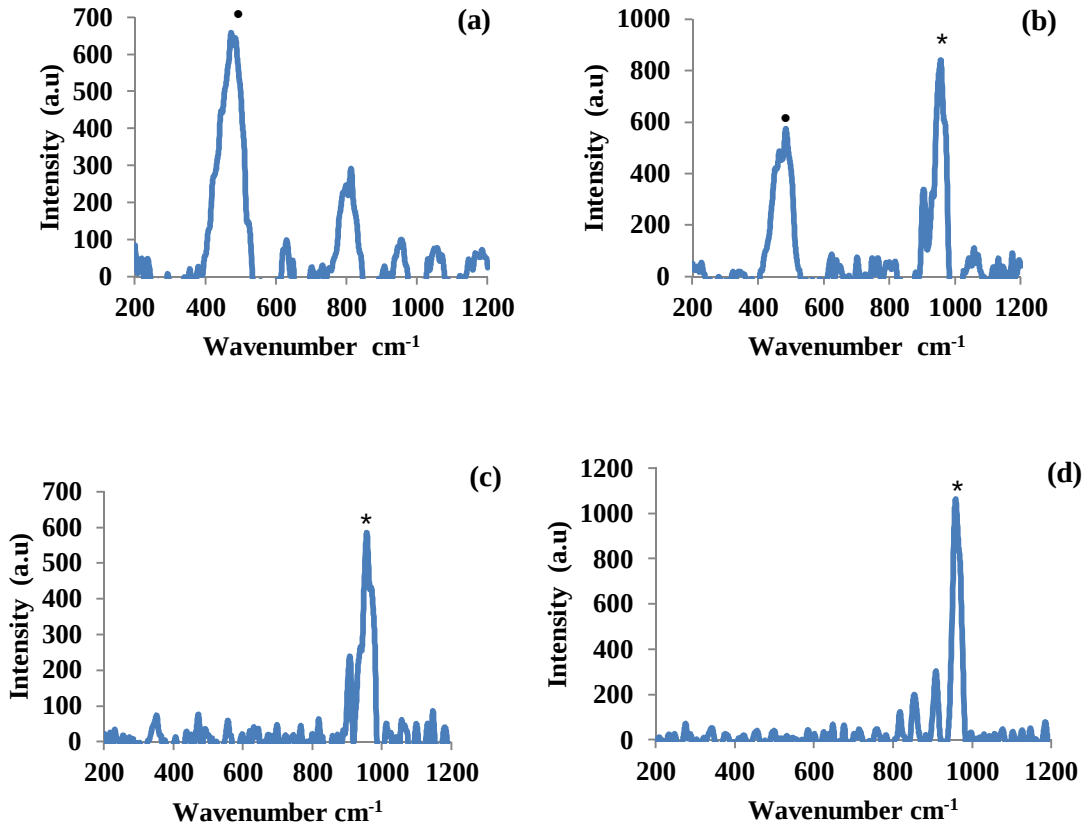

Figure 3.12: Raman spectra of the used magnesium molybdate catalyst at different C:O ratios; 8:0 (a), 8:1 (b), 8:2 (c), and 8:4 (d), MoO_3 (•) and $MgMoO_4$ (*).

3.4) Conclusion

Magnesium molybdate is active in the oxidative dehydrogenation and dehydrogenation of *n*-octane. Oxygen concentration in the feed influenced the catalyst stability (the catalyst undergoes partial reduction under oxygen lean environments). Oxygen content also influenced the activity of the catalyst in terms of *n*-octane conversion (the conversion increased with increase in oxygen content, due to reaction equilibrium manipulation) and the selectivity to value added products was also influenced by the oxygen content, where high oxygen content lead to an increase in COx selectivity, however, selectivity to aromatics increased also. The optimum C:O ratio was determined at *iso*-conversion at 500 °C to be 8:2, where up to 71% selectivity to olefins and aromatics was obtained.

3.5) Acknowledgements

We thank NRF, SASOL and THRIP (grant Number TP 1208035643) for financial support.

The electron microscopy unit in UKZN for their help with TEM imaging.

3.6) References

[1] V.D.B.C. Dasireddy, S. Singh, H.B. Friedrich, Appl. Catal., A: Gen., 421–422 (2012) 58-69.
[2] H.B. Friedrich, N. Govender, M.R. Mathebula, Appl. Catal., A: Gen., 297 (2006) 81-89.
[3] B. Pillay, M.R. Mathebula, H.B. Friedrich, Appl. Catal., A: Gen., 361 (2009) 57-64.
[4] M.M. Bhasin, J.H. McCain, B.V. Vora, T. Imai, P.R. Pujadó, Appl. Catal., A: Gen., 221 (2001) 397-419.
[5] A. Kaddouri, R. Del Rosso, C. Mazzocchia, P. Gronchi, D. Fumagalli, J. Therm. Anal. Calorim. 66 (2001) 63-78.
[6] Y. Yoon, W. Ueda, Y. Moro-oka, Top. Catal., 3 (1996) 265-275.
[7] J. Miller, N. Jackson, L. Evans, A. Sault, M. Gonzales, Catal. Lett., 58 (1999) 147-152.
[8] L.E. Cadus, M.C. Abello, M.F. Gomez, J.B. Rivarola, Ind. Eng. Chem.Res., 35 (1996) 14-18.
[9] W. Ueda, K.H. Lee, Y.S. Yoon, Y. Moro-oka, Catal. Today, 44 (1998) 199-203.
[10] L.E. Cadus, M.F. Gomez, M.C. Abello, Catal. Lett., 43 (1997) 229-233.
[11] B. Pillay, M.R. Mathebula, H.B. Friedrich, Catal. Lett., 141 (2011) 1297-1304.
[12] Y.J. Zhang, I. Rodríguez-Ramos, A. Guerrero-Ruiz, Catal. Today, 61 (2000) 377-382.
[13] S. Pradhan, J.K. Bartley, D. Bethell, A.F. Carley, M. Conte, S. Golunski, M.P. House, R.L. Jenkins, R. Lloyd, G.J. Hutchings, Nat. Chem., 4 (2012) 134-139.
[14] Y.S. Yoon, K. Suzuki, T. Hayakawa, S. Hamakawa, T. Shishido, K. Takehira, Catal. Lett., 59 (1999) 165-172.
[15] M. Dieterle, G. Mestl, J. Jäger, Y. Uchida, H. Hibst, R. Schlögl, J. Mol. Catal. A: Chem., 174 (2001) 169-185.
[16] V.D.B.C. Dasireddy, S. Singh, H.B. Friedrich, Appl. Catal., A: Gen., 456 (2013) 105-117.
[17] E. A. Elkhalifa, H. B. Friedrich, Catal. Lett., 141 (2011) 554-564.
[18] R. Burch, M.J. Hayes, J. Mol. Catal. A: Chem., 100 (1995) 13-33.
[19] E.A. Elkhalifa, H.B. Friedrich, Appl. Catal., A: Gen., 373 (2010) 122-131.
[20] W.P. Addiego, W. Liu, T. Boger, Catal. Today, 69 (2001) 25-31.
[21] W. Liu, W.P. Addiego, C.M. Sorensen, T. Boger, Ind. Eng. Chem.Res., 41 (2002) 3131-3138.
[22] W. Oganowski, J. Hanuza, H. Drulis, W. Miśta, L. Macalik, Appl. Catal., A: Gen., 136 (1996) 143-159.
[23] M. Narayanappa, V.D.B.C. Dasireddy, H.B. Friedrich, Appl. Catal., A: Gen., 447–448 (2012) 135-143.
[24] E.A. Elkhalifa, H.B. Friedrich, J. Mol. Catal. A: Chem., 392 (2014) 22-30.
[25] V.D.B.C. Dasireddy, H.B. Friedrich, S. Singh, Appl. Catal., A: Gen., 467 (2013) 142-153.
[26] L.M. Madeira, F.J. Maldonado-Hódar, M.F. Portela, F. Freire, R.M. Martin-Aranda, M. Oliveira, Appl. Catal., A: Gen., 135 (1996) 137-153.

[27] B. Solsona, J.M. López Nieto, P. Concepción, A. Dejoz, F. Ivars, M.I. Vázquez, J. Catal., 280 (2011) 28-39.
[28] M.I. Fadlalla, H.B. Friedrich, Catal. Sci. Tech., 4 (2014) 4378-4385.
[29] P. Meriaudeau, A. Thangaraj, C. Naccache, S. Narayanan, J. Catal., 146 (1994) 579-582.

Chapter four

The effect of the oxidation environment on the activity and selectivity to aromatics and octenes over cobalt molybdate in the oxidative dehydrogenation of n-octane

Abstract

A cobalt molybdate catalyst was synthesised by the co-precipitation method and characterized by XRD, BET-surface area measurements, ICP-OES, Raman, TPR, TPO, SEM and SEM-EDX. XRD results showed that the dominate phase in the catalyst is the β-phase. The ratio of Co:Mo was determined by ICP-OES to be 1:1.04. The excess molybdenum is found in the molybdenum trioxide phase as shown by the Raman results. The TPR/O/R/O/R results showed that the catalyst can undergo the redox cycle where cobalt molybdate reduces to the molybdite and spinel form of cobalt molybdate (by 5% hydrogen) and oxidize back to the cobalt molybdate after oxygen exposure. The catalytic testing was carried out in a continuous flow fixed bed reactor at atmospheric pressure and a temperature range of 350 to 550 °C in 50 °C intervals with different oxygen content (*i.e.* C:O ratio of 8:0, 8:1, 8:2, 8:3 and 8:4) in the reaction mixture. The conversion of *n*-octane increased with increase in the oxygen content in the reaction mixture, which was accompanied by changes in the selectivity patterns. The dominant products were the octenes at all temperatures and different carbon to oxygen ratios. Furthermore, the selectivity to aromatic products increased with increase in the strength of the oxidising environment in the feed mixture and was dominated by styrene and ethylbenzene (both products of 1,6-cyclization). The yields of octenes, aromatics, cracked products and COx at 500 °C showed that an increase in the oxygen content resulted in a decrease in the yield to octenes and an increase in what can be considered secondary products (*i.e.* aromatics, cracked products and COx). The total selectivity % of value-added products (*i.e.* octenes and aromatics) also decreased with increase in the oxygen content, due to the increase in cracked products and COx yields (which are not considered value added products). Characterization of the spent catalysts at the different conditions showed that the catalyst maintains the cobalt molybdate phase under the 8:2, 8:3 and 8:4 C:O conditions, while complete segregation took place under dehydrogenation conditions and partial segregation occurred at an 8:1 C:O ratio.

Keywords: Cobalt molybdate, oxidative dehydrogenation, dehydrogenation, carbon to oxygen ratio, selectivity to octenes and aromatics.

4.1) Introduction

Alkenes have been produced by dehydrogenation for the past six decades, and have large scale applications in the petrochemical industry. They are used as feedstock in the production of value added products (though functionalization) [1, 2]. In recent years, the petrochemical industry has looked towards using paraffins to produce value-added products through oxidative dehydrogenation or partial oxidation of paraffins, since paraffins are abundant and cheap, in part due to the increase in the number of the coal to liquid and gas to liquid plants (CTL and GTL) worldwide [3]. Oxidative dehydrogenation of paraffins offers a number of advantages, namely; the reaction is exothermic, low energy costs, low environmental impact, lower greenhouse gas emissions [3] and it does not suffer from equilibrium limitation. Moreover, dehydrogenation of alkanes is accompanied by low selectivities and high yields of coke and cracked products, moreover, carbon deposit results in blockage of the active site in the catalyst leading to a shorting of the life span of the catalyst [4]. The use of oxygen in the reaction mixture reduces coke formation and overcomes equilibrium and thermodynamic limitations of the dehydrogenation reaction [1, 5, 6]. Therefore, activation of paraffins via oxidative dehydrogenation is gaining a lot of interest academically and industrially [7, 8].

Molybdates are considered one of the better catalysts for the oxidation of olefins due to their suitable solid-state redox [9-15]. Furthermore, the advantage of molybdates is that the metal-oxygen bond can be tailored, based on the structure and the nature of the molybdate [16]. It has been shown that the different phases (*i.e.* α and β) nickel molybdate have different activity and selectivity to hexenes in the oxidative dehydrogenation of *n*-hexane [3]. Also the effect of carbon to oxygen ratio affects the selectivity to hexenes over the β-nickel molybdate [17].

Cobalt molybdate has been used in different types of catalysis such as hydrodesulfurization [18], hydrolysis of carbonyl sulphide (COS) [19] and the oxidative dehydrogenation of light paraffins, mainly propane [20-23]. For the latter processes selectivity to useful products was

64% at 7% conversion of propane, however, an increase in the conversion to 15% resulted in a decrease in the selectivity to useful products [23]. Moreover, cobalt molybdate showed good activity and selectivity to propene among different molybdates studied, such as Cu, Fe, Mn and Zn [20-22].

Based on the activity and selectivity of cobalt molybdate in the oxidative dehydrogenation of light paraffins and the increase in the amount of *n*-octane worldwide, we decided to investigate the activity and selectivity of cobalt molybdate in the oxidative dehydrogenation of *n*-octane. In addition, the effect of the carbon to oxygen ratio on the catalyst activity, selectivity and stability was explored.

4.2) Experimental

4.2.1) Catalyst synthesis

The cobalt molybdate catalyst was prepared by the co-precipitation method modified from literature [21]. Equi-concentration solutions of molybdenum ($(NH_4)Mo_7O_{24}.4H_2O$, Merck) and cobalt ($Co(NO_3)_2.6H_2O$), ACE) were prepared with deionized water. The molybdenum solution was stirred at room temperature and the pH was adjusted to 6 using aqueous ammonia (Saarchem). Then the cobalt solution was added drop-wise with continuous stirring. Upon addition of the cobalt solution the mixture turned purple. After complete addition of the cobalt solution, the mixture was heated to 90 °C. Once part of the water had evaporated a purple precipitate formed. The slurry was then dried in an oven for 12 hours at 110 °C. The purple precipitate was calcined at 550 °C for 2 hours to produce cobalt molybdate.

4.2.2) Catalyst characterization

The phase composition of the catalyst was analysed by X-Ray diffraction (XRD) using a Bruker D8 Advance operated with a copper radiation source (1.5406 nm) and an Anton Paar XRK 900 reaction chamber. BET-surface area measurements were carried out after the sample was degassed at 200 °C overnight under nitrogen flow using a Micromeritics flow prep 060 and analysed using a Micromeritics Tristar II. The Raman analyses were carried out using an Advantage 532 series spectrometer with Nuspec software. The molar ratio of the two metals (*i.e.* cobalt and molybdenum) in the bulk of the catalyst was determined by

inductively coupled plasma-optical emission spectroscopy (ICP-OES) using a PerkinElmer Precisely Optima 5300DV, after the sample was digested using hydrochloric acid (HCl 32%, Merck). Temperature programme reduction (TPR), temperature programme desorption (TPD) and temperature programmed reduction/oxidation/reduction (TPR/O/R/O/R) were carried out in a Micromeritics 2920 Autochem II chemisorption analyser following a reported method [1]. The catalyst structure and surface morphology were viewed using a Ziess Ultra Plus scanning electron microscope (SEM). Samples were placed on aluminium stubs using a double sided carbon tape and the samples were coated with carbon.

4.2.3) Catalytic testing

The catalytic testing was carried out using a continuous flow fixed bed reactor in vertical flow mode. The catalyst was placed in the middle of the isothermal region in the stainless steel tube (10 mm ID and 210 mm length). All voids in the reactor tube were filled with carborandum (24 gritt, Polychem). 1 mL (0.8091 g) of the catalyst was freshly used for each reaction, with a particle size between 1000-600 µm. All reactions were carried out in the temperature range of 350 – 550 °C at 50 °C intervals. The molar ratio of carbon to oxygen was adjusted to obtain the different C:O ratios (*i.e.* 8:1, 8:2, 8:3 and 8:4) using air as the oxygen source. The target GHSV of 4000 h^{-1} (total flow of gases 67 mL/min) was obtained by using nitrogen as diluent inert gas. All liquids (unreacted octane and products) were collected in a catch-pot that is cooled to 2 °C. The volume of the gaseous products were measured using a Ritter Drum-Type gas flow meter. All the reaction products (liquid and gas) were identified and quantified using gas chromatography (GC). The gaseous products were injected into a PerkinElmer Clarus 400 (GC) equipped with a thermal conductivity detector (TCD) (COx analysis) and also in a PerkinElmer Clarus 400 (GC) equipped with a flame ionization detector (FID). The liquid products from the catch-pot were analysised by the GC with the FID detector. All reactions reported have a carbon balance between 95-105% and the results reported are the average of at least two runs.

4.2.4) Used catalyst characterization

The used catalyst was kept under nitrogen after the reaction and characterized by XRD, BET-surface area measurements and Raman spectroscopy as described in Section 4.2.2.

4.3) Results and discussion

4.3.1) Catalyst characterization

The X-Ray diffraction results (Fig. 4.1 a) showed the two phases of the cobalt molybdate present, which are the α- and β-$CoMoO_4$. The main difference between these two phases is in the co-ordination environment around the molybdenum center. The co-ordination around the molybdenum centre in β-$CoMoO_4$ is partially distorted tetrahedral, while in the α-$CoMoO_4$ phase the co-ordination is octahedral around the molybdenum centre [24]. The α- and β- phases of cobalt molybdate also differ in colour is the physical appearance, where the former is purple in colour and the latter is green. The transformation between the two phases can be achieved by applying pressure or increasing the temperature. The dominance of the β-phase at room temperature is expected, since that phase is the more stable form of $CoMoO_4$ at room temperature and atmospheric pressure [24].

The Raman analysis (Fig. 4.1 b) showed two peaks at 940 and 818 cm^{-1}. The peak at 940 cm^{-1} corresponds to the cobalt molybdate phase, in particular the β-form of cobalt molybdate [25]. Thus, these results relate well with the XRD results showing that the β-$CoMoO_4$ is the dominant phase. Moreover, the expected Raman peak for the α-$CoMoO_4$ (at 950 cm^{-1}) was not clearly observed. However, the broadening of the peak at 940 cm^{-1} suggested that the peak due to α-$CoMoO_4$ could be overlapping with the characteristic peak of the β-$CoMoO_4$. The presence of MoO_3 was indicated by the Raman peak at 818 cm^{-1}, which corresponds to the Mo-O asymmetric frequency [26]. The presence of the excess molybdenum (likely in the form of MoO_3) was also detected by ICP-OES which gave a Co:Mo ratio of 1:1.04. The surface area of the material was 12 m^2/g, which is in the normal range for molybdates [21].

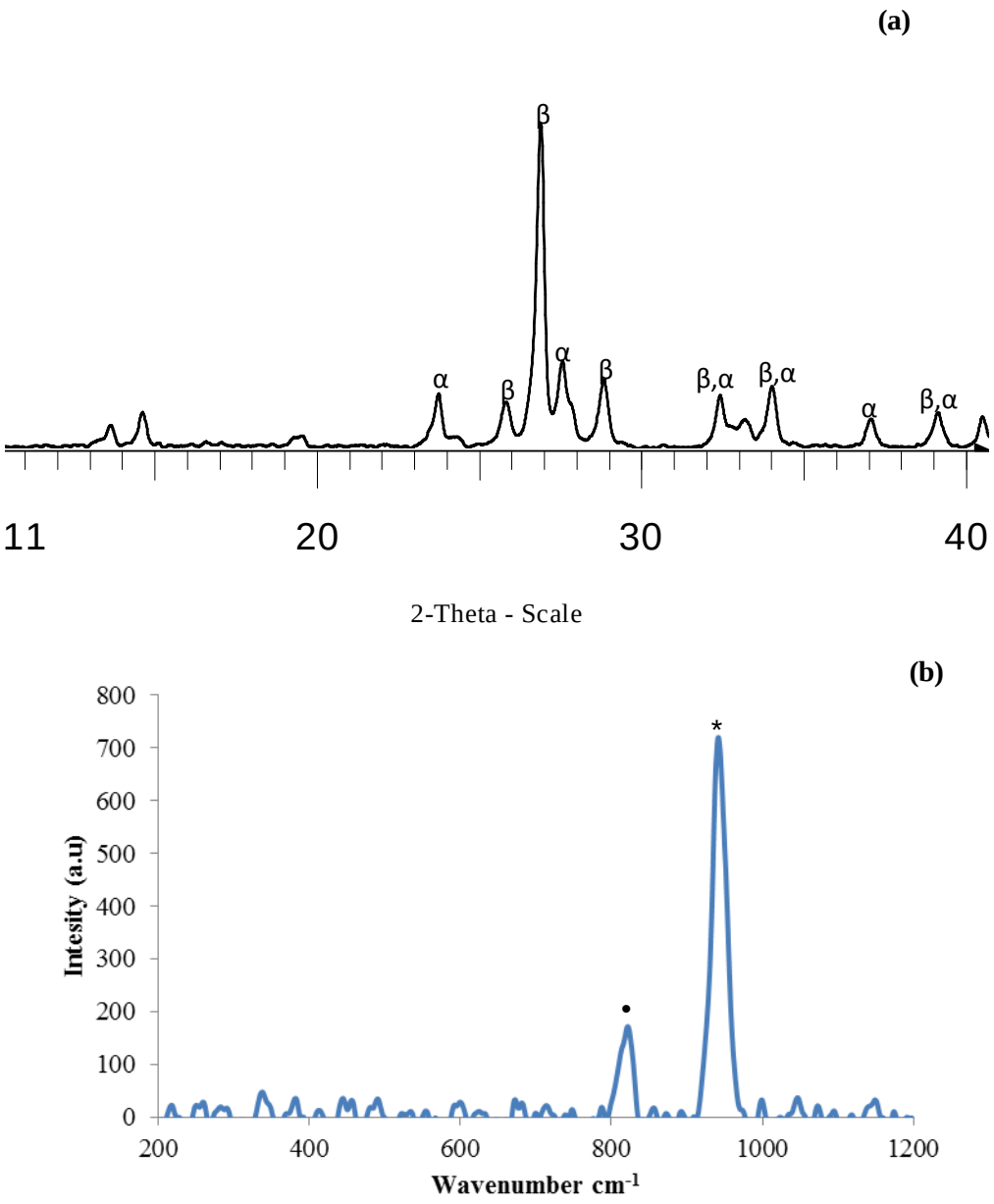

Figure 4.1: XRD pattern (a) of the cobalt molybdate catalyst synthesised by co-precipitation (α and β cobalt molybdate phases and only the major peaks are labelled) and Raman spectrum (b) molybdenum oxide (•) and cobalt molybdate (*)

The temperature programmed reduction, oxidation and repeat cycles of reduction and oxidation (Fig. 4.2) showed two reduction peaks (Fig. 4.2, reduction 1), the first peak at around 650 °C, the second peak at around 850 °C. The lower temperature reduction peak is due to the reduction of cobalt molybdate to molybdite ($Co_2Mo_3O_8$) and the spinel form of

cobalt molybdate (Co_2MoO_4), both present in equimolar quantities [27]. The higher temperature reduction peak is due to complete reduction of molybdite and the spinel to the metal form (*i.e.* cobalt and molybdenum) [27]. Also, the small quantity of molybdenum trioxide present is likely reducing to the molybdenum dioxide phase at around 650 °C [27]. Furthermore, the reduction-oxidation-reduction-oxidation-reduction cycle shows that the catalyst can go through the redox cycle without permanently changing phase, *i.e.* as long as there is enough oxygen to oxidize the catalyst back to the cobalt molybdate phase, phase segregation does not take place.

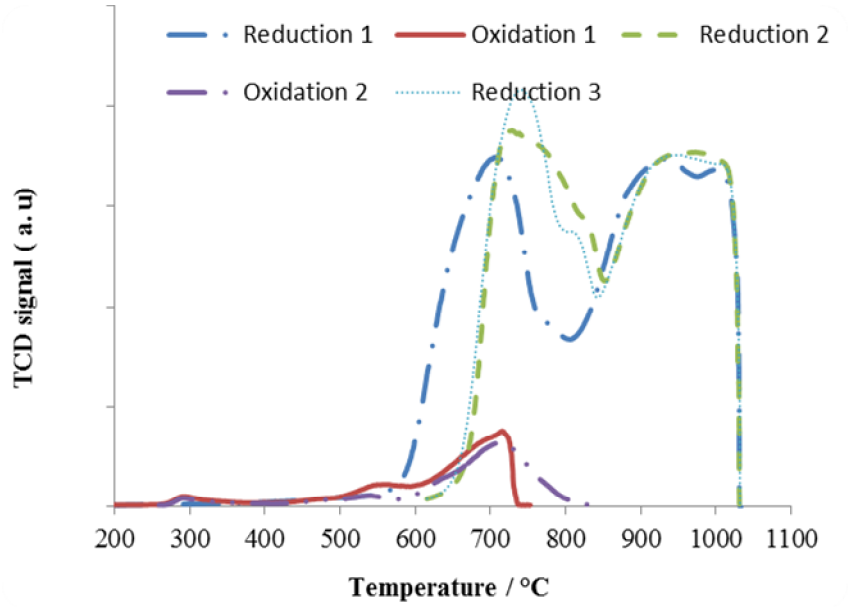

Figure 4.2: TPR/O/R/O/R of the cobalt molybdate catalyst synthesised by the co-precipitation method.

The surface morphology of the catalyst (Appendix 4.1) was observed by SEM. The results showed that the catalyst consists of round shaped particles and some plate like particles. The plate like particles are believed to be due to the free molybdenum trioxide that is present in the catalyst in small quantity and the round particles are the cobalt molybdate. This also would agree with the Raman results, since this shows that the catalyst is dominated by the cobalt molybdate phase.

4.3.2) Catalytic results

4.3.2.1) n-Octane activation at a C:O ratio of 8:0 (dehydrogenation)

There was low conversion of *n*-octane over cobalt molybdate under reducing conditions (no oxygen), with a highest conversion of 11% at 550 °C. The low conversion could be attributed to the equilibrium of the reaction not being pushed towards product formation due to the absence of the formation of the thermodynamically stable products (such as COx and water) [28]. Furthermore and/or in addition, the strong reducing environment resulted in reduction of the catalyst, since there is not sufficient lattice oxygen to maintain the initial phase of the catalyst. This was confirmed by the spent catalyst characterization, where the XRD of the spent catalyst (Fig. 4.3) showed the formation of cobalt oxide and molybdenum oxide. These phases are the same phases that were found to form in the TPR analysis of cobalt molybdate. The Raman analysis (Appendix 4.2) confirmed the formation of the cobalt oxide. At 350 °C the only products observed were the dehydrogenation products (*i.e.* octenes and octadienes). As the reaction temperature increased (400-450 °C), the selectivity to the dehydrogenation products decreased and the selectivity to the dehydrocyclization products (aromatization) increased. This change occurs at the onset reduction temperature of molybdenum trioxide as observed in the TPR profile. However, at the onset temperature for the reduction of cobalt molybdate (~ 500 °C) the catalyst again favoured dehydrogenation only, rather than the dehydrocyclization path, as demonstrated by the increase in the selectivity to the octenes and decrease in the selectivity to aromatics (Fig. 4.4 a).

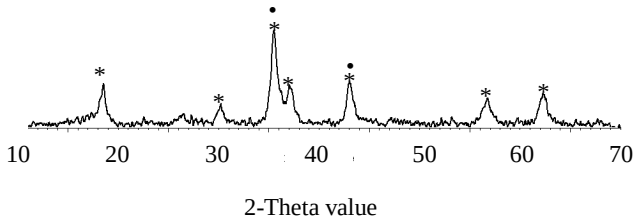

Figure 4.3: XRD diffractogram of the used catalyst under *n*-octane at an 8:0 C:O ratio at 4000 h^{-1} showing Co_3O_4 (*) and MoO_2 (•).

The breakdown of the octenes selectivity (Fig. 4.4 b) shows the dominance of the 2-octene isomer, that is accompanied by o-xylene dominating in the aromatic product breakdown (Fig. 4.4 c). This correlation suggests that 2-octene is the precursor to xylene through 2,7-cyclization. There was no 1-octene observed at the different temperatures, however, ethylbenzene and styrene were detected at 400 and 450 °C, respectively. This could be attributed to the high reactivity of 1-octene, which can be explained by the fact that 1-octene contains six sp^3 carbon atoms in a sequence providing the free rotation that is required for 1,6 cyclization to take place leading to the formation of ethylbenzene and styrene [28-31]. At higher temperatures the other octenes isomers (*i.e.* 3 and 4-octenes) were detected with low selectivities.

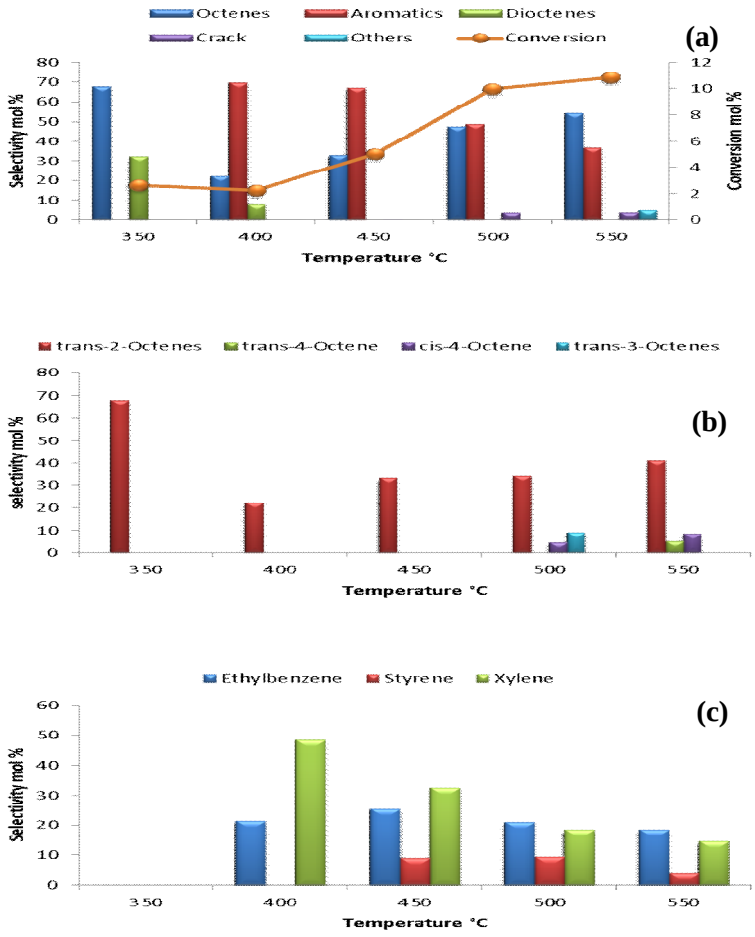

Figure 4.4: Conversion and general selectivity pattern (a), octenes (b) and aromatics selectivity breakdown (c) of cobalt molybdate under *n*-octane at an 8:0 C:O ratio at 4000 h^{-1}

A time on stream experiment was carried to study the stability of the catalyst under dehydrogenation conditions at 500 °C. Fig. 4.5 shows the catalyst activity and selectivity to octenes and aromatics. Reaction time has clear effects on both catalyst activity and selectivity. As the conversion of *n*-octane decreased with time so too did the aromatics selectivity. The selectivity to octenes increased as the selectivity to aromatics decreased. This is likely due to the stripping of the lattice oxygen from the catalyst that is required for the aromatization of the octenes products to produce aromatics. The catalyst was removed and characterized, once after 4 hours and again in a repeat run after 18 hours on stream to investigate any changes in the catalyst. Fig. 4.6 shows the XRD pattern of the used catalyst. The cobalt molybdate has been reduced to the oxide forms of cobalt and molybdenum. Thus, the change in the catalyst activity and selectivity is likely due to phase changes in the catalyst brought upon by the strong reducing environment. Furthermore, the change in the catalyst structure, activity and selectivity indicates that the reaction goes through, at least in part, goes through the oxidative dehydrogenation pathway rather than the dehydrogenation pathway.

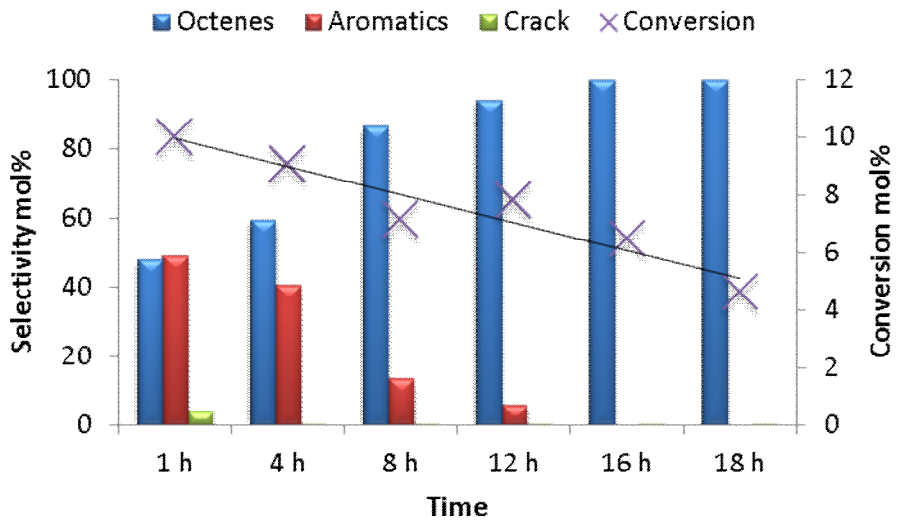

Figure 4.5: Cobalt molybdate catalyst activity and selectivity as function of time in the dehydrogenation of *n*-octane at 4000 h^{-1} and 500 °C

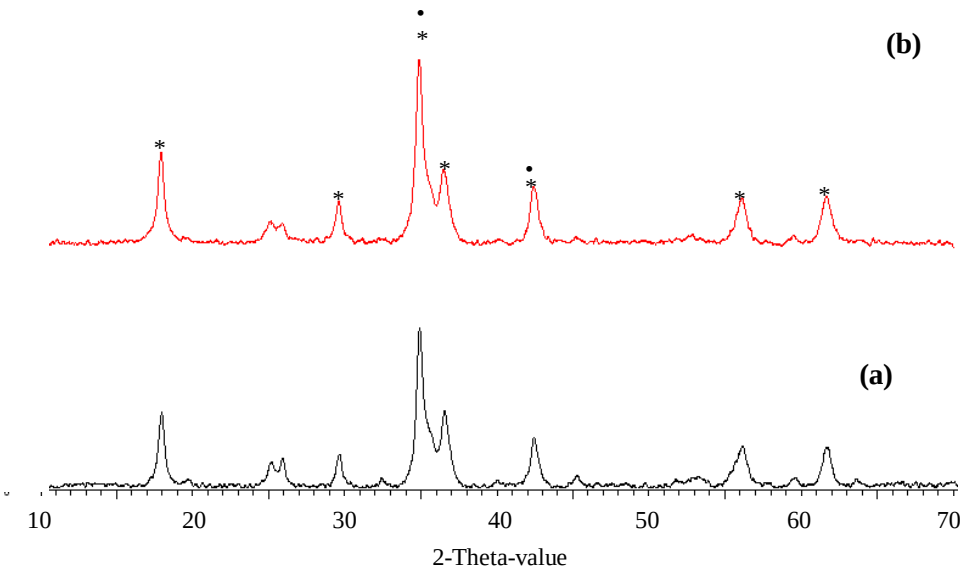

Figure 4.6: XRD patterns for the used catalyst under dehydrogenation conditions at 500 °C and 4000 h^{-1} after 4 hours (a) and 18 hours (b) reaction. The two phases detected were Co_3O_4 (*) and MoO_2 (•).

4.3.2.2) Effect of oxygen content on activity and selectivity

Four different carbon to oxygen (C:O) ratios were investigated to shed light on their effect on the conversion and the selectivity of the cobalt molybdate to non-COx products. As the oxygen content in the reaction mixture increased in the order 8:1 < 8:2 < 8:3 < 8:4, so did the conversion of *n*-octane (Fig. 4.7 a). The *iso*-thermal increase, with increasing oxygen concentration, in the conversion is due to the shift in the reaction equilibrium towards the products, which is brought on by the increase in the formation of COx (Fig. 4.7 b) and water as a function of oxygen in the reaction mixture [28]. The highest selectivity to COx was obtained at 400 °C with a carbon to oxygen ratio of 8:1 (oxygen deficient environment), after which the selectivity decreased with increasing temperature to the lowest COx selectivity among the different carbon to oxygen ratios. A similar pattern was observed for the carbon to oxygen ratio of 8:2, however, the increase at 400 °C was lower in comparison to that at the 8:1 ratio. The selectivity to COx generally decreased with an increase in the reaction temperature, as a result of the formation of more ODH products. The selectivity to octenes in general increased with a decrease in the oxygen content in the reaction mixture. At low oxygen content (*i.e.* C:O ratio of 8:1 and 8:2) the formation of octenes was favoured and became less favoured with higher oxygen content (*i.e.* 8:3 and 8:4) due to secondary reactions [28-32]. Moreover, the selectivity to octenes (Fig. 4.7 c) decreased or reached a plateau at higher temperatures due to subsequent reactions forming aromatics and cracked products.

The increase in the selectivity towards aromatics at high temperatures (Fig. 4.7 d) supports the belief that octenes are the precursors to aromatics through cyclization.

The dominant octene isomer is 2-octene (as in the dehydrogenation reaction) across the different temperatures and carbon to oxygen ratios. However, as the oxygen content increased in the reaction mixture other isomers were formed (*i.e.* 3- and 4-octenes), though their selectivities remained lower than that to 2-octene. With regards to the aromatics breakdown, the selectivity to xylene was the highest under oxygen deficient environment conditions (*i.e.* 8:1), however, an increase in oxygen content in the reaction mixture favoured the formation of ethylbenzene and, more so, styrene (*i.e.* products of 1,6-cyclization). The increase in the selectivity to ethylbenzene and styrene can be attributed to the increase in the oxygen available for the 1,6-cyclization and dehydrogenation to give styrene. The increase in the 1,6-cyclization was accompanied by a decrease in the selectivity to 1-octene, which is believed to be the precursor for the 1,6-cyclization. This hypothesis was supported by the increase in the selectivity toward 4-octene relative to the other octenes in oxygen rich environments, since its less reactive than the other isomers and the position of the double bond hinders cyclization.

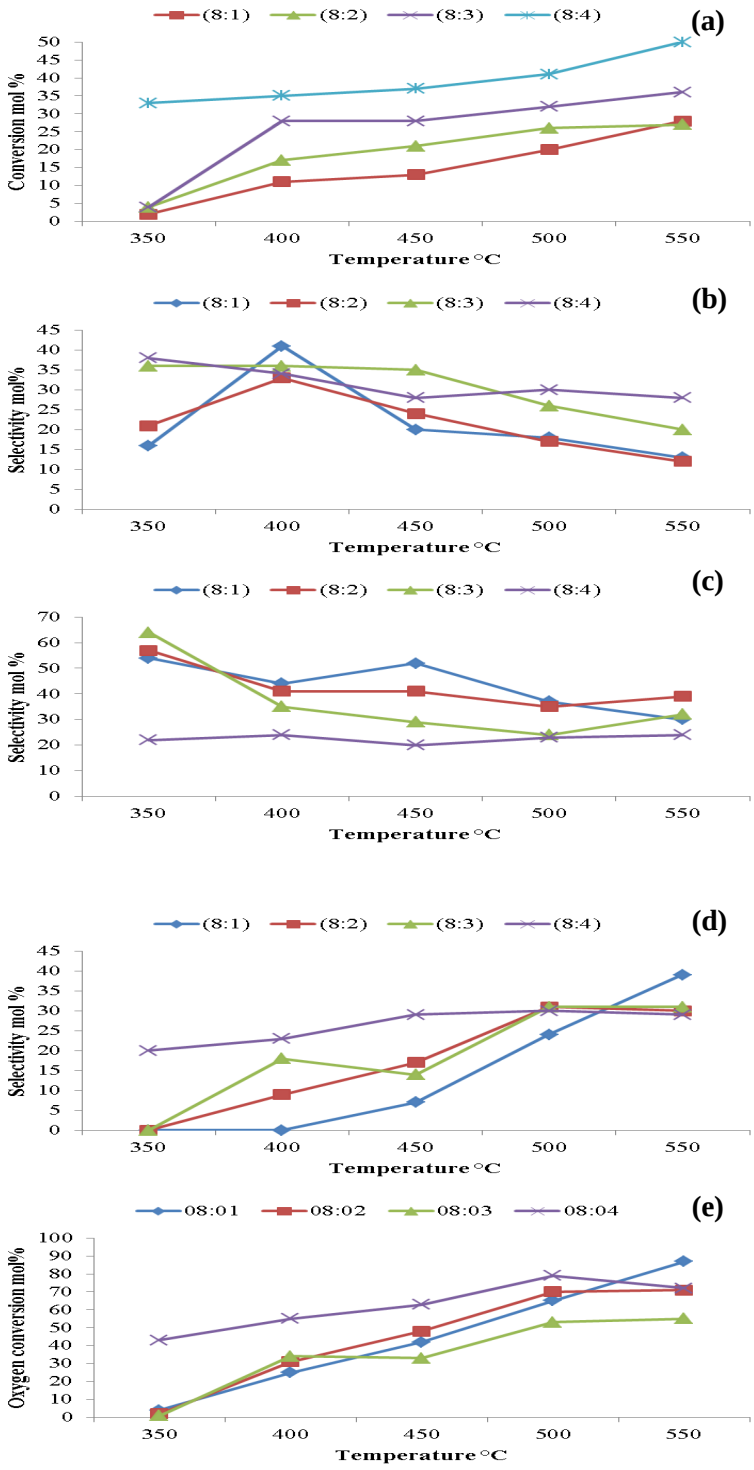

Figure 4.7: Effect of oxygen on the conversion of *n*-octane (a), COx selectivity (b), octenes selectivity (c), aromatics selectivity (d) and oxygen conversion (e) over cobalt molybdate at 4000 h^{-1} as function of reaction temperature.

The general trend observed for oxygen conversion over cobalt molybdate (Fig. 4.7 e) is that the conversion increased as the reaction temperature increased, consequently, the *n*-octane conversion also increased. Selectivity to COx and aromatics plateaued at 500 and 550 °C, the

conversion of oxygen also generally plateaued at the same temperatures indicating the correlation between oxygen and formation of those products. This trend was also observed in the ODH of *n*-octane over Co/ceria [33] and vanadium [28] based catalysts. At 550 °C and a C:O ratio of 8:1 the selectivity to aromatics increased and that was accompanied by an increase in the oxygen conversion, which indicates that oxygen has been consumed to produce aromatics. Furthermore, the results obtained showed that the system is always oxygen sufficient and at no temperature or C:O ratio was the system oxygen deficient. Furthermore, the ratio of CO and CO_2 was constant at all ratios (Appendix 4.3), which indicates that CO does not undergo deep oxidation to form CO_2 [34].

A further way to investigate the effect of both oxygen concentration and reaction temperature on the reaction is by determining the formation rate of value added products (*i.e.* octenes and aromatics). The formation rate of octenes (Fig. 4.8 a) and aromatics (Fig. 4.8 b) were calculated as reported by Solsona *et al.* [34]. The general trend in the formation rate of octenes (Fig. 4.8 a) is an increase in the formation rate of octenes as the oxygen concentration in the feed increased, the exception is the 8:2 C:O ratio, which showed the highest formation rate. The increase in the oxygen concentration was also accompanied by an increase in the formation rate of C8 aromatics (Fig. 4.8 b). This indicates that aromatics are formed through subsequent reactions starting from octane, through cyclization and dehydrogenation where oxygen is required [28, 35].

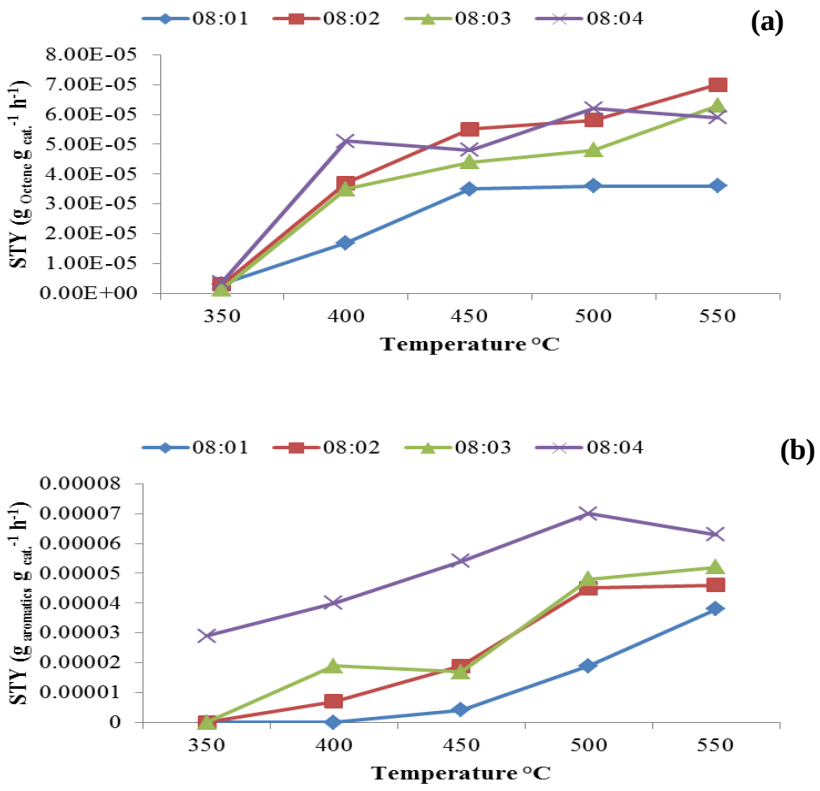

Figure 4.8: Formation rate of octenes (a) and aromatics (b) as a function of oxygen concentration and reaction temperature in ODH of *n*-octane over cobalt molybdate.

4.3.2.3) Effect of C:O ratio on product distribution

The yields of octenes, aromatics, cracked products and COx at 500 °C as a function of the oxygen content in the reaction mixture are shown in Fig. 4.9 a. The yields of the octenes in general slightly increase with increase in the oxygen content in the reaction, since these are the reagent for the formation of the secondary products (*i.e.* aromatics, cracked products and COx). This is indicated by the clear increase in the yield of the secondary products as the oxygen content increased. The increase in the COx yield could be as a direct result of the increase in the oxygen content causing over oxidation of octenes to the thermodynamically stable COx products. The value-added C8 selectivity % (VAP%) (Fig. 4.9 b) decreased with increase in the oxygen content in the reaction. This observation emphasises that the yield of undesired products (mainly COx) increased with oxygen content. At lower oxygen content (*i.e.* C:O ratios of 8:1 and 8:2) the VAP% was mainly due to the high yields of octenes, as the oxygen content increased so did the contribution from the aromatics to the VAP%. Thus, the

ratio of 8:3 can be considered ideal for obtaining both octenes and aromatics and a lower ratio (*i.e* 8:2) is best for octenes formation.

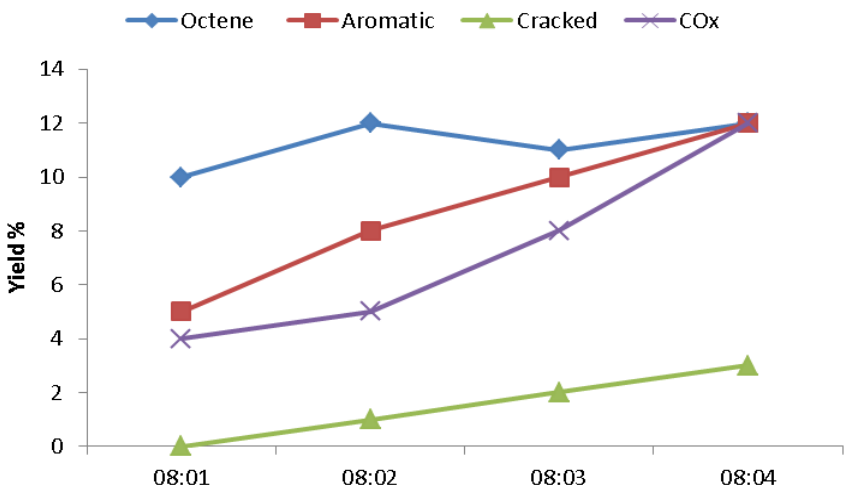

Figure 4.9 a: Yield % of octene, aromatics, cracked and COx products at 500 °C as function of the oxygen content in the reaction mixture.

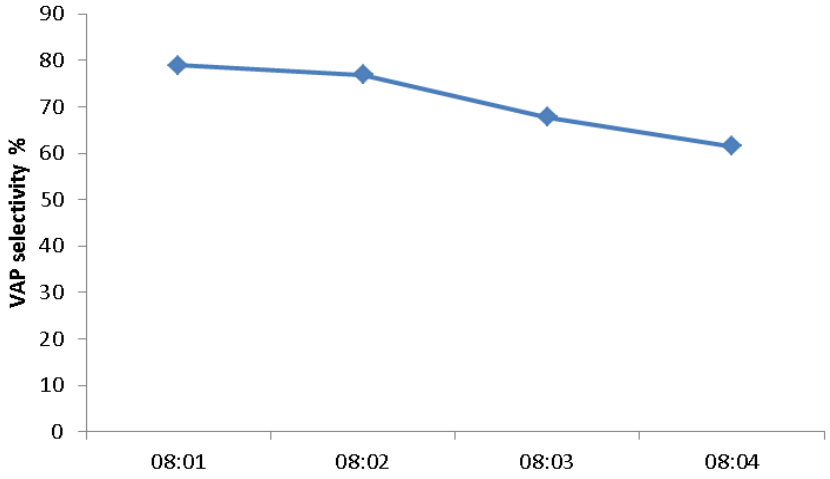

Figure 4.9 b: VAP% plot as effect of oxygen content over cobalt molybdate catalyst at 500 °C and GHSV of 4000 h^{-1}

4.3.3) Used catalyst characterization

The used catalyst was characterized using XRD, Raman and BET surface area measurements, in order to investigate any phase change that may have been brought on by the reaction conditions. Therefore, the catalyst was characterized without any pre-treatment to avoid any

changes to the used catalyst. The XRD (Appendix 4.4) confirms the presence of cobalt molybdate as the dominant phase in the used catalyst regardless of the oxygen content in the reaction mixture. However, the Raman analyses (Fig. 4.10) showed more clearly the effect of the oxygen content in the reaction mixture. For the catalyst under oxygen deficient conditions (*i.e.* an 8:1 C:O ratio) a peak at ~ 468 cm^{-1} was detected (Fig. 4.10) and it corresponded to Co-O in cobalt oxide. The ratio between the cobalt oxide to the cobalt molybdate (peak at ~ 937 cm^{-1}) indicated that the dominant phase is the cobalt molybdate. The Raman analyses (Fig. 4.10) of the used catalysts obtained under oxygen richer environments (*i.e.* C:O ratios of 8:2, 8:3 and 8:4) showed the presence of cobalt molybdate only (peak at ~ 937 cm^{-1}). These results indicate that the catalyst maintains its phase during the reaction as long as there is sufficient oxygen to re-oxidize the catalyst and maintain the initial phase (*i.e.* cobalt molybdate).

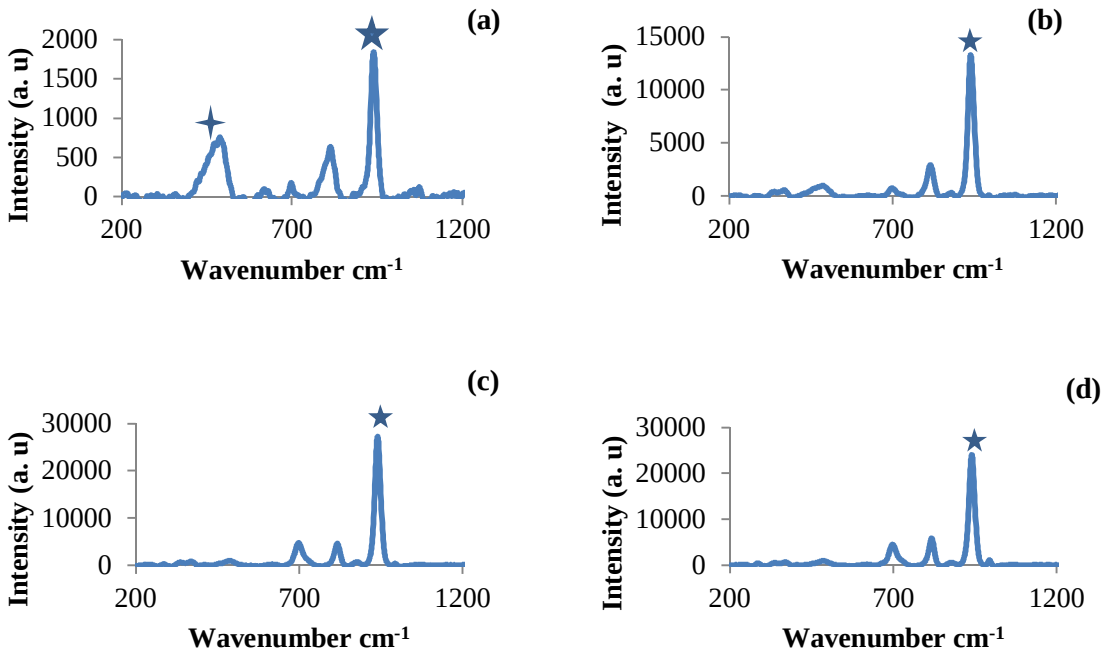

Figure 4.10: Raman spectra of the used catalysts tested under different oxygen contents (a) 8:1, (b) 8:2, (c) 8:3 and (d) 8:4. Cobalt oxide(✦) and cobalt molybdate (★).

4.4) Summary and Conclusion

The cobalt molybdate catalyst synthesised by the co-precipitation method consisted of a mixture of the β- and α-$CoMoO_4$ phases, however, the catalyst was dominated by the β-$CoMoO_4$ phase and this is the more stable phase of cobalt molybdate. The TPR/O/R/O/R results showed that the catalyst can undergo the redox cycle without undergoing any irreversible transformation. The catalyst was tested in the oxidative dehydrogenation of *n*-octane under different carbon to oxygen ratios (*i.e.* 8:0, 8:1, 8:2, 8:3 and 8:4). The catalyst showed low conversion under dehydrogenation conditions and this resulted in the complete segregation of the cobalt molybdate catalyst. However, introduction of oxygen to the system significantly improved the conversion and also the selectivity to aromatics, and the catalyst maintained the cobalt molybdate phase after the reaction. The highest selectivity to octene of ~55% was obtained at an 8:1 carbon to oxygen ratio at 450 °C, while the highest selectivity to aromatics was obtained at an 8:3 carbon to oxygen ratio at the same temperature. At low temperature (350 °C), conversion was low and octene formation was favoured at all carbon to oxygen ratios again shows octenes are primary products. There is a slight increase in the yield of the octenes with increase in the oxygen content, which is accompanied by a clear increase in the yield of aromatics, cracked and COx products. This resulted in a decrease in the value-added product yields. Therefore, the best carbon to oxygen ratio for octenes production is an 8:1 C:O ratio, while for aromatics it is 8:3.

4.5) Acknowledgments

The authors are thankful to SASOL, the NRF and THRIP (grant number TP1208035643) for financial support, and the EM unit at UKZN for helping with the SEM analyses.

4.6) References

[1] V.D.B.C. Dasireddy, S. Singh, H.B. Friedrich, Appl. Catal., A: Gen., 421–422 (2012) 58-69.
[2] F. Cavani, F. Trifirò, Appl. Catal., A: Gen., 88 (1992) 115-135.
[3] B. Pillay, M.R. Mathebula, H.B. Friedrich, Appl. Catal., A: Gen., 361 (2009) 57-64.
[4] C. Téllez, M. Abon, J.A. Dalmon, C. Mirodatos, J. Santamaría, J. Catal., 195 (2000) 113-124.
[5] A. de Lucas, P. Sánchez, F. Dorado, M.J. Ramos, J.L. Valverde, Appl. Catal., A: Gen., 294 (2005) 215-225.

[6] K.A. Williams, L.D. Schmidt, Appl. Catal., A: Gen., 299 (2006) 30-45.
[7] A.A. Lemonidou, Appl. Catal., A: Gen., 216 (2001) 277-284.
[8] M. Machli, E. Heracleous, A.A. Lemonidou, Appl. Catal., A: Gen., 236 (2002) 23-34.
[9] R.K. Grasselli, J. Chem. Educ., 63 (1986) 216.
[10] J.D. Burrington, C.T. Hartisch, R.K. Grasselli, J. Catal., 81 (1983) 489-488.
[11] J.D. Burrington, C.T. Hartisch, R.K. Grasselli, J. Catal., 87 (1984) 363-380.
[12] D. Halvorson. K. Aykan, A. W. Sleight, D. B. Rogers, J. Catal., 35 (1975) 401-406.
[13] A.Mazurkiewicz. B. Grzybowska, J. Sloczinsky, Appl. Catal., A: Gen., 13 (1985).
[14] G.L.Schrader. U. Ozkan, J. Catal., 95 (1985) 120-136.
[15] C.Martin. S. R. G. Carrazan, V. Rives, R. Vidal, Appl. Catal., A: Gen., 135 (1996).
[16] A. Kaddouri, R. Del Rosso, C. Mazzocchia, P. Gronchi, D. Fumagalli, J. Therm. Anal. Calorim., 66 (2001) 63-78.
[17] B. Pillay, M.R. Mathebula, H.B. Friedrich, Catal. Lett., 141 (2011) 1297-1304.
[18] J.M.J.G. Lipsch, G.C.A. Schuit, J. Catal., 15 (1969) 163-173.
[19] Z.M. George, J. Catal., 32 (1974) 261-271.
[20] Y. S. Yoon, W. Ueda, Y. Moro-oka, Top. Catal., 3 (1996) 265-275.
[21] Y.S. Yoon, N. Fujikawa, W. Ueda, Y. Moro-oka, K.W. Lee, Catal. Today, 24 (1995) 327-333.
[22] L.A. Palacio, A. Echavarría, L. Sierra, E.A. Lombardo, Catal. Today, 107–108 (2005) 338-345.
[23] D.L. Stern, R.K. Grasselli, J. Catal., 167 (1997) 550-559.
[24] J. Vila, F. Sapina, E. Martinez, V. Cortes, J. Podobinski, Contrib. Sci., 4 (2008) 223-229.
[25] K. H. Jeziorowski, P. Grange, P. Gajardo, J. Phys. Chem., 84 (1980) 1825-1829.
[26] S.C. Chang, M.A. Leugers, S.R. Bare, J. Phys. Chem., 96 (1992) 10358-10365.
[27] J. L. Brito, A.L. Barbosa, J. Catal., 171 (1997) 467-475.
[28] E. A. Elkhalifa, H. B. Friedrich, Catal. Lett., 141 (2011) 554-564.
[29] E.A. Elkhalifa, H.B. Friedrich, Appl. Catal., A: Gen., 373 (2010) 122-131.
[30] P. Meriaudeau, A. Thangaraj, C. Naccache, S. Narayanan, J. Catal., 146 (1994) 579-582.
[31] B.C. Shi, B.H. Davis, J. Catal., 157 (1995) 626-630.
[32] A.A. Lemonidou, G.J. Tjatjopoulos, I.A. Vasalos, Catal. Today, 45 (1998) 65-71.
[33] M. Narayanappa, V.D.B.C. Dasireddy, H.B. Friedrich, Appl. Catal., A: Gen., 447–448 (2012) 135-143.
[34] B. Solsona, J.M. López Nieto, P. Concepción, A. Dejoz, F. Ivars, M.I. Vázquez, J. Catal., 280 (2011) 28-39.
[35] V.D.B.C. Dasireddy, H.B. Friedrich, S. Singh, Appl. Catal., A: Gen., 467 (2013) 142-153.

Chapter five

Effect of the cation in the molybdate structure: activity and selectivity in n-octane ODH

Abstract

Two molybdates with different cations (magnesium molybdate and cobalt molybdate) were synthesised by co-precipitation with similar ratios of cation:molybdenum (~ 1:1). The two molybdates were characterized by XRD, BET-surface area measurements, Raman spectroscopy, inductively coupled plasma-optical emission spectroscopy, infra-red spectroscopy, electron imaging (reported elsewhere), *in situ* XRD under *n*-octane and porosity studies. The *in situ* XRD results showed that magnesium and cobalt molybdate are stable under reducing environment up to 600 and 500 °C, respectively, after which phase segregation takes place. The catalytic testing was carried out at a GHSV of 4000 h^{-1}, carbon to oxygen ratio of 8:3 and in the temperature range of 350 to 500 °C in 50 °C intervals. The highest activity (in terms of *n*-octane conversion) was obtained over cobalt molybdate (CM) with the highest selectivity to aromatics. However, magnesium molybdate (MM) was the most selective to octenes, as observed at *iso* conversion. The space time yields of value added products over the two molybdates showed that MM is most selective to octenes and CM to aromatics. Increasing the reaction temperature had a positive effect over both catalysts by increasing the activity and decreases the selectivity to COx, especially at high temperature (*i.e.* 500 °C).

Keywords: n-octane, cations, molybdates, octenes, C8 aromatics, COx.

5.1) Introduction

Since world war II there has been a lot of interest in the production of olefins from the cheap and readily available paraffins [1]. Some processes have been developed to mainly produce olefins and aromatics, which are both considered as being valuable starting materials in the petrochemical industries. Currently, olefins are produced commercially through dehydrogenation of paraffin (*e.g.* Pacol™) and steam cracking, among other methods. However, these two processes suffer from two key disadvantages, which are economic impact from the shutdown period (for catalyst regeneration) and the environmental impact (extensive use of energy). These two

disadvantages motivated researchers to investigate oxidative dehydrogenation (ODH), in which the use of oxygen eliminates or limits those two disadvantages. However, for ODH process to be commercially utilized there is a great need to development active and selective catalyst(s) for the production of olefins, aromatics and oxygenates with low selectivity to the thermodynamically stable COx.

Molybdates are among the materials that have been extensively investigated in the oxidative dehydrogenation of light paraffins, due to the possibility of modifying their thermal stability, metal-oxygen bond strength, oxygen mobility in their lattice and structure defects by changing the nature of the cation in the molybdate structure (*e.g.* Ni, Fe, Co, Mg, Zn, *etc.*) [2]. Various approaches have been taken to tailor the activity and selectivity of molybdates, mainly in ODH of light paraffins. Lee *et al.* [3] and Yoon *et al.* [4-7] investigated the effect of excess molybdenum trioxide on the activity and selectivity of magnesium molybdate, showing that a slight excess of molybdenum trioxide improves the activity of the catalyst without compromising its selectivity to olefins. Combination of cations in the molybdate structure were also investigated [8, 9] and these showed different activity and selectivity to the corresponding mono-molybdates. Changing the cation in the molybdate structure also influences the structure or the co-ordination of the molybdenum centre (*e.g.* α- *vs* β-molybdate). Pillay *et al.* [10, 11] showed the effect of the different molybdate phases (*i.e.* α- *vs* β- molybdate) using nickel molybdate in the ODH of *n*-hexane, where the α-phase is more active than the β-phase, however, the latter is more selective than the former phase. Few researchers focused their work on the effect of the cation in molybdates in the ODH of light paraffins [6, 12], however, no work was done on medium linear chain paraffins.

The motivation of this work was to investigate the effect of the cations (*i.e.* Mg and Co) in the ODH of *n*-octane, focusing on activity and selectivity to value added products (*i.e.* octenes and C8 aromatics)

5.2) Experimental

5.2.1) Catalysts preparation

All catalyst were synthesised by the co-precipitation method for magnesium molybdate (MM) and cobalt molybdate (CM) [4]. The synthesis of MM (as an example) was carried out by preparing equi-concentrations of molybdenum solution

(ammonia heptamolybdate-tetrahydrate, Merck) and magnesium solution (magnesium nitrate, Aldrich). The pH of the molybdenum solution was adjusted to 6 by aqueous ammonia solution (25%). The magnesium solution was added drop-wise to the molybdenum solution with continuous stirring, and after complete addition, the solution was heated until slurry formation. The white slurry was dried in an oven at 110 °C overnight and calcined at 550 °C for 2 h, yielding the MM catalyst. A similar method was followed to prepare the CM catalyst, although in this case the slurry was purple in colour.

5.2.2) Catalysts characterization

All catalysts were characterized using the same techniques in order to determine the chemical and physical effect of changing the cation in the molybdate. Powder and *in situ* X-Ray diffraction (XRD) under *n*-octane, with C:O of 8:1 was carried using Bruker D8 advanced equipped with a copper radiation source, BET-surface area measurements, Raman spectroscopy, inductively coupled plasma-optical emission spectroscopy (reported in chapter 3 and 4) were used as characterisation techniques. The effect of the cation in porosity of molybdate was investigated using a Micromeritics Tristar (II), the samples were degased at 200 ºC overnight under nitrogen flow. The analysis of the two samples was carried out at liquid nitrogen temperature and 55 point analyses were carried out.

5.2.3) Catalytic testing

The catalytic testing was carried out in a continuous flow fixed bed reactor at a carbon to oxygen ratio of 8:3 and GHSV of 4000 h^{-1}. These conditions were based on previous work (Chapters 3 and 4). Products identification and quantification were carried out using gas chromatography (GC). The liquid (organic) products collected from the catch pot were injected into a Perkin Elmer Clarus 400 (GC) equipped with a flame ionization detector (FID), the gaseous sample were injected in the GC-FID and a PerkinElmer Clarus 400 GC equipped with thermal conductivity detector (TCD).

5.3) Results and discussion

5.3.1) Catalyst characterization

The chemical stability of the molybdate was greatly influenced by the choice of cation in the molybdate. The *in situ* XRD results under near reaction conditions (8:1 C:O) showed that the catalyst reduced at different temperatures based on the cation of choice. In the case of MM, the molybdate phase is stable up to 600 °C (Fig. 5.1 a) and only under goes reduction after 4 hours at 600 ºC, while the CM catalyst (Fig. 5.1 b) undergoes reduction from 500 ºC under *n*-octane flow. Moreover, in the cooling cycle these phases (segregated metal oxides) did not oxidize back to the initial phases (*i.e.* molybdate) (Fig. 5.1 c and d for MM and CM, respectively). In terms of the thermal stability, both MM and CM were thermally stable up to 600 ^{O}C without undergoing lattice expansion or contraction.

The effect of the cation in the molybdate structure in terms of surface porosity was investigated by N_2 adsorption/desorption. Both molydates showed a Type IV isotherm which indicated that the material was completely filled through the secondary capillary condensation process and which is characteristic of mesoporous materials. Furthermore, the molybdates showed a H1 type hysteresis loops (Fig. 5.2) which indicates that these molybdates consist of channels with uniform sizes and shapes [13] regardless of the cation choice. In terms of the amount of gas adsorped, the cations had a clear effect, where the highest amount adsorped was over the CM (~ 39 cm^3/g) catalyst, followed by the MM catalyst (~ 32 cm^3/g). This might be the reason for the higher conversion observed over the CM catalyst compared to the MM catalyst (see Section 5.3.2).

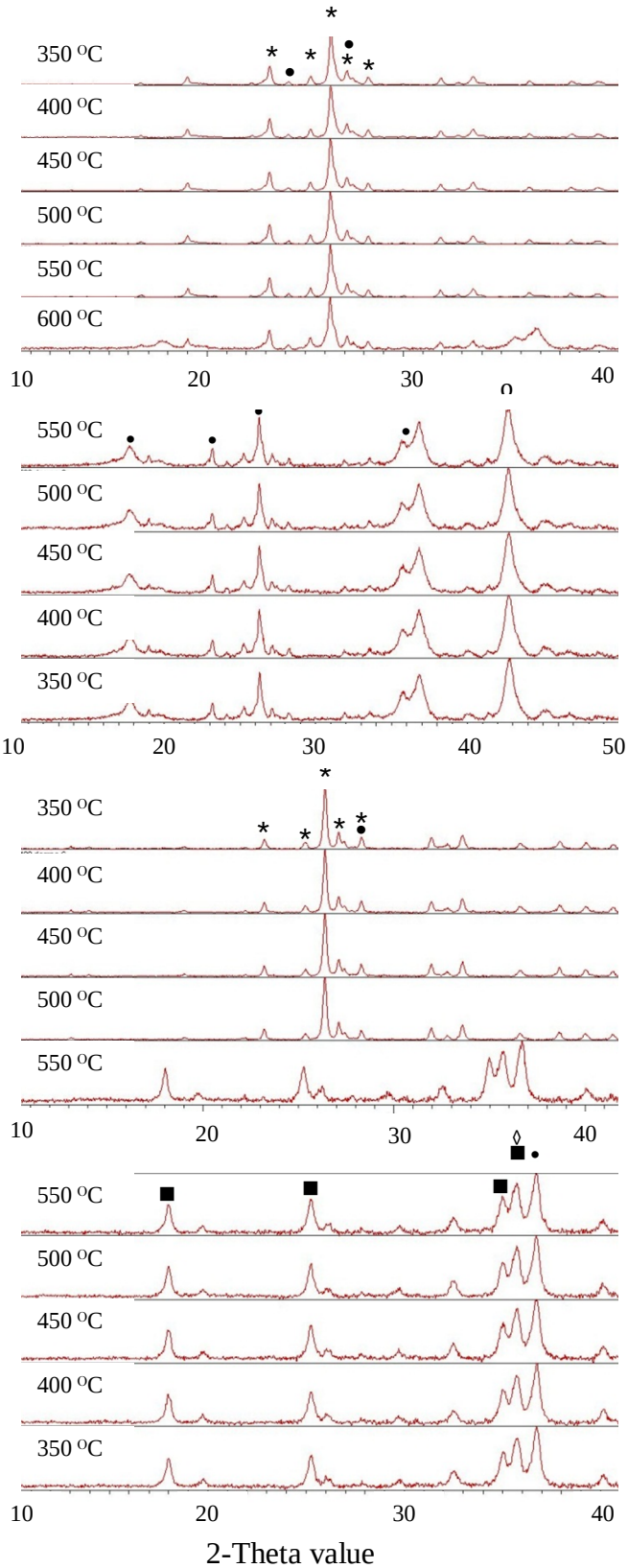

Figure 5.1: XRD diffractograms for MM and CM under *n*-octane flow with a C:O ratio of 8:1, MM heating (a), MM cooling (b), CM heating (c) and CM cooling (d). $MgMoO_4$ (*), MoO_3 (•) $CoMoO_4$ (*), MgO (o), Co_3O_4 (▮) and MoO_2 (◊).

The effect of the cation in the molybdate structure in terms of surface porosity was investigated by N_2 adsorption/desorption. Both molydates showed a Type IV isotherm which indicated that the material was completely filled through the secondary capillary condensation process and which is characteristic of mesoporous materials. Furthermore, the molybdates showed a H1 type hysteresis loops (Fig. 5.2) which indicates that these molybdates consist of channels with uniform sizes and shapes [13] regardless of the cation choice. In terms of the amount of gas adsorped, the cations had a clear effect, where the highest amount adsorped was over the CM (~ 39 cm^3/g) catalyst, followed by the MM catalyst (~ 32 cm^3/g). This might be the reason for the higher conversion observed over the CM catalyst compared to the MM catalyst (see Section 5.3.2).

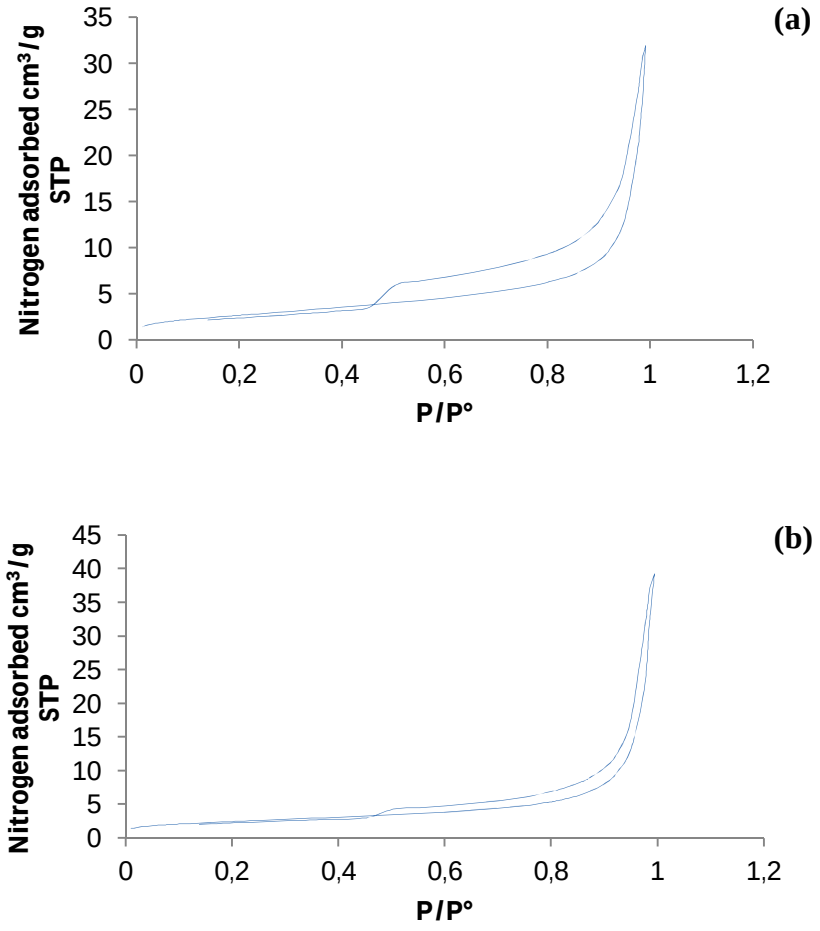

Figure 5.2: The effect of cation in molybdates in terms of surface porosity as determined by N_2 adsorption analysis, MM (a) and CM (b).

5.3.2) Catalytic testing

All the catalytic testing was carried out at carbon to oxygen atomic ratio of 8:3 (C:O) and a gas hourly space velocity of 4000 h^{-1} in a continuous flow fixed bed reactor using air as oxidant and nitrogen as diluent. The concentration of *n*-octane in the feed was maintained at ~11% and the reaction temperature was in the range of 350 to 500 °C and increased at 50 °C intervals. The effect of the cation in the molybdate was investigated by considering the *n*-octane conversion, selectivity to value added products and COx.

The cation in molybdate did influence the activity of molybdate (Fig. 5.3 a), where at all the different reaction temperature studied, the highest conversion of *n*-octane was obtained over the CM catalyst. These results agree with those reported in literature for CM and MM, where CM was found to be slightly more active in the oxidative dehydrogenation of light alkanes [6]. The effect of the cation in the molybdate was more profound in terms of the selectivity to different products. In terms of the selectivity to octenes (Fig. 5.3 b), the most selective catalyst was the MM catalyst. This could be brought on due to the different basicity of those cations, since for octene to form it must desorb from the catalyst surface before undergoing any further reactions [14]**.** Therefore, the acidity of the catalyst plays a key role in this step. Since magnesium is basic, it will reduce the acidity of molybdates and therefore octenes will be desorbing faster from the MM surface as compared to the surface of CM, thus giving a higher selectivity to octenes. The trend was different in terms of the selectivity to C8 aromatics (Fig. 5.3 c) (*i.e.* ethylbenzene, styrene and xylene), where CM was the most selective. The selectivity to aromatics increased with an increase in the reaction temperature for both molybadates, this observation is well documented in literature for different alkanes and in particular for *n*-octane over vanadium based catalysts [15-17]. This trend is likely due to the high activation energy required to form aromatics and could also be due to the multiple steps that take place to form those aromatics (*e.g.* cyclization and oxidative dehydrogenation and/or dehydrogenation) [18-20].

The selectivities to COx (*i.e.* CO and CO_2) (Fig. 5.3 d) over both CM and MM were similar at high reaction temperatures. However, the majority of COx detected was in the form of CO_2, indicating the over-oxidation of *n*-octane [21].

The space time yield (STY) for value added products (*i.e.* octenes and aromatics) (Fig. 5.4) shows clearly the effect of the different cations in the molybdates. In terms of STY for octenes (Fig. 5.4 a) both MM and CM showed acceptable to good activity depending on the temperature. At low temperature (below 450 °C) the CM gave higher STY than MM, which could be due to the superior conversion of *n*-octane at those temperatures over CM, leading to an increased mass of octenes formed. However, at high temperatures (above 450 °C) MM gave higher STY than CM. This was expected, since MM is known to be selective to olefins [22] and at high temperatures (*i.e.* 450 and 500 °C), the activity of the catalyst increased thus increasing the amount of octene formed. In terms of the STY for aromatics (Fig. 5.4 b), CM showed the highest STY when compared to MM. This could be due to cobalt being slightly more acidic than magnesium, thus promoting further reaction of octenes to aromatics. The cation in the molybdate structure favours one reaction pathway over another as shown in Scheme 5.1. The magnesium molybdate favours the formation of octenes, therefore favouring step 1, while cobalt molybdate favours step 2.

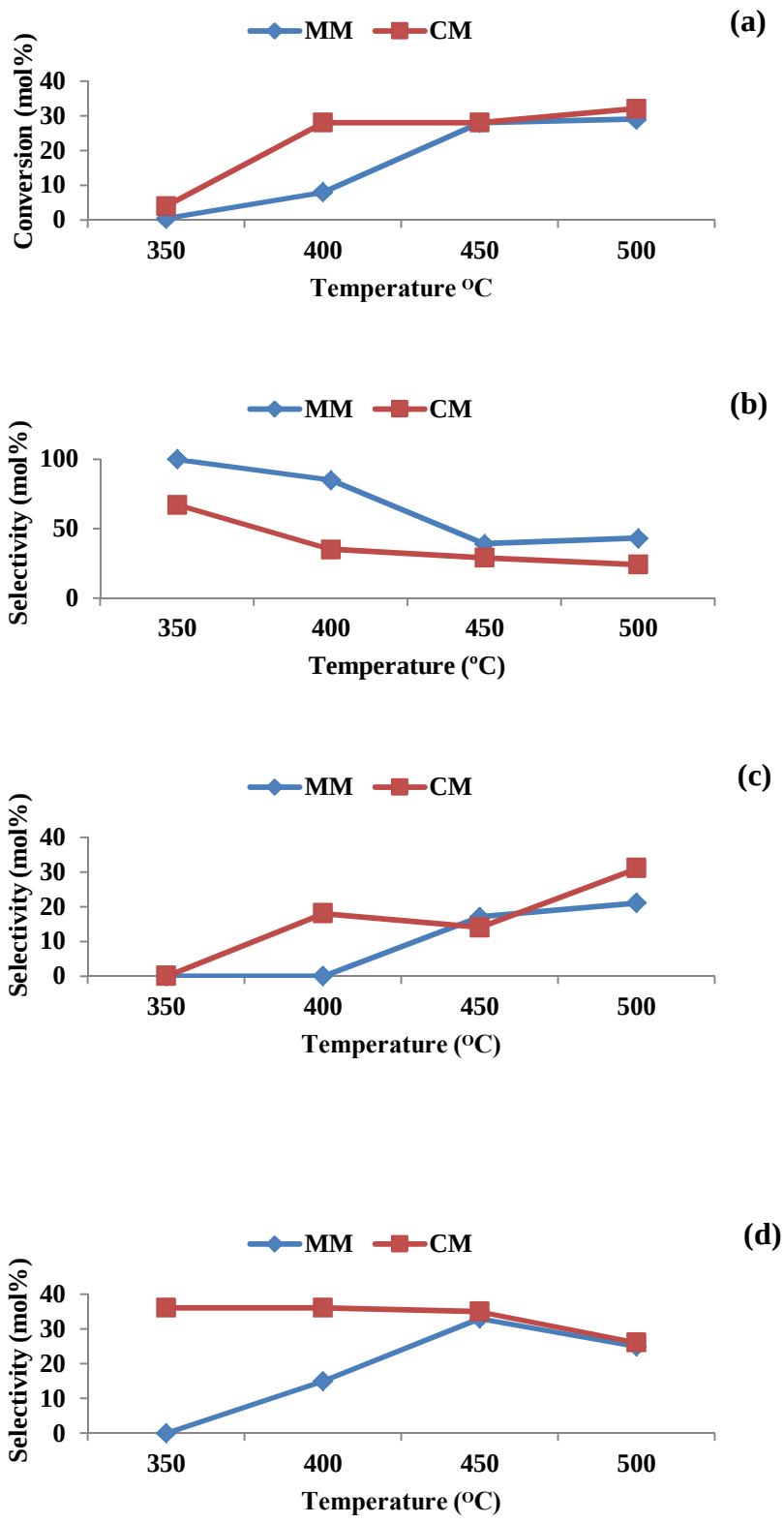

Figure 5.3: Effect of the cation in molybdate in *n*-octane ODH in terms of conversion (a), selectivity to octenes (b), selectivity to aromatics (c) and selectivity to COx (d).

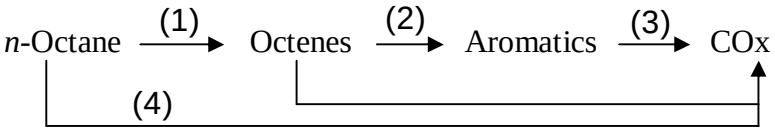

Scheme 5.1: Proposed reaction sequence in the ODH of *n*-octane based on literature.

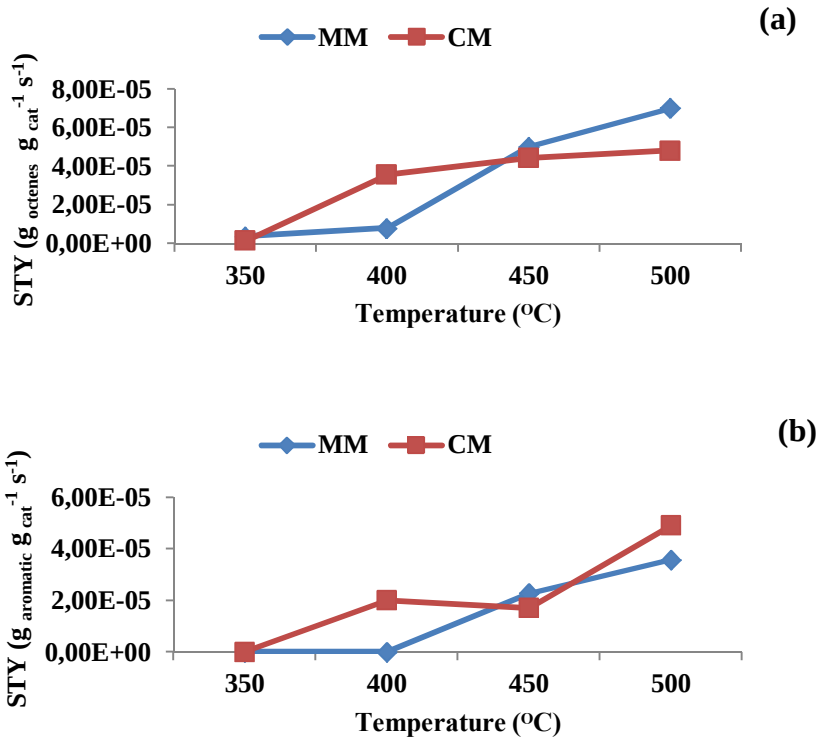

Figure 5.4: The influence of the cation in molybdate space time yield in the ODH of *n*-octane for octenes (a) and aromatics (b) at carbon to oxygen ratio of 8:3 and 4000 h^{-1} GHSV.

5.3.3) Conversion at iso-thermal and selectivity at iso-conversion

The effect of the carbon to oxygen ratio on the different molybdates was investigated at *iso*-thermally (*i.e.* 500 °C) (Fig. 5.5 a). CM showed the highest activity at all different carbon to oxygen ratios. The activity of both molybdates increased as the

oxygen concentration in the feed increased. This could be due to manipulation in the reaction equilibrium to the direction of products formation or improving the redox cycle of the catalyst leading to higher activity.

In terms of the selectivity to value added products and COx (Fig. 5.5 b) at iso-conversion (~ 29%) at 500 °C and 8:3 carbon to oxygen ratio, MM and CM showed a similar selectivity to value added products (*i.e.* octenes and aromatics). However, there is a clear difference in the selectivity between MM and CM, the former being more selective to octenes, while the latter is more selective to aromatics. If one considers that aromatics are likely formed from octenes, then this indicates that the octenes remain adsorbed longer on CM than on MM, allowing them to react further to form C8 aromatics. This indicates the effect of the cation on the acidity of the catalyst. Furthermore, cobalt has also been reported to be a good aromatization catalyst [23].

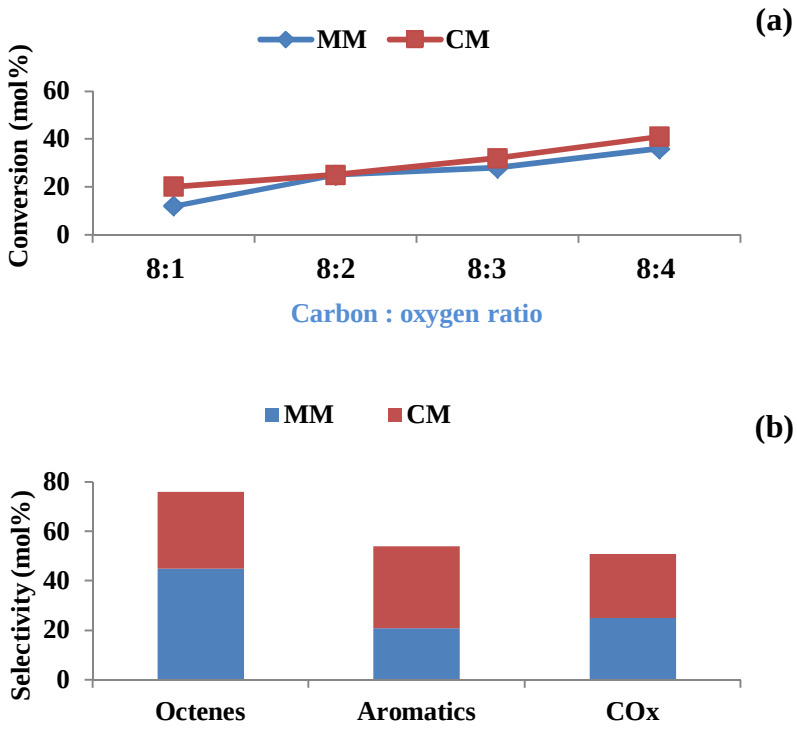

Figure 5.5: Influence of the cation in the molybdate and the oxygen concentration on the conversion of *n*-octane in ODH at 500 ^{O}C (a) and the effect of the cation in the selectivity at *iso* conversion (~ 29%) at 8:3 (C:O) and 500 °C.

5.4) Summary and conclusion

The different cations in the molybdate structures affected the activity and selectivity of the molybdates in the ODH of *n*-octane. The highest conversion of *n*-octane was obtained with cobalt as cation followed by magnesium. The most selective catalysts to octenes was magnesium molybdate and to C8 aromatics was cobalt molybdate. Likely, due to the cation altering the surface acidity of the catalyst.

5.5) Acknowledgements

The authors would like to thanks National Research Foundation (NRF), THRIP (grant number TP1208035643) and SASOL for financial support. Dr. M. Conte for his assistance with the *in situ* XRD work.

5.6) References

[1] M.M. Bhasin, J.H. McCain, B.V. Vora, T. Imai, P.R. Pujadó, Appl. Catal., A: Gen., 221 (2001) 397-419.
[2] A. Kaddouri, R. Del Rosso, C. Mazzocchia, P. Gronchi, D. Fumagalli, J. Therm. Anal. Calorim., 66 (2001) 63-78.
[3] K.H. Lee, Y.S. Yoon, W. Ueda, Y. Moro-oka, Catal. Lett., 46 (1997) 267-271.
[4] Y.S. Yoon, W. Ueda, Y. Moro-oka, Catal. Lett., 35 (1995) 57-64.
[5] Y. Yoon, W. Ueda, Y. Moro-oka, Top. Catal., 3 (1996) 265-275.
[6] Y.S. Yoon, N. Fujikawa, W. Ueda, Y. Moro-oka, K.W. Lee, Catal. Today, 24 (1995) 327-333.
[7] Y.S. Yoon, K. Suzuki, T. Hayakawa, S. Hamakawa, T. Shishido, K. Takehira, Catal. Lett., 59 (1999) 165-172.
[8] M.M. Barsan, F.C. Thyrion, Catal. Today, 81 (2003) 159-170.
[9] D.L. Stern, R.K. Grasselli, J. Catal., 167 (1997) 560-569.
[10] B. Pillay, M.R. Mathebula, H.B. Friedrich, Appl. Catal., A: Gen., 361 (2009) 57-64.
[11] B. Pillay, M.R. Mathebula, H.B. Friedrich, Catal. Lett., 141 (2011) 1297-1304.
[12] D.L. Stern, R.K. Grasselli, J. Catal., 167 (1997) 550-559.
[13] S.-S. Chang, B. Clair, J. Ruelle, J. Beauchêne, F. Di Renzo, F. Quignard, G.-J. Zhao, H. Yamamoto, J. Gril, J. Exp. Bot., 60 (2009) 3023-3030.
[14] E.A. Elkhalifa, H.B. Friedrich, J. Mol. Catal. A: Chem., 392 (2014) 22-30.
[15] E.A. Elkhalifa, H.B. Friedrich, Appl. Catal., A: Gen., 373 (2010) 122-131.
[16] V.D.B.C. Dasireddy, S. Singh, H.B. Friedrich, Appl. Catal., A: Gen., 456 (2013) 105-117.
[17] E.A. Elkhalifa, H.B. Friedrich, Catal. Lett., 141 (2011) 554-564.
[18] M. Narayanappa, V.D.B.C. Dasireddy, H.B. Friedrich, Appl. Catal., A: Gen., 447–448 (2012) 135-143.
[19] V.D.B.C. Dasireddy, S. Singh, H.B. Friedrich, Appl. Catal., A: Gen., 421–422 (2012) 58-69.

[20] V.D.B.C. Dasireddy, H.B. Friedrich, S. Singh, Appl. Catal., A: Gen., 467 (2013) 142-153.
[21] L.M. Madeira, M.F. Portela, Appl. Catal., A: Gen. 281 (2005) 179-189.
[22] J. Miller, N. Jackson, L. Evans, A. Sault, M. Gonzales, Catal. Lett. 58 (1999) 147-152.
[23] J.F. Liu, Y. Liu, L.F. Peng, J. Mol. Catal. A: Chem. 280 (2008) 7-15.

Chapter six

Summary and conclusion

The effect of the molybdenum content in the magnesium molybdate catalyst system (using four different Mg/Mo catalysts) in terms of activity (*i.e.* conversion of *n*-octane) and selectivity to value added products (*i.e.* octenes and C8 aromatics) was investigated in the oxidative dehydrogenation of *n*-octane. The Raman results demonstrated that the excess molybdenum was present in the α-MoO_3 form, this was supported by the SEM imaging analysis where the plate like structures become more dominant at high molybdenum content. In terms of the catalytic behavior, the catalysts with near stoichiometric Mg:Mo ratios (*i.e.* MM0.98 and MM1.06) showed the highest conversion of *n*-octane especially at high reaction temperatures (~ 28% at 500 ^{O}C) and in terms of selectivity trend, as the molybdenum content in the catalyst increased the selectivity to octenes decreased, accompanied by an increase in the selectivity to aromatics and COx. This could be explained in that as the acidity of the catalysts increased, the desorbtion of octenes was slower leading to these molecules reacting further to form aromatics and COx. Those catalysts were also the most selective to octenes (~ 45%) and C8 aromatics (~ 19 %) as determined at *iso*-conversion (~24% at 500 ^{O}C). The catalyst with the highest molybdenum trioxide content showed the lowest selectivity to octenes and C8 aromatics. Characterization of the used catalyst by Raman spectroscopy showed that the catalysts maintain their initial phases (*i.e.* $MgMoO_4$).

Furthermore, the effect of the oxygen concentration on the magnesium (Mg:Mo 1:1.06) molybdate catalyst's activity, selectivity and stability in the ODH of *n*-octane was investigated. Four carbon to oxygen ratios were investigated (*i.e.* 8:0, 8:1, 8:2 and 8:4 carbon to oxygen ratio) in the temperature range of 350 to 500 ^{O}C in 50 ^{O}C intervals. The conversion on *n*-octane increased as the oxygen concentration in the feed increased; however, the selectivity to octenes decreased as the oxygen concentration increased and that was accompanied by an increase in the selectivity to C8 aromatics and COx. The highest selectivity to octenes (~ 58%) was obtained at an 8:2 carbon to oxygen ratio and the highest selectivity to C8 aromatics (~ 19%) was obtained at an 8:4 carbon to oxygen ratio, as determined at *iso*-conversion (~26%) at 500 ^{O}C. In terms of

the catalyst stability, the oxygen concentration also played an important role, where in oxygen lean environments (*i.e.* 8:0 and 8:1 carbon to oxygen ratios) the catalyst underwent partial reduction to the molybdenum trioxide phase. Under oxygen rich environments (*i.e.* 8:2 and 8:4 carbon to oxygen ratios) the $MgMoO_4$ phase was the dominant phase (as in the fresh catalyst).

The effect of the oxygen content in the reaction feed was again investigated using cobalt molybdate as catalyst in the ODH of *n*-octane. The XRD analysis indicated the presence of both the α- and β-$CoMoO_4$ phases and the bulk metal ratios was determined by ICP-OES to be 1:1.04 Co:Mo. Similar trends to $MgMoO_4$ with respect to conversion and selectivity with changing oxygen concentration were observed. Characterization of the used catalyst by Raman spectroscopy showed that the catalyst is stable at moderate to high oxygen content (*i.e.* 8:2, 8:3 and 8:4 carbon to oxygen ratios). The STY (space time yield) for both octenes and C8 aromatics increased with increase in the oxygen content in the reaction mixture.

The effect of oxygen content in the reaction mixture for both magnesium molybdate and cobalt molybdate indicate that the adsorbed oxygen species improve the activity of the catalyst, however, that was accompanied by increase in the selectivity to aromatics and mainly COx, leading to the belief that the lattice oxygen is rather more selective than the adsorbed oxygen molecules, since under a lean oxygen environment the catalyst is more selective to value added products.

Finally, the effect of the cation in the molybdate structure was investigated by comparing the catalysts magnesium molybdate and cobalt molybdate at *iso*-conversion at 500 ^{O}C. The results obtained showed that the magnesium molybdate catalyst showed inferior *n*-octane conversion compared to cobalt molybdate. In term of selectivity to value added products (as determined under the *iso*-conversion conditions), magnesium molybdate and cobalt molybdate showed similar total selectivity to octane and aromatics. Further breakdown of the total selectivity to value added products indicated that magnesium molybdate is more selective for octenes, while cobalt molybdate is more selective for aromatics.

Appendix

Chapter two

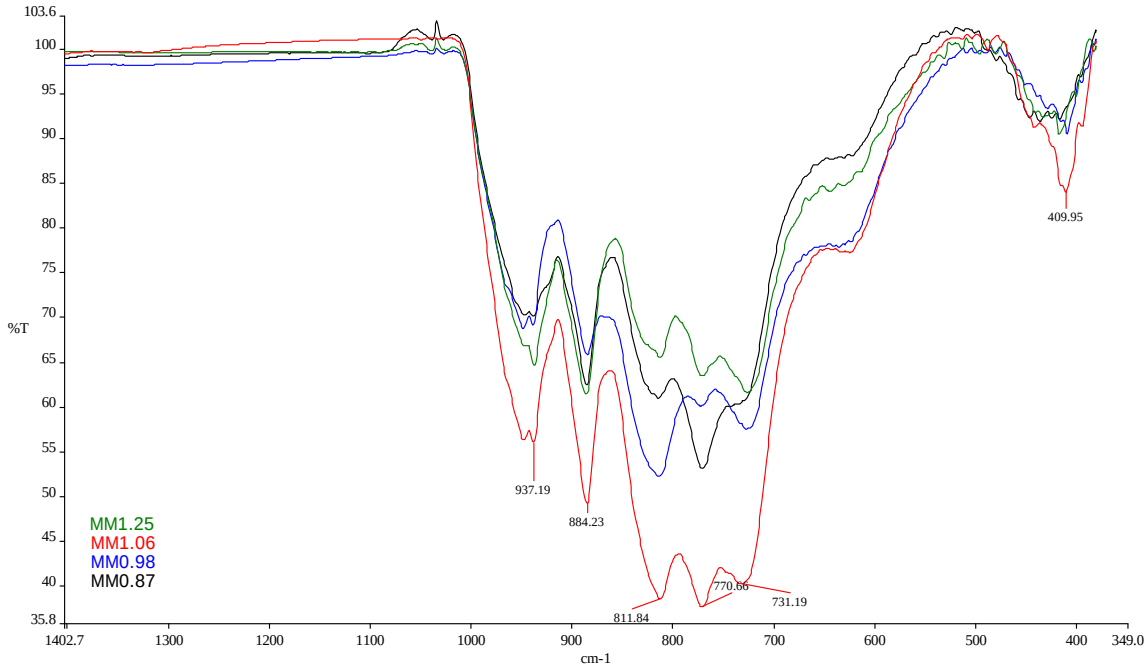

Appendix 2.1: IR spectra of the different magnesium molybdate catalyst with different molybdenum content for the ODH of *n*-octane at carbon to oxygen ratio of 8:3 and GHSV of 4000 h^{-1}

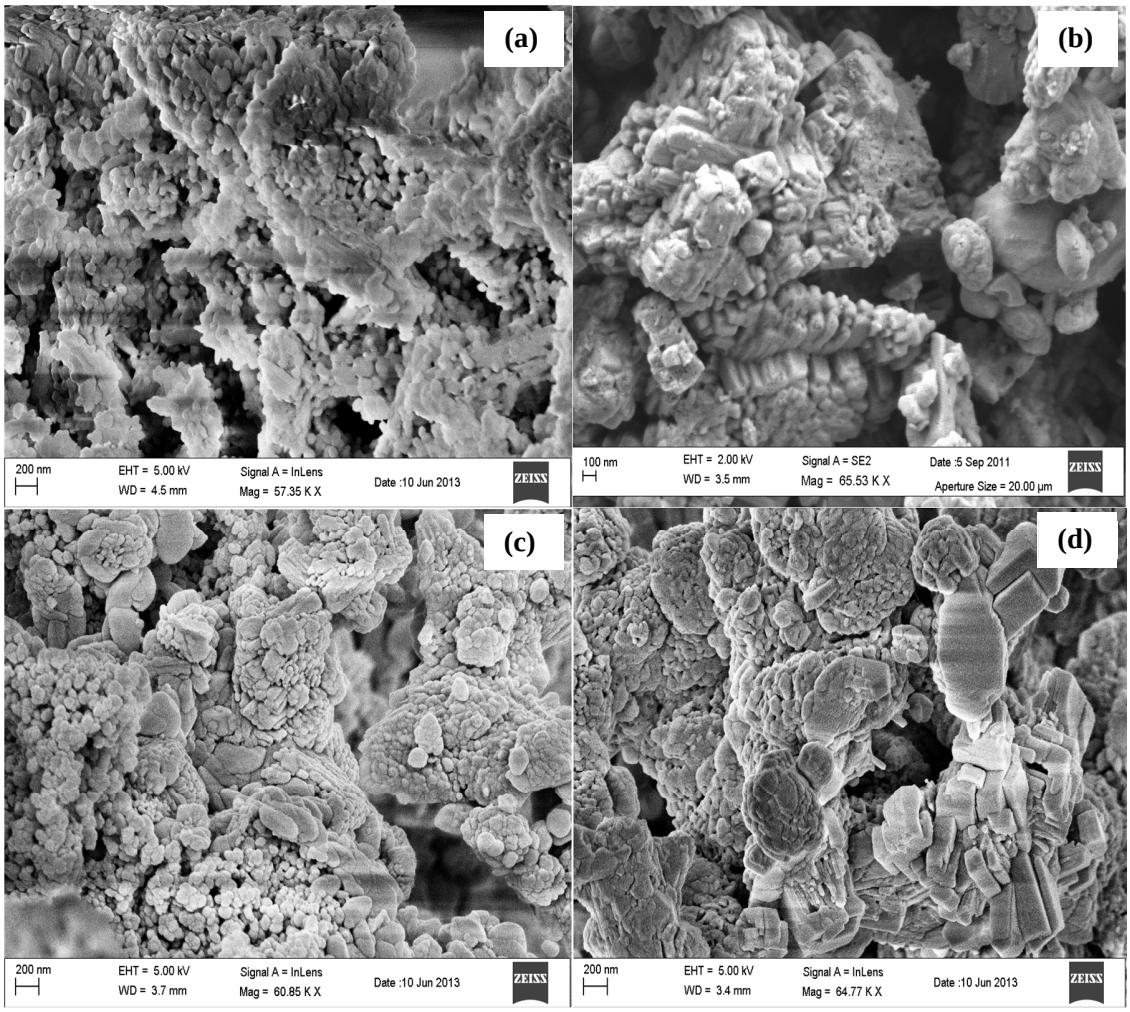

Appendix 2.2: SEM images of all four catalyst with different molybdenum content, MM0.87 (a), MM0.98 (b), MM1.06 (c) and MM1.25 (d).

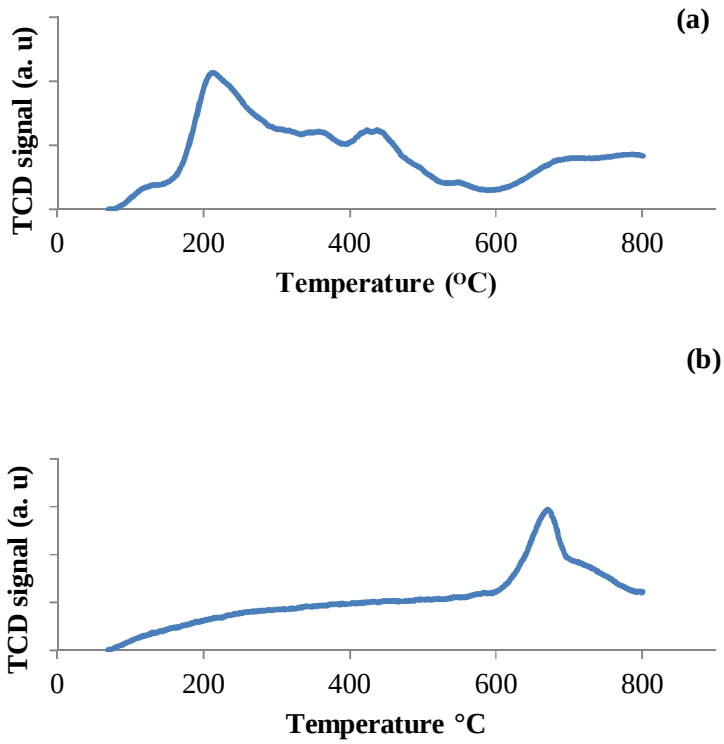

Appendix 2.3: NH_3-TPD of MM0.87 (a), MM 1.25 (b).

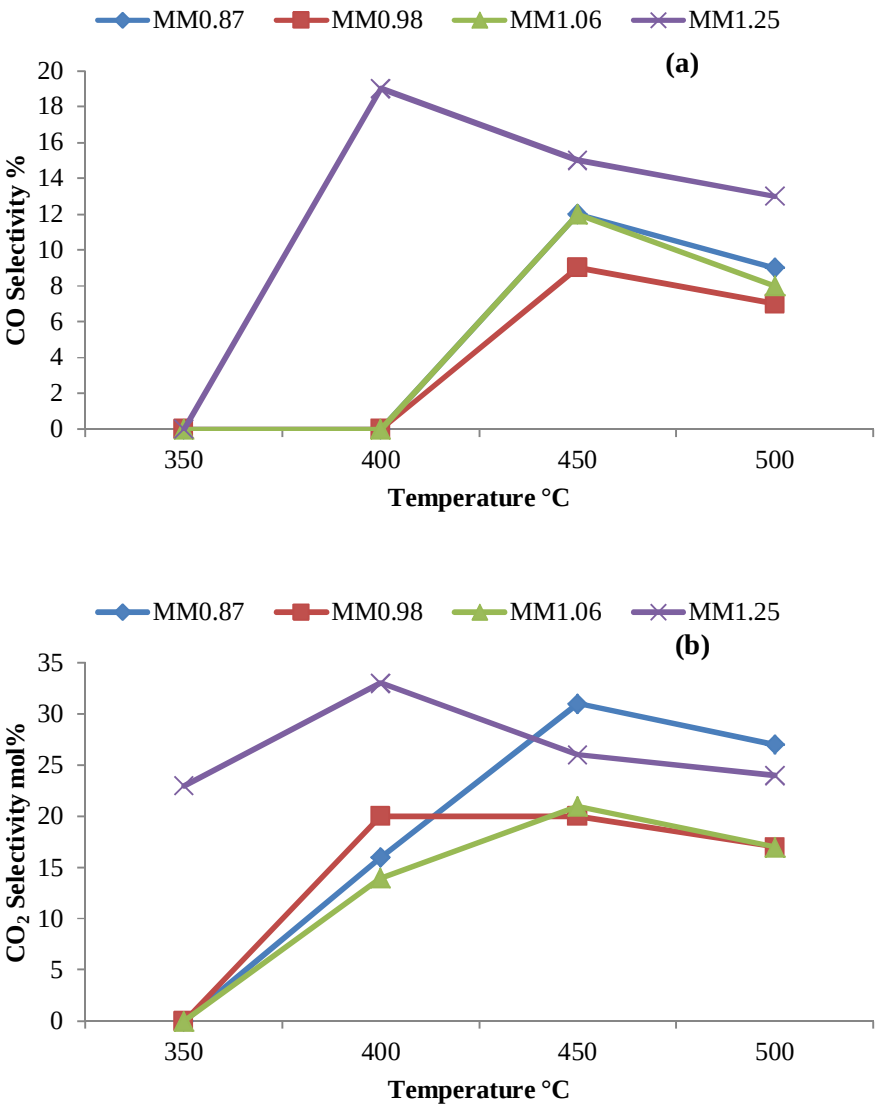

Appendix 2.4: Selectivity to CO (a) and CO_2 (b) as function of the molybdenum content and the reaction temperature in the ODH of *n*-octane.

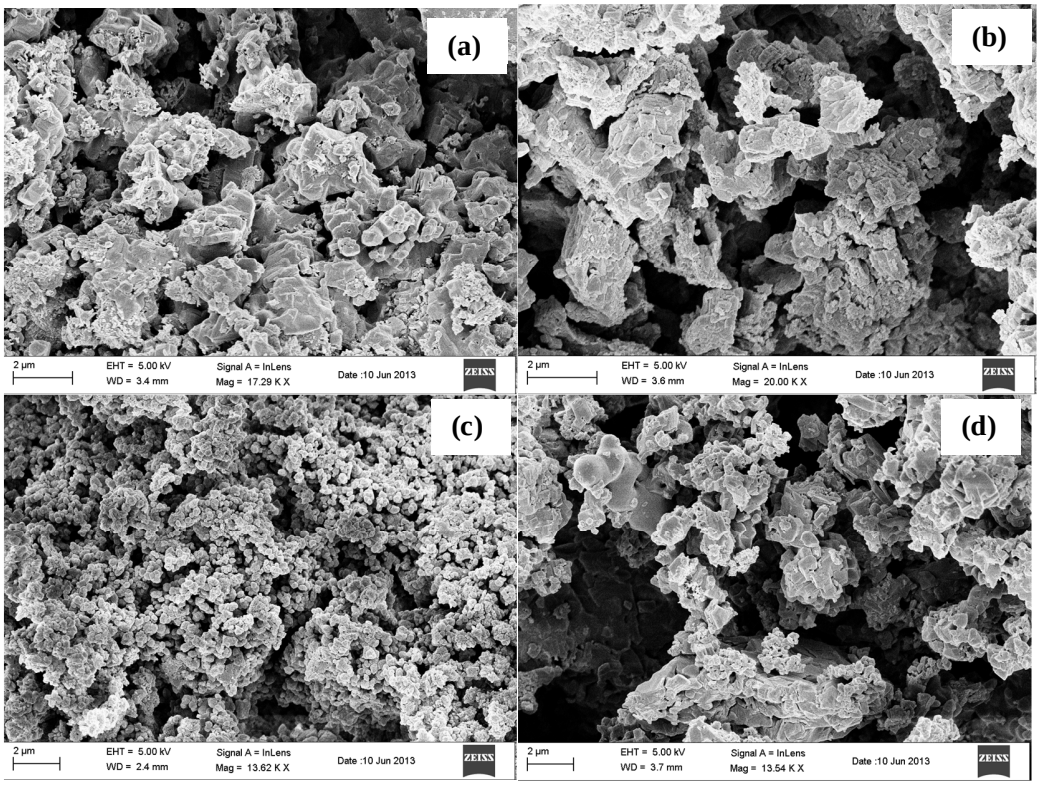

Appendix 2.5: SEM images of all four used catalysts in the ODH of *n*-octane MM0.87 (a), MM0.98 (b), MM1.06 (c) and MM1.25 (d) at carbon to oxygen ratio of 8:3 and 4000 h^{-1} GHSV.

Appendix

Chapter three

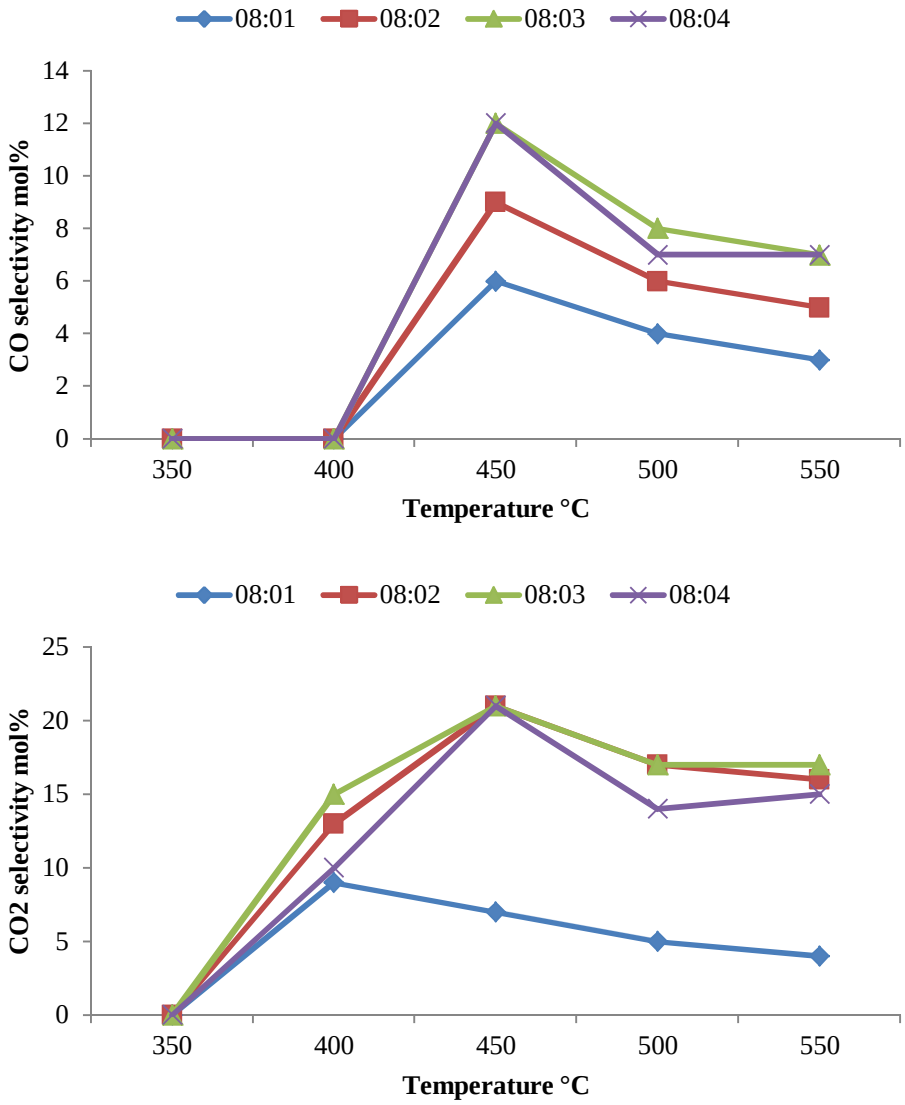

Appendix 3.1: The effect of C:O ratio on the selectivity breakdown of CO and CO_2 in the ODH of *n*-octane over magnesium molybdate catalyst.

Appendix

Chapter four

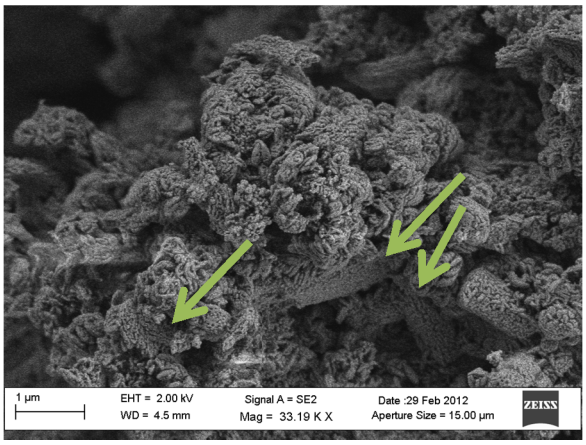

Appendix 4.1: SEM image of the cobalt molybdate catalyst, showing the presence of both cobalt molybdate and molybdenum trioxide.

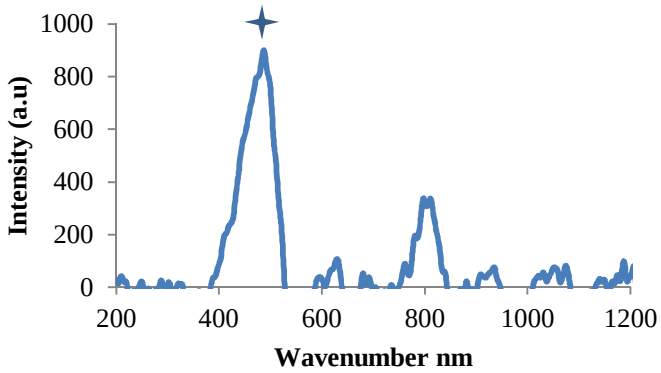

Appendix 4.2: Raman spectrum of the used catalyst under *n*-octane at an 8:0 C:O ratio at 4000 h^{-1}, ✦ (cobalt oxide)

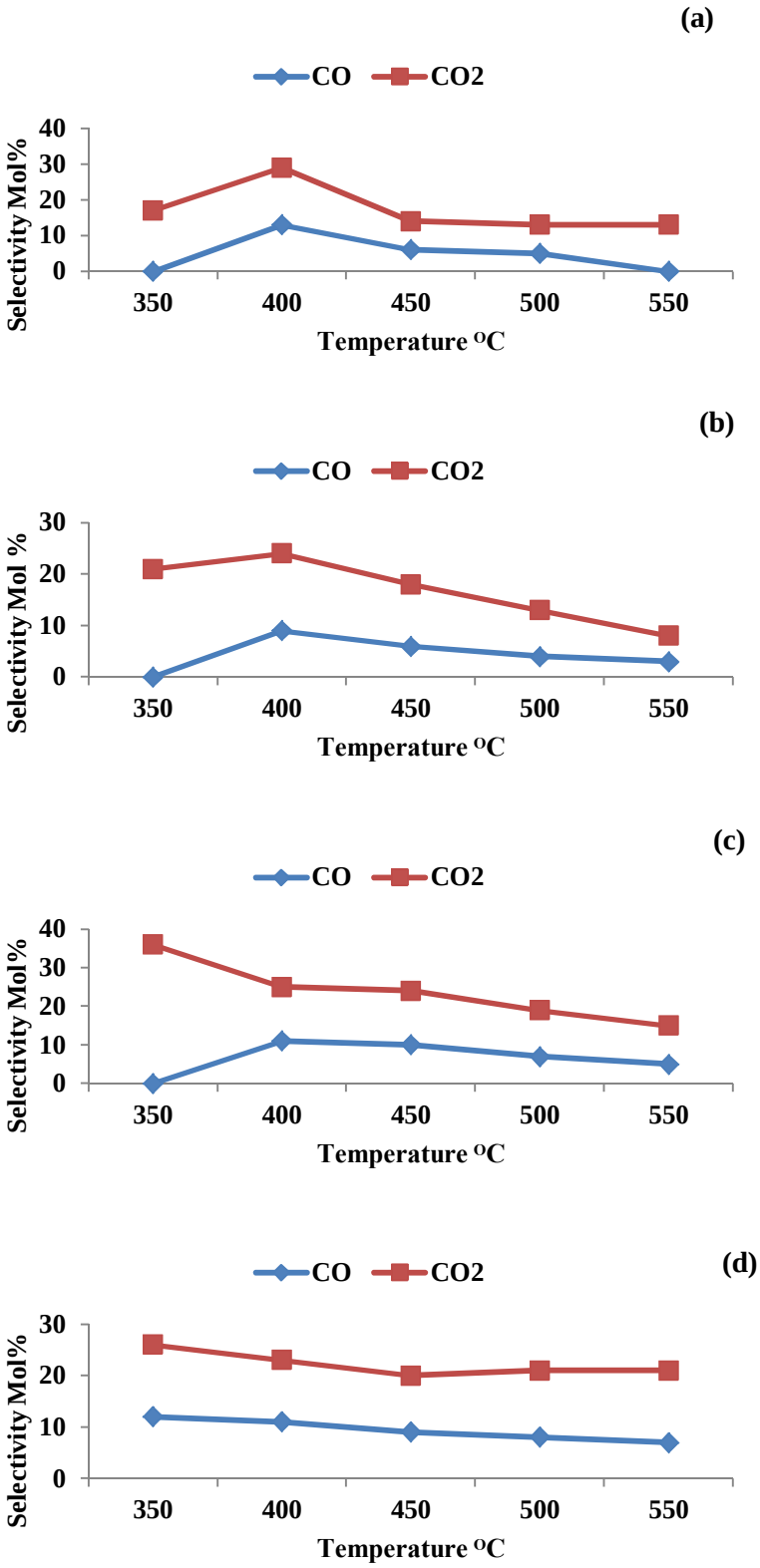

Appendix 4.3: The effect of the oxygen concentration in the ODH of *n*-octane on the ratio of CO and CO_2, C:O 8:1 (a), 8:2 (b), 8:3 (c) and 8:4 (d)

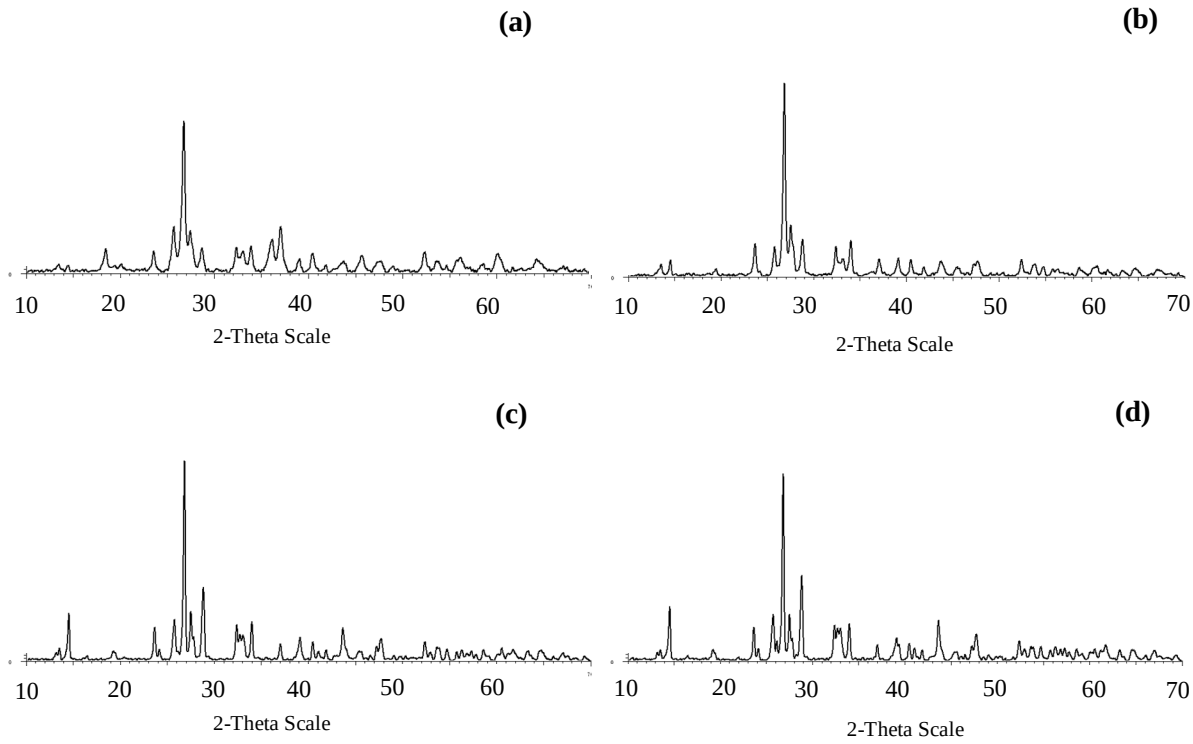

Appendix 4.4: XRD patterns of the used catalysts tested under different oxygen content in the activation of the *n*-octane at a GHSV of 4000 h^{-1}, a (8:1), b (8:2), c (8:3) and d (8:4).

Table 1: Example of GC standards used for calibration

Component	Purity %	Supplier
n-Octane	99	Merck
1-Octene	98	Aldrich
cis-2-Octene	98	Fluka
trans-2-Octene	98	Alfa Aesar
trans-3-Octene	98	Aldrich
cis-4-Octene	97	Alfa Aesar
trans-4-Octene	98	Fluka
Ethylbenzene	99	Alfa Aesar
Styrene	99	Aldrich
o-Xylene	99	Alfa Aesar

Table 2 : GC gaseous multicomponent standards used for calibration

Cylinder	Component	Concentration %	Supplier
1	Ethane	3	Afrox
	Ethylene	6	
	Butane	9	
	Nitrogen	Balance	
2	Methane	2	Afrox
	Propane	4	
	Propene	6	
	Nitrogen	Balance	
3	Carbon monoxide	5	Afrox
	Carbon dioxide	15	
	Nitrogen	Balance	

Table 3: GC settings and column description used for analysis of organic products

Column type	PONA
Column length	50 m
Column width	530 µm
Carrier gas	He
Split ratio	150:1
Detector type	FID
Detector temperature	250 ^{O}C
Detector range	1
Detector gas flows	Air 450 ml/min
	H_2 45 ml/min
Injector temperature	220 ^{O}C
Injection volume	0.2 µL

Table 4: Temperature program CG method used for organic products

Steps (ramping rate ^{O}C/min)	Temperature (^{O}C)	Hold (min)
1	40	15
2 (20)	100	5
3 (20)	200	2

Table 5: GC settings and column description used for analysis of COx

Column type	Carboxen 106 PLOT
Column length	30 m
Column width	530 µm
Carrier gas	He
Split flow	500 ml/min
Detector type	TCD
Detector temperature	250 ^{O}C
Detector range	1
Detector gas flows	He 30 ml/min
Injector temperature	180 ^{O}C

Table 6: Temperature program CG method used for COx

Steps (ramping rate ^{O}C/min)	Temperature (^{O}C)	Hold (min)
1	40	2.5
2 (20)	80	2.5

The methods used are the relative response factor and calibration method for quantification of the products obtained from the reaction. Standards used were multistandards solution where a number of different components (with different retention times mixed together) injected in different volumes to obtain calibration factors. The relative response factor was calculated as shown in Eq. 1 for all compounds and used to correct for their percentage from the GC analysis. The calculation for conversion, selectivity and yield are shown in Eq. 2, 3 and 4, respectively.

$$\text{Relative response factor} = \frac{Peak\ area\ of\ component\ A\ x\ mass\ of\ n-octane}{Mass\ of\ component\ A\ x\ peak\ area\ of\ n-octane} \qquad \text{Eq.1}$$

$$\text{Conversion} = \left(\frac{mole\ of\ octane\ in - mole\ octane\ out}{mole\ of\ octane\ in}\right) X\ 100 \qquad \text{Eq. 2}$$

$$\text{Selectivity} = \left(\frac{Moles\ of\ carbon\ in\ \ selected\ product}{Total\ moles\ of\ carbon\ in\ all\ products}\right)\ X\ 100 \qquad \text{Eq. 3}$$

$$\text{Yield} = \frac{Selectivity\ \%\ x\ conversion\ \%}{100} \qquad \text{Eq.}$$

Reactor setup

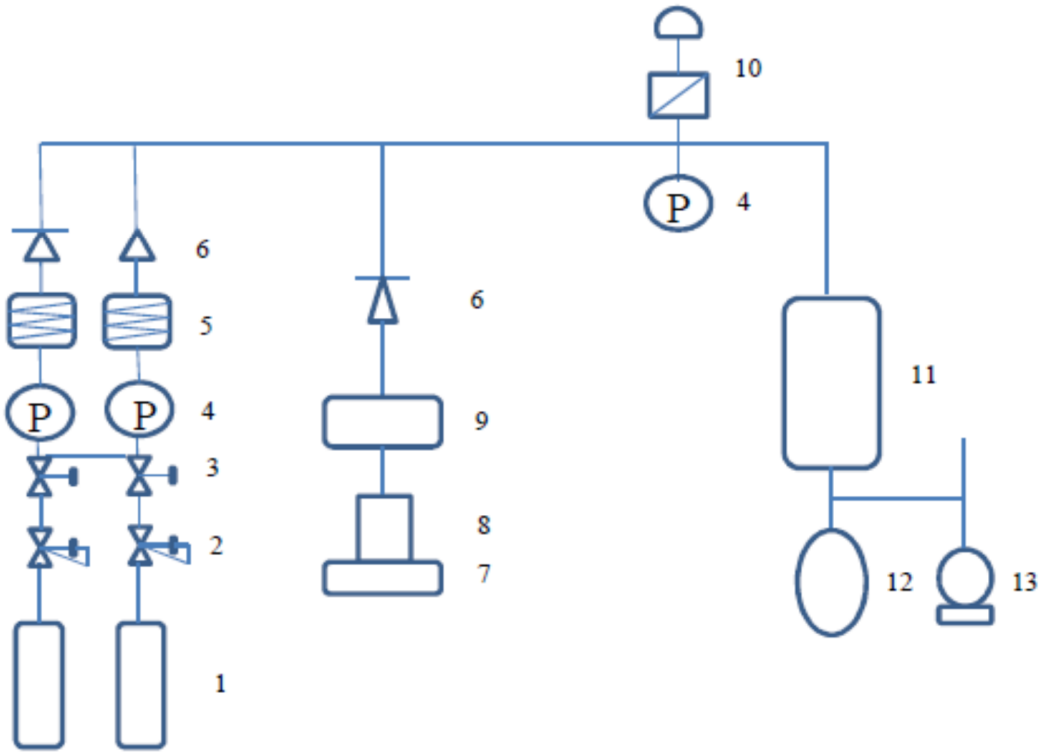

Figure 1: continuous flow vertical reactor step.

Table 7: Description of parts used in the continuous flow vertical reactor step.

Part number	Description
1	Gas cylinders (air and N_2)
2	Pressure regulator
3	Ball valve
4	Pressure gauge
5	Flow controllers
6	One way valve
7	Digital balance
8	Octane container
9	HPLC pump
10	Pressure relief valve
11	Heating block
12	Catch pot
13	Wet gas flow meter

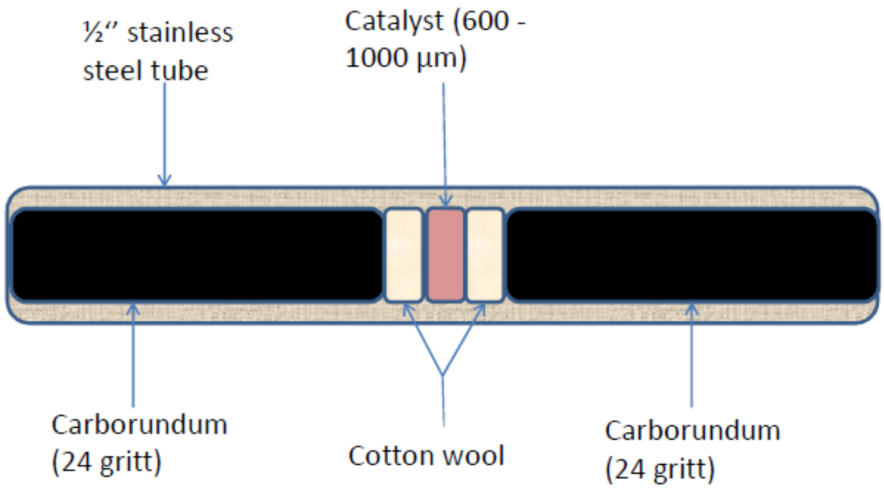

Figure 2: Reactor tube configuration used in the continuous flow vertical reactor step placed in the heating block.